CHAPTER 1 CHANGED PAGES

TABLE 1.0.1

HI-STORM FW SYSTEM COMPONENTS

Item	Designation (Model Number)
Overpack	HI-STORM FW
PWR Multi-Purpose Canisters	MPC-37, MPC-32ML, MPC-31C
BWR Multi-Purpose Canister	MPC-89
Transfer Cask	HI-TRAC VW

1.1 INTRODUCTION TO THE HI-STORM FW SYSTEM

This section and the next section (Section 1.2) provide the necessary information on the HI-STORM FW System pursuant to 10CFR72 paragraphs 72.2(a)(1),(b); 72.122(a),(h)(1); 72.140(c)(2); 72.230(a),(b); and 72.236(a),(c),(h),(m).

HI-STORM (acronym for Holtec International Storage Module) FW System is a spent nuclear fuel storage system designed to be in full compliance with the requirements of 10CFR72. The model designation "FW" denotes this as a system which has been specifically engineered to withstand sustained Flood and Wind.

The HI-STORM FW System consists of a sealed metallic multi-purpose canister (MPC) contained within an overpack constructed from a combination of steel and concrete. The design features of the HI-STORM FW components are intended to simplify and reduce the on-site SNF loading and handling work effort, to minimize the burden of in-use monitoring, to provide utmost radiation protection to the plant personnel, and to minimize the site boundary dose.

The HI-STORM FW System can safely store either PWR or BWR fuel assemblies, in the MPC ~~-37 or MPC-89, respectively~~s identified in Table 1.0.1. The MPC is identified by the maximum number of fuel assemblies it can contain in the fuel basket. The MPC external diameters are identical to allow the use of a single overpack design, however the height of the MPC, as well as the overpack and transfer cask, are variable based on the SNF to be loaded.

Figure 1.1.1 shows the HI-STORM FW System with two of its major constituents, the MPC and the storage overpack, in a cut-away view. The MPC, shown partially withdrawn from the storage overpack, is an integrally welded pressure vessel designed to meet the stress limits of the ASME Boiler and Pressure Vessel Code, Section III, Subsection NB [1.1.1]. The MPC defines the Confinement Boundary for the stored spent nuclear fuel assemblies. The HI-STORM FW storage overpack provides structural protection, cooling, and radiological shielding for the MPC.

The HI-STORM FW overpack is equipped with thru-wall penetrations at the bottom of the overpack and in its lid to permit natural circulation of air to cool the MPC and the contained SNF. The HI-STORM FW System is autonomous inasmuch as it provides SNF and radioactive material confinement, radiation shielding, criticality control and passive heat removal independent of any other facility, structures, or components at the site. The surveillance and maintenance required by the plant's staff is minimized by the HI-STORM FW System since it is completely passive and is composed of proven materials. The HI-STORM FW System can be used either singly or as an array at an ISFSI. The site for an ISFSI can be located either at a nuclear reactor facility or an away-from-a-reactor (AFR) location.

The information presented in this report is intended to demonstrate the acceptability of the HI-STORM FW System for use under the general license provisions of Subpart K by meeting the criteria set forth in 10CFR72.236.

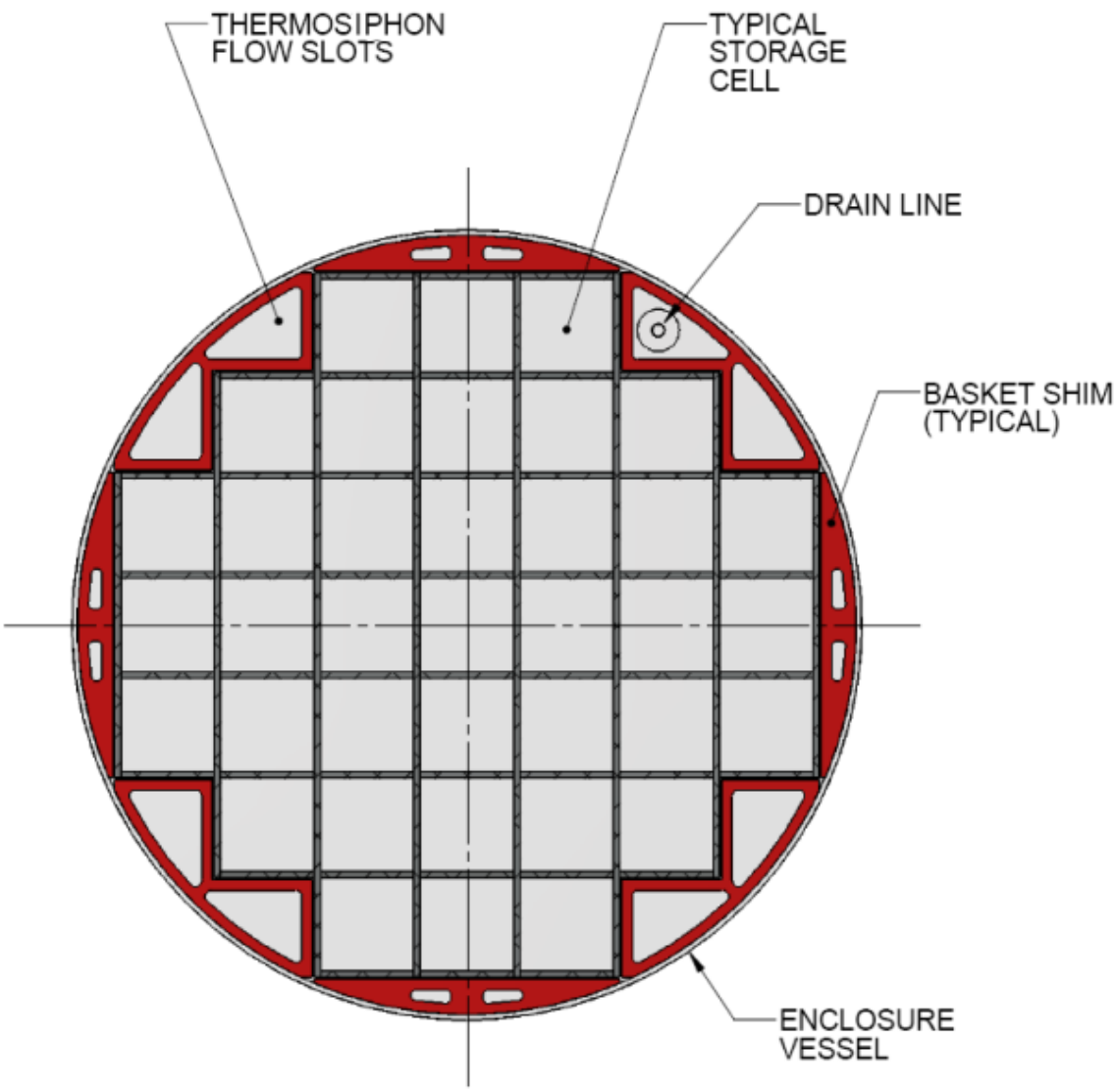

1.1.4A MPC-37 IN CROSS SECTION

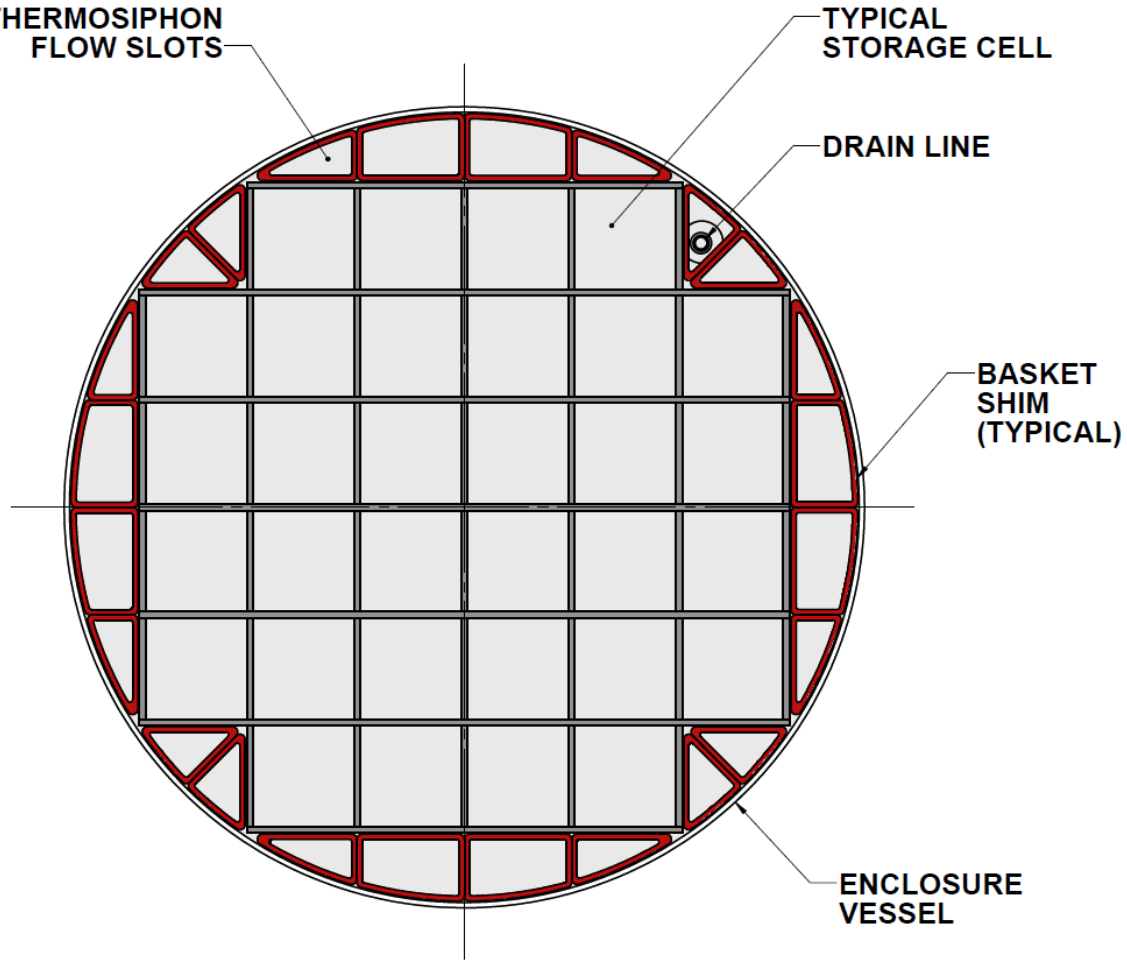

1.1.4B MPC-32ML IN CROSS SECTION

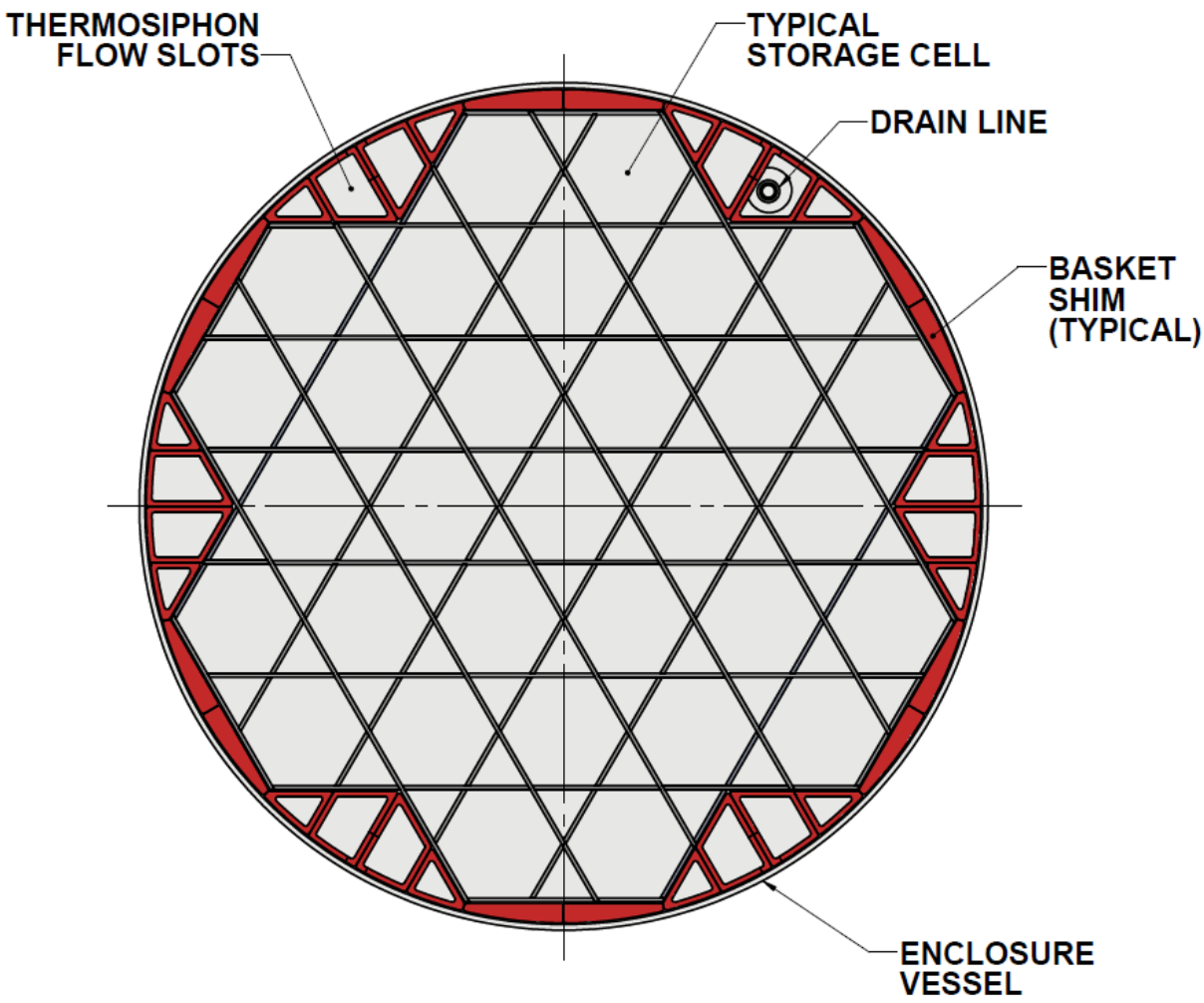

1.1.4C MPC-31C IN CROSS SECTION

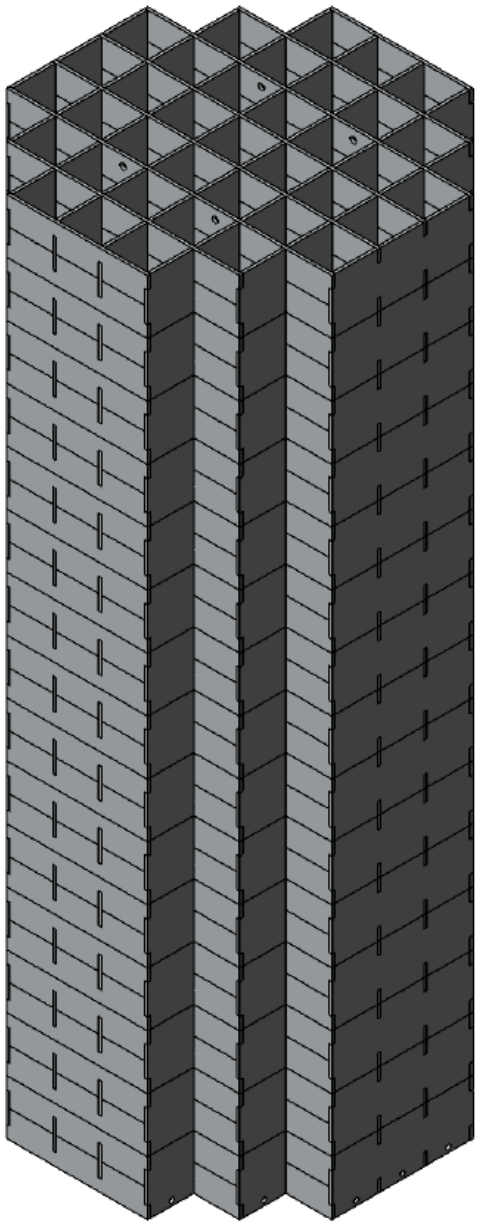

FIGURE 1.1.6A: MPC-37 PWR FUEL BASKET (37 STORAGE CELLS) IN PERSPECTIVE VIEW

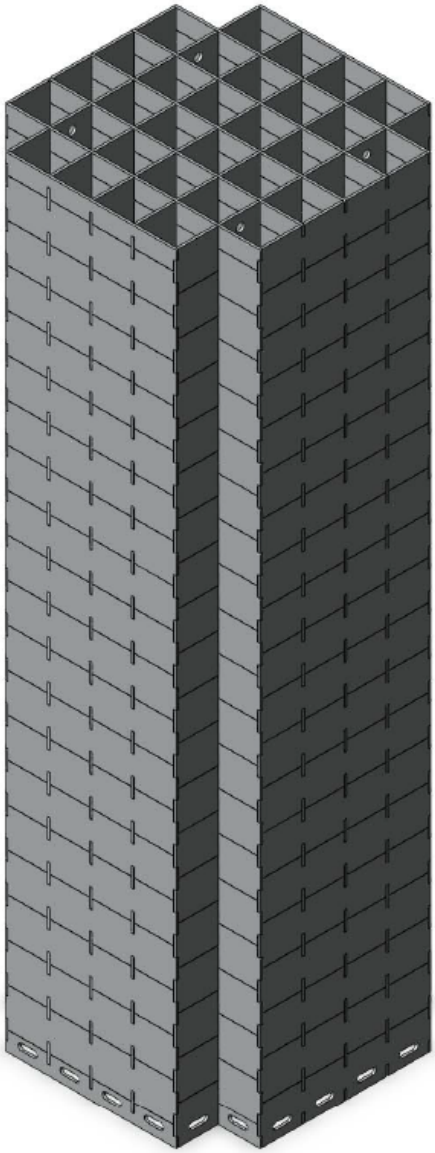

FIGURE 1.1.6B: MPC-32ML PWR FUEL BASKET (32 STORAGE CELLS) IN PERSPECTIVE VIEW

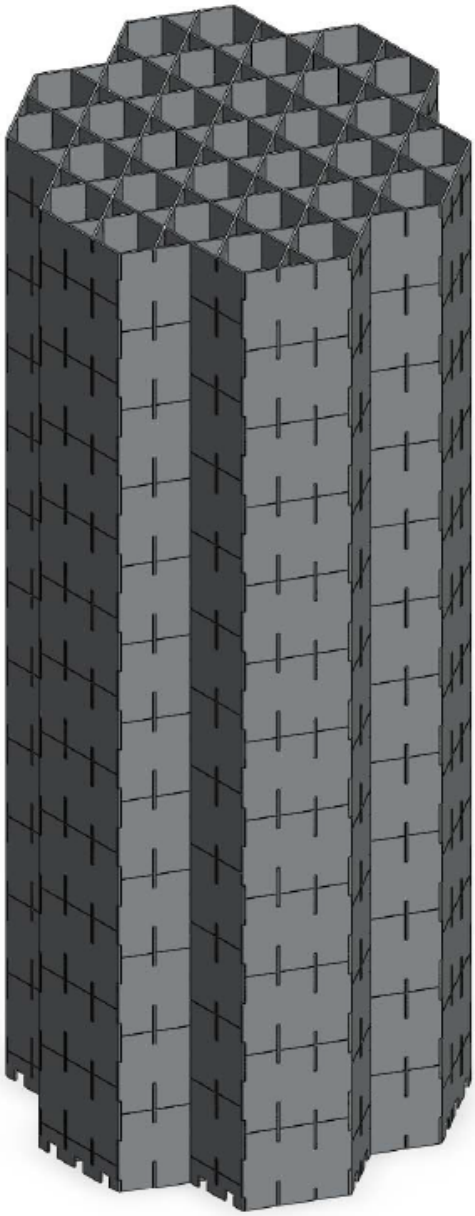

FIGURE 1.1.6C: MPC-31C PWR FUEL BASKET (31 STORAGE CELLS) IN PERSPECTIVE VIEW

The HI-STORM FW System shares certain common attributes with the HI-STORM 100 System, Docket No. 72-1014, namely:

i. the honeycomb design of the MPC fuel basket;
ii. the effective distribution of neutron and gamma shielding materials within the system;
iii. the high heat dissipation capability;
iv. the engineered features to promote convective heat transfer by passive means;
v. a structurally robust steel-concrete-steel overpack construction.

The honeycomb design of the MPC fuel baskets renders the basket into a multi-flange egg-crate structure where all structural elements (i.e., cell walls) are arrayed in two orthogonal sets of plates. Consequently, the walls of the cells are either completely co-planar (i.e., no offset) or orthogonal with each other. There is complete edge-to-edge continuity between the contiguous cells to promote conduction of heat.

The composite shell construction in the overpack, steel-concrete-steel, allows ease of fabrication and eliminates the need for the sole reliance on the strength of concrete.

A description of each of the components is provided in this section, along with fabrication and safety feature information.

1.2.1.1 Multi-Purpose Canisters

The MPC enclosure vessels are cylindrical weldments with identical and fixed outside diameters. Each MPC is an assembly consisting of a honeycomb fuel basket (Figures 1.1.6 and 1.1.7), a baseplate, a canister shell, a lid, and a closure ring. The number of SNF storage locations in an MPC depends on the type of fuel assembly (PWR or BWR) to be stored in it.

Subsection 1.2.3 and Table 1.2.1 summarize the allowable contents for each MPC model listed in Table 1.0.1. Subsection 2.1.8 provides the detailed specifications for the contents authorized for storage in the HI-STORM FW System. Drawings for the MPCs are provided in Section 1.5.

The MPC enclosure vessel is a fully welded enclosure, which provides the confinement for the stored fuel and radioactive material. The MPC baseplate and shell are made of stainless steel (Alloy X, see Appendix 1.A). The lid is a two piece construction, with the top structural portion made of Alloy X. The confinement boundary is defined by the MPC baseplate, shell, lid, port covers, and closure ring.

The HI-STORM FW System MPCs shares external and internal features with the HI-STORM 100 MPCs certified in the §72-1014 docket, as summarized below.

i. ~~MPC-37 and MPC-89~~All HI-STORM FW MPCs have an identical enclosure vessel which mimics the enclosure vessel design details used in the HI-STORM 100 counterparts including the shell thickness, the vent and drain port sizes, construction details of the top lid and closure ring, and closure weld details. The baseplate is made slightly thicker to ensure its bending rigidity is comparable to its counterpart in the HI-STORM 100 system. The material

of construction of the pressure retaining components is also identical (options of austenitic stainless steels, denoted as Alloy X, is explained in Appendix 1.A herein as derived from the HI-STORM 100 FSAR with appropriate ASME Code edition updates). There are no gasketed joints in the MPCs.

ii. The top lid of the MPCs contains the same attachment provisions for lifting and handling the loaded canister as the HI-STORM 100 counterparts.

iii. The drain pipe and sump in the bottom baseplate of the MPCs (from which the drain pipe extracts the water during the dewatering operation) are also similar to those in the HI-STORM 100 counterparts.

iv. The fuel basket is assembled from a rectilinear gridwork of plates so that there are no bends or radii at the cell corners. This structural feature eliminates the source of severe bending stresses in the basket structure by eliminating the offset between the cell walls which transfer the inertia load of the stored SNF to the basket/MPC interface during the various postulated accident events (such as non-mechanistic tipover). This structural feature is shared with the HI-STORM 100 counterparts. Figures 1.1.6 and 1.1.7 show the PWR and BWR fuel baskets, respectively, in perspective view.

v. Precision extruded and/or machined blocks of aluminum alloy with axial holes (basket shims) are installed in the peripheral space between the fuel basket and the enclosure vessel to provide conformal contact surfaces between the basket shims and the fuel basket and between the basket shims and the enclosure vessel shell. The axial holes in the basket shims serve as the passageway for the downward flow of the helium gas under the thermosiphon action. This thermosiphon action is common to all MPCs including those of the HI-STORM 100. Various options are available to install these extruded shims in the basket periphery as summarized in Table 1.2.9.

vi. To facilitate an effective convective circulation inside the MPC, the operating pressure is set the same as that in the HI-STORM 100 counterparts.

vii. Like the high capacity baskets in the HI-STORM 100 MPCs, the fuel baskets do not contain flux traps (with the exception of the MPC-31C fuel basket).

Because of the above commonalities, the HI-STORM FW System is loaded in the same manner as the HI-STORM 100 system, and will use similar ancillary equipment, (e.g., lift attachments, lift yokes, lid welding machine, weld removal machine, cask transporter, mating device, low profile transporter or zero profile transporter, drying system, the hydrostatic pressure test system).

Lifting lugs, attached to the inside surface of the MPC shell, are used to place the empty MPC into the HI-TRAC VW transfer cask. The lifting lugs also serve to axially locate the MPC lid prior to welding. These internal lifting lugs cannot be used to handle a loaded MPC. The MPC lid is installed prior to any handling of a loaded MPC and there is no access to the internal lifting lugs once the MPC lid is installed.

1.2.2.3 Identification of Subjects for Safety and Reliability Analysis

1.2.2.3.1 Criticality Prevention

Criticality is controlled by geometry and neutron absorbing materials in the fuel basket. The entire basket is made of Metamic-HT, a uniform dispersoid of boron carbide and nano-particles of alumina in an aluminum matrix, serves as the neutron absorber. This accrues four major safety and reliability advantages:

(i) The larger B-10 areal density in the Metamic-HT allows higher enriched fuel (i.e., BWR fuel with planar average initial enrichments greater than 4.5 wt% U-235) ~~without relying on gadolinium or burn-up credit~~.
(ii) The neutron absorber cannot be removed from the basket or displaced within it.
(iii) Axial movement of the fuel with respect to the basket has no reactivity consequence because the entire length of the basket contains the B-10 isotope.
(iv) The larger B-10 areal density in the Metamic-HT reduces the reliance on soluble boron credit during loading/unloading of PWR fuel.

1.2.2.3.2 Chemical Safety

There are no chemical safety hazards associated with operations of the HI-STORM FW System. A detailed evaluation is provided in Section 3.4.

1.2.2.3.3 Operation Shutdown Modes

The HI-STORM FW System is totally passive and consequently, operation shutdown modes are unnecessary.

1.2.2.3.4 Instrumentation

As stated earlier, the HI-STORM FW MPC, which is seal welded, non-destructively examined, and pressure tested, confines the radioactive contents. The HI-STORM FW is a completely passive system with appropriate margins of safety; therefore, it is not necessary to deploy any instrumentation to monitor the cask in the storage mode. At the option of the user, temperature elements may be utilized to monitor the air temperature of the HI-STORM FW overpack exit vents in lieu of routinely inspecting the vents for blockage.

1.2.2.3.5 Maintenance Technique

Because of its passive nature, the HI-STORM FW System requires minimal maintenance over its lifetime. No special maintenance program is required. Chapter 10 describes the maintenance program set forth for the HI-STORM FW System.

1.2.3 Cask Contents

This sub-section contains information on the cask contents pursuant to 10 CFR72, paragraphs 72.2(a)(1),(b) and 72.236(a),(c),(h),(m).

The HI-STORM FW System is designed to house both BWR and PWR spent nuclear fuel assemblies. Tables 1.2.1 and 1.2.2 provide key system data and parameters for the MPCs. A description of acceptable fuel assemblies for storage in the MPCs is provided in Section 2.1. This includes fuel assemblies classified as damaged fuel assemblies and fuel debris in accordance with the definitions of these terms in the Glossary. All fuel assemblies, non-fuel hardware, and neutron sources authorized for packaging in the MPCs must meet the fuel specifications provided in Section 2.1. All fuel assemblies classified as damaged fuel or fuel debris must be stored in damaged fuel containers (DFC).

As shown in Figure 1.2.1a (MPC-37) and Figure 1.2.2 (MPC-89), each storage location is assigned to one of three regions, denoted as Region 1, Region 2, and Region 3 with an associated cell identification number. For example, cell identified as 2-4 is Cell 4 in Region 2. A DFC can be stored in the outer peripheral locations of ~~both~~ the MPC-37/MPC-32ML/MPC-31C and MPC-89 as shown in Figures 2.1.1 and 2.1.2, respectively. The permissible heat loads for each cell, region, and the total canister are given in Tables 1.2.3 and 1.2.4 for MPC-37/MPC-32ML/MPC-31C and MPC-89, respectively. The sub-design heat loads for each cell, region and total canister are in Table 4.4.11.

TABLE 1.2.1

KEY SYSTEM DATA FOR HI-STORM FW SYSTEM

ITEM	QUANTITY	NOTES
Types of MPCs[†]	~~2~~4	~~1~~3 for PWR 1 for BWR
MPC storage capacity:	MPC-37	Up to 37 undamaged ZR clad PWR fuel assemblies with or without non-fuel hardware, of classes specified in Table 2.1.1a. Up to 12 damaged fuel containers containing PWR damaged fuel and/or fuel debris may be stored in the locations denoted in Figure 2.1.1a with the remaining basket cells containing undamaged fuel assemblies, up to a total of 37.
MPC storage capacity:	MPC-89	Up to 89 undamaged ZR clad BWR fuel assemblies. Up to 16 damaged fuel containers containing BWR damaged fuel and/or fuel debris may be stored in locations denoted in Figure 2.1.2 with the remaining basket cells containing undamaged fuel assemblies, up to a total of 89.
MPC storage capacity:	MPC-32ML	Up to 32 undamaged ZR clad PWR fuel assemblies, of classes specified in Table 2.1.1b. Up to 8 damaged fuel containers containing PWR damaged fuel and/or fuel debris may be stored in the locations denoted in Figure 2.1.1b with the remaining basket cells containing undamaged fuel assemblies, up to a total of 32.
MPC storage capacity:	MPC-31C	Up to 31 undamaged ZR clad PWR fuel assemblies, of classes specified in Table 2.1.1c. Up to 6 damaged fuel containers containing PWR damaged fuel and/or fuel debris may be stored in the locations denoted in Figure 2.1.1c with the remaining basket cells containing undamaged fuel assemblies, up to a total of 31 (additional restrictions apply to total storage capacity, see Chapter 2).

[†] See Chapter 2 for a complete description of authorized cask contents and fuel specifications.

TABLE 1.2.2

KEY PARAMETERS FOR HI-STORM FW MULTI-PURPOSE CANISTERS

Parameter	PWR	BWR
Pre-disposal service life (years)	100	100
Design temperature, max./min. (°F)	752†/-40††	752†/-40††
Design internal pressure (psig) Normal conditions Off-normal conditions Accident Conditions	 100 120 200	 100 120 200
Total heat load, max. (kW)	See Table 1.2.3a/b/c	See Table 1.2.4
Maximum permissible peak fuel cladding temperature: Long Term Normal (°F) Short Term Operations (°F) Off-normal and Accident (°F)	 752 752 or 1058††† 1058	 752 752 or 1058††† 1058
Maximum permissible multiplication factor (k_{eff}) including all uncertainties and biases	< 0.95	< 0.95
B_4C content (by weight) (min.) in the Metamic-HT Neutron Absorber (storage cell walls)	10%	10%
[Withheld in Accordance with 10 CFR 2.390]	**[Withheld in Accordance with 10 CFR 2.390]**	**[Withheld in Accordance with 10 CFR 2.390]**
[Withheld in Accordance with 10 CFR 2.390]	**[Withheld in Accordance with 10 CFR 2.390]**	**[Withheld in Accordance with 10 CFR 2.390]**
End closure(s)	Welded	Welded
Fuel handling	Basket cell openings compatible with standard grapples	Basket cell openings compatible with standard grapples
Heat dissipation	Passive	Passive

† Maximum normal condition design temperatures for the MPC fuel basket. A complete listing of design temperatures for all components is provided in Table 2.2.3.

†† Temperature based on off-normal minimum environmental temperatures specified in Section 2.2.2 and no fuel decay heat load.

††† See Section 4.5 for discussion of the applicability of the 1058°F temperature limit during short-term operations, including MPC drying.

TABLE 1.2.3a
MPC-37 HEAT LOAD DATA (See Figure 1.2.1a)

Number of Regions: 3

Number of Storage Cells: 37

Maximum Design Basis Heat Load (kW): 44.09 (Pattern A); 45.0 (Pattern B)

Region No.	Decay Heat Limit per Cell, kW		Number of Cells per Region	Decay Heat Limit per Region, kW	
	Pattern A	Pattern B		Pattern A	Pattern B
1	1.05	1.0	9	9.45	9.0
2	1.70	1.2	12	20.4	14.4
3	0.89	1.35	16	14.24	21.6

Note: See Chapter 4 for decay heat limits per cell when vacuum drying high burnup fuel.

TABLE 1.2.3b MPC-32ML HEAT LOAD DATA (See Figure 1.2.1b)	
Number of Regions:	1
Number of Storage Cells:	32
Maximum Design Basis Heat Load (kW):	44.16
Decay Heat Limit per Cell, kW:	1.38

Note: See Chapter 4 for decay heat limits per cell when vacuum drying moderate or high burnup fuel.

TABLE 1.2.3c MPC-31C HEAT LOAD DATA (See Figure 1.2.1c)	
Number of Regions:	1
Number of Storage Cells:	31
Maximum Design Basis Heat Load (kW):	43.4
Decay Heat Limit per Cell, kW:	1.4

Note: See Chapter 4 for decay heat limits per cell when vacuum drying moderate or high burnup fuel.

TABLE 1.2.5 CRITICALITY AND SHIELDING SIGNIFICANT SYSTEM DATA		
Item	**Property**	**Value**
Metamic-HT Neutron Absorber	Nominal Thickness (mm)	8.9 (MPC-31C) 10 (MPC-89) 15 (MPC-37) 15 (MPC-32ML)
	Minimum B_4C Weight %	10 (MPC-31C) 10 (MPC-89) 10 (MPC-37) 10 (MPC-32ML)
Concrete in HI-STORM FW overpack body and lid	Installed Nominal Density (lb/ft^3)	150 (reference) 200 (maximum)

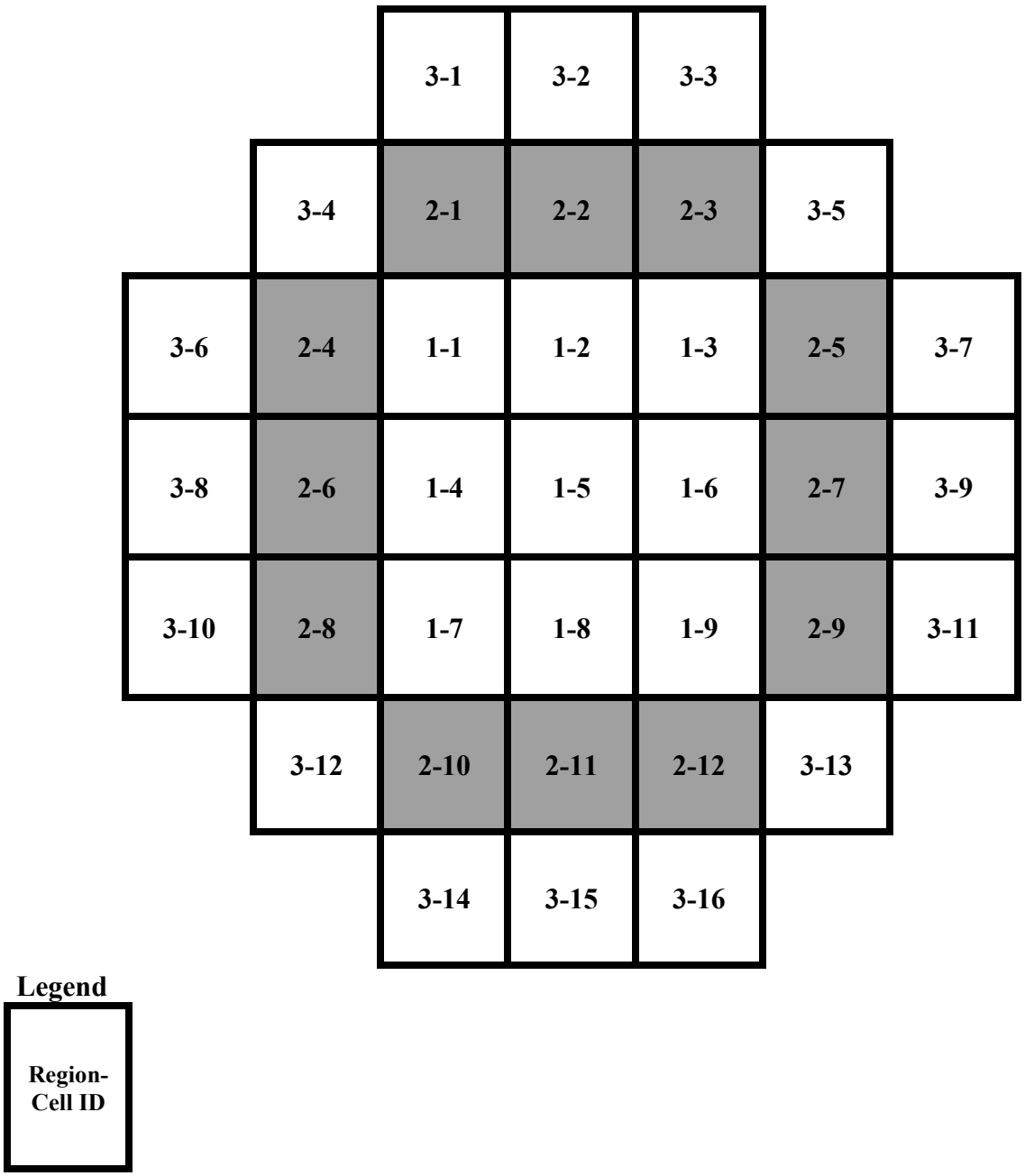

Figure 1.2.1a: MPC-37 Basket, Region and Cell Identification

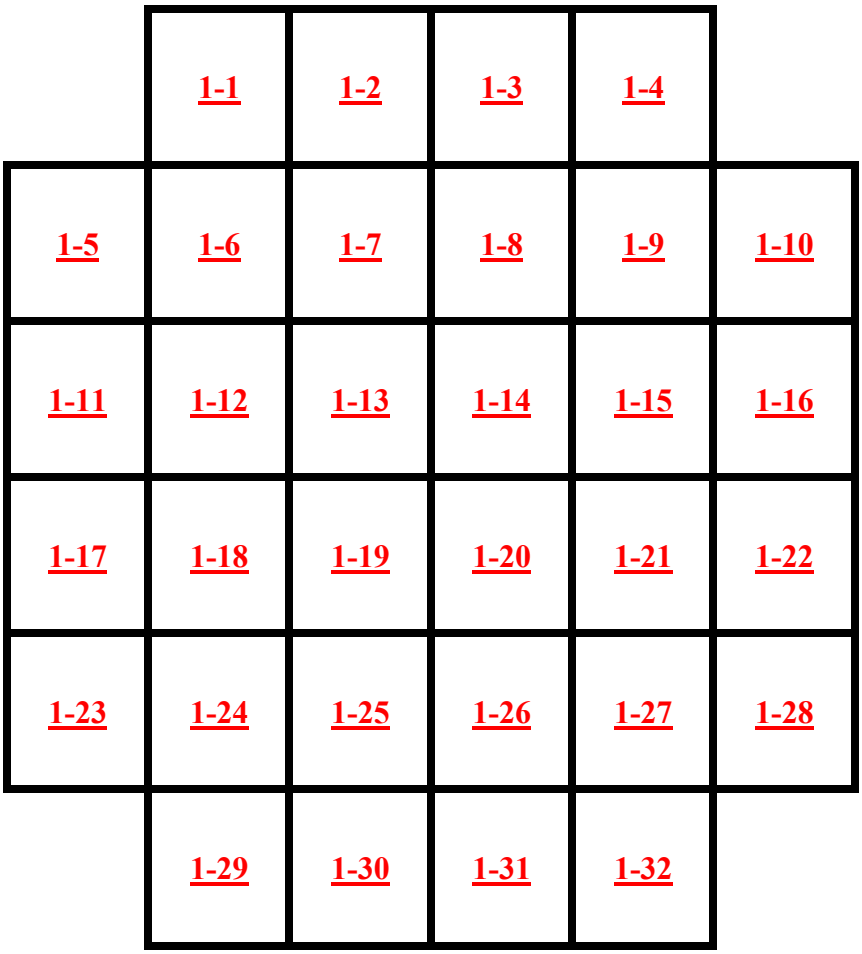

Figure 1.2.1b: MPC-32ML Basket Cell Identification

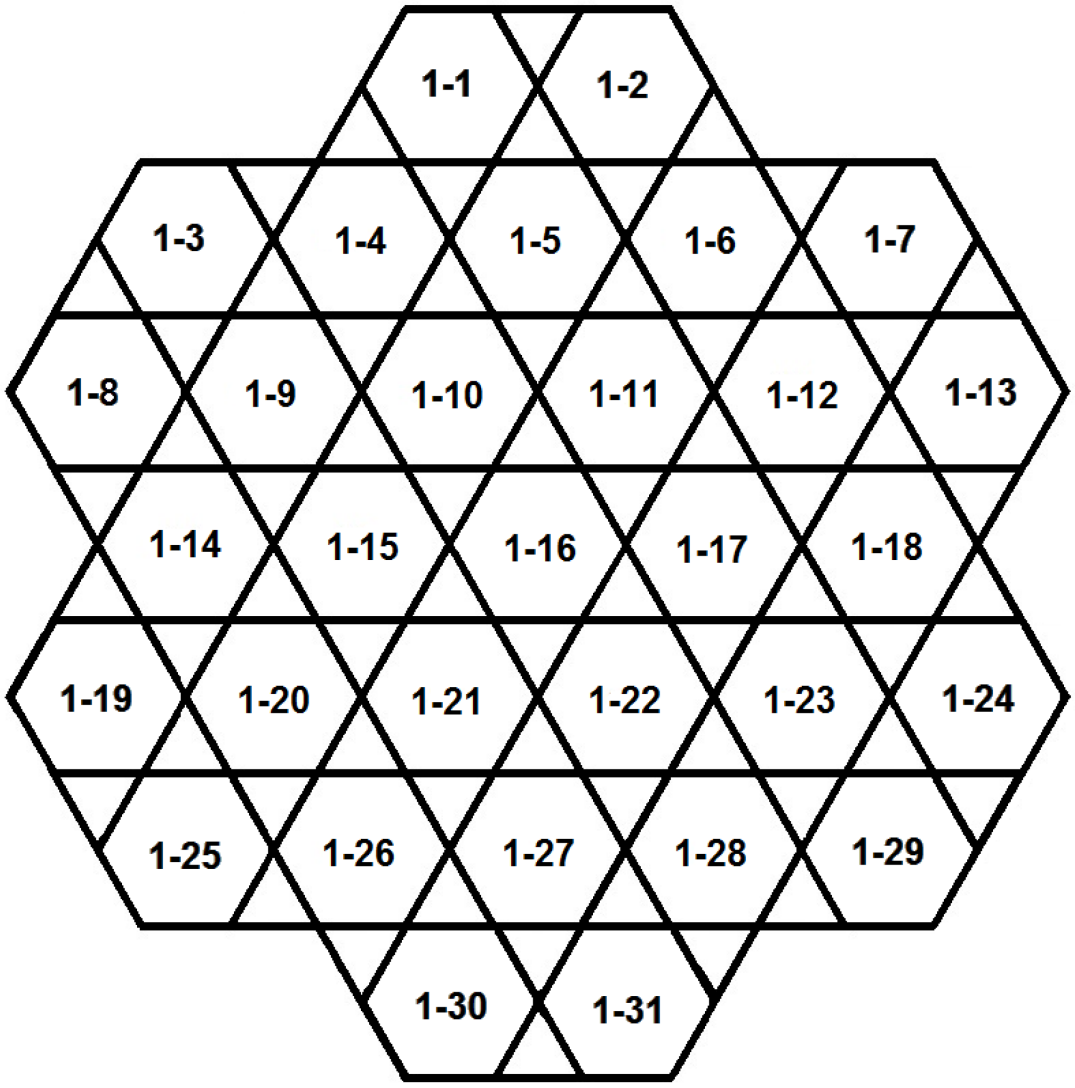

Figure 1.2.1c: MPC-31C Basket Cell Identification

1.5 DRAWINGS

The following HI-STORM FW System drawings are provided on subsequent pages in this section to fulfill the requirements in 10 CFR 72.2(a)(1),(b) and 72.230(a):

Drawing No.	Title	Revision
6494	HI-STORM FW BODY	12
6508	HI-STORM LID ASSEMBLY	8
6514	HI-TRAC VW – MPC-37	9
6799	HI-TRAC VW – MPC-89	9
6505	MPC-37 ENCLOSURE VESSEL	13
6506	MPC-37 FUEL BASKET	12
6512	MPC-89 ENCLOSURE VESSEL	15
6507	MPC-89 FUEL BASKET	11
10464	MPC-32ML ENCLOSURE VESSEL	0
10457	MPC-32ML FUEL BASKET	0
10465	MPC-31C ENCLOSURE VESSEL	0
10462	MPC-31C FUEL BASKET	0

Notes:

1. The HI-TRAC VW for MPC-37 is the designated HI-TRAC for all PWR MPCs (MPC-37, MPC-32ML, and MPC-31C).

CHAPTER 2 CHANGED PAGES

To achieve compliance with the above criteria, certain design and operational changes are necessary, as summarized below.

i. The peak fuel cladding temperature limit (PCT) for long term storage operations and short term operations is generally set at 400ºC (752ºF). However, for MPCs containing all moderate burnup fuel, the fuel cladding temperature limit for short-term operations is set at 570ºC (1058ºF) because the nominal fuel cladding stress is shown to be less than 90 MPa [2.0.2]. Appropriate analyses have been performed as discussed in Chapter 4 and operating restrictions have been added to ensure these limits are met.

ii. A method of drying, such as forced helium dehydration (FHD) is used if the above temperature limits for short-term operations cannot be met.

iii. The off-normal and accident condition PCT limit remains unchanged at 570 ºC (1058ºF).

The MPC cavity is dried, either with FHD or vacuum drying, and then it is backfilled with high purity helium to promote heat transfer and prevent cladding degradation.

The normal condition design temperatures for the stainless steel components in the MPC are provided in Table 2.2.3.

~~Each~~ The MPC-37 and MPC-89 models allow~~s~~ for regionalized storage where the basket is segregated into three regions as shown in Figures 1.2.1a and 1.2.2. Decay heat limits for regionalized loading are presented in Tables 1.2.3a and 1.2.4 for MPC-37 and MPC-89 respectively. Specific requirements, such as approved locations for DFCs and non-fuel hardware are given in Section 2.1.

Shielding

The dose limits for an ISFSI using the HI-STORM FW System are delineated in 10CFR72.104 and 72.106. Compliance with these regulations for any particular array of casks at an ISFSI is necessarily site-specific and must be demonstrated by the licensee. Dose for a single cask and a representative cask array is illustrated in Chapter 5.

The MPC provides axial shielding at the top and bottom ends to maintain occupational exposures ALARA during canister closure and handling operations. The HI-TRAC VW bottom lid also contains shielding. The occupational doses are controlled in accordance with plant-specific procedures and ALARA requirements (discussed in Chapter 9).

The dose evaluation is performed for a reference fuel (Table 1.0.4) as described in Section 5.2. Calculated dose rates for each MPC are provided in Section 5.1. These dose rates are used to perform an occupational exposure (ALARA) evaluation, as discussed in Chapter 11.

Criticality

The MPC provides criticality control for all design basis normal, off-normal, and postulated accident conditions, as discussed in Section 6.1. The effective neutron multiplication factor is limited to $k_{eff} < 0.95$ for fresh (unirradiated) fuel with optimum water moderation and close reflection, including all biases, uncertainties, and manufacturing tolerances.

Criticality control is maintained by the geometric spacing of the fuel assemblies and the spatially distributed B-10 isotope in the Metamic-HT fuel basket, and for the PWR MPC model, the additional soluble boron in the MPC water or use of burnup credit. The minimum specified boron concentration in the purchasing specification for Metamic-HT must be met in every lot of the material manufactured. The guaranteed B-10 value in the neutron absorber, assured by the manufacturing process, is further reduced by 10% (90% credit is taken for the Metamic-HT) to accord with NUREG/CR-5661. No credit is taken for fuel burnup or integral poisons such as gadolinia in BWR fuel. However, a partial gadolinium credit is taken to qualify certain BWR fuel delineated in Section 2.1 with a greater maximum fuel enrichment limit, as defined in Table 2.1.3. For PWR fuel, the soluble boron concentration requirements or burnup requirements based on the initial enrichment of the fuel assemblies are delineated in Section 2.1 consistent with the criticality analysis described in Chapter 6.

Confinement

The MPC provides for confinement of all radioactive materials for all design basis normal, off-normal, and postulated accident conditions. As discussed in Section 7.1, the HI-STORM FW MPC design meets the guidance in Interim Staff Guidance (ISG)-18 so that leakage of radiological matter from the confinement boundary is non-credible. Therefore, no confinement dose analysis is required or performed. The confinement function of the MPC is verified through pressure testing, helium leak testing of the MPC shell, base plate, and lid material along with the shell to base plate and shell to shell seam welds, and a rigorous weld examination regimen executed in accordance with the acceptance test program in Chapter 10.

Operations

There are no radioactive effluents that result from storage or transfer operations. Effluents generated during MPC loading are handled by the plant's radioactive waste system and procedures.

Generic operating procedures for the HI-STORM FW System are provided in Chapter 9. Detailed operating procedures will be developed by the licensee using the information provided in Chapter 9 along with the site-specific requirements that comply with the 10CFR50 Technical Specifications for the plant, and the HI-STORM FW System Certificate of Compliance (CoC).

Acceptance Tests and Maintenance

Table 2.0.9 – MPC-32ML Enclosure Vessel (Drawing # 10464)		
Item Number*	Part Name	ITS QA Safety Category
1	Shell, Enclosure Vessel	A
2	Plate, Enclosure Vessel Base	A
3	Plate, Enclosure Vessel Lower Lid	B
4	Plate, Enclosure Vessel Upper Lid	A
5	Ring, Enclosure Vessel Closure	A
6	Plate, Enclosure Vessel Lift Lug	C
8	Block, Enclosure Vessel Vent/Drain Upper	B
9	Block, Enclosure Vessel Lower Drain Shield	C
10	Block, Enclosure Vessel Lower Vent Shield	C
11	Port, Enclosure Vessel Vent/Drain	C
12	Plug, Enclosure Vessel Vent /Drain	C
16	Purge Tool Port Plug	C
18	Plate, Enclosure Vessel Vent/Drain Port Cover	A

*Item Numbers are non-consecutive because they are consistent with Parts List on drawing.

Table 2.0.10 – Assembly, MPC-32ML Fuel Basket (Drawing # 10457)		
Item Number	Part Name	ITS QA Safety Category
1	Panel, Type 1 Cell Wall	A
2	Panel, Type 2 Cell Wall	A
3	Panel, Type 3 Cell Wall	A
4	Panel, Type 4 Cell Wall	A
5	Basket Shim, Type 1	C
6	Basket Shim, Type 2	C
7	Basket Shim, Type 3	C

Table 2.0.11 – MPC-31C Enclosure Vessel (Drawing # 10465)		
Item Number*	Part Name	ITS QA Safety Category
1	Shell, Enclosure Vessel	A
2	Plate, Enclosure Vessel Base	A
3	Plate, Enclosure Vessel Lower Lid	B
4	Plate, Enclosure Vessel Upper Lid	A
5	Ring, Enclosure Vessel Closure	A
6	Plate, Enclosure Vessel Lift Lug	C
8	Block, Enclosure Vessel Vent/Drain Upper	B
9	Block, Enclosure Vessel Lower Drain Shield	C
10	Block, Enclosure Vessel Lower Vent Shield	C
11	Port, Enclosure Vessel Vent/Drain	C
12	Plug, Enclosure Vessel Vent /Drain	C
16	Purge Tool Port Plug	C
18	Plate, Enclosure Vessel Vent/Drain Port Cover	A

*Item Numbers are non-consecutive because they are consistent with Parts List on drawing.

Table 2.0.12 – Assembly, MPC-31C Fuel Basket (Drawing # 10462)		
Item Number	Part Name	ITS QA Safety Category
1	Panel, Type 1 Cell Wall	A
2	Panel, Type 2 Cell Wall	A
3	Panel, Type 3 Cell Wall	A
4	Panel, Type 4 Cell Wall	A
5	Panel, Type 5 Cell Wall	A
6	Panel, Type 6 Cell Wall	A
7	Panel, Type 7 Cell Wall	A
8	Panel, Type 8 Cell Wall	A
9	Panel, Type 9 Cell Wall	A
10	Basket Shim, Type 1	C
11	Basket Shim, Type 2	C
12	Basket Shim, Type 3	C

The design basis dose rates can be met by a variety of burnup levels and cooling times. Table 2.1.1 provides the acceptable ranges of burnup, enrichment and cooling time for all of the authorized fuel assembly array/classes. Table 2.1.5 and Figures 2.1.3 and 2.1.4 provide the axial distribution for the radiological source terms for PWR and BWR fuel assemblies based on the axial burnup distribution. The axial burnup distributions are representative of fuel assemblies with the design basis burnup levels considered. These distributions are used for analyses only, and do not provide a criteria for fuel assembly acceptability for storage in the HI-STORM FW System.

Non-fuel hardware, as defined in the Glossary, has been evaluated and is also authorized for storage in the PWR MPCs as specified in Table 2.1.1.

2.1.7 Criticality Parameters for Design Basis SNF

Criticality control during loading of the MPC-37 is achieved through either meeting the soluble boron limits in Table 2.1.6 OR verifying that the assemblies meet the minimum burnup requirements in Table 2.1.7. Criticality control during loading of the MPC-32ML is achieved through meeting the soluble boron limits in Table 2.1.6.

Criticality control during loading of certain BWR fuel with a greater maximum fuel enrichment limit, as seen in Table 2.1.3, is achieved through meeting the criteria of Table 2.1.9.

For those spent fuel assemblies that need to meet the burnup requirements specified in Table 2.1.7, a burnup verification shall be performed in accordance with either Method A OR Method B described below.

Method A: Burnup Verification Through Quantitative Burnup Measurement

For each assembly in the MPC-37 where burnup credit is required, the minimum burnup is determined from the burnup requirement applicable to the loading configuration chosen for the cask (see Table 2.1.7). A measurement is then performed that confirms that the fuel assembly burnup exceeds this minimum burnup. The measurement technique may be calibrated to the reactor records for a representative set of assemblies. The assembly burnup value to be compared with the minimum required burnup should be the measured burnup value as adjusted by reducing the value by a combination of the uncertainties in the calibration method and the measurement itself.

Method B: Burnup Verification Through an Administrative Procedure and Qualitative Measurements

Depending on the location in the basket, assemblies loaded into a specific MPC-37 can either be fresh, or have to meet a single minimum burnup value. The assembly burnup value to be compared with the minimum required burnup should be the reactor record burnup value as adjusted by reducing the value by the uncertainties in the reactor record value. An administrative procedure shall be established that prescribes the following steps, which shall be performed for each cask loading:

Table 2.1.1a

MATERIAL TO BE STORED

PARAMETER	VALUE	
	MPC-37	MPC-89
Fuel Type	Uranium oxide undamaged fuel assemblies, damaged fuel assemblies, and fuel debris meeting the limits in Table 2.1.2 for the applicable array/class.	Uranium oxide undamaged fuel assemblies, damaged fuel assemblies, with or without channels, fuel debris meeting the limits in Table 2.1.3 for the applicable array/class.
Cladding Type	ZR (see Glossary for definition)	ZR (see Glossary for definition)
Maximum Initial Rod Enrichment	Depending on soluble boron levels or burnup credit and assembly array/class as specified in Table 2.1.6 and Table 2.1.7.	≤ 5.0 wt. % U-235
Post-irradiation cooling time and average burnup per assembly	Minimum Cooling Time: 3 years Maximum Assembly Average Burnup: 68.2 GWd/mtU	Minimum Cooling Time: 3 years Maximum Assembly Average Burnup: 65 GWd/mtU
Non-fuel hardware post-irradiation cooling time and burnup	Minimum Cooling Time: 3 years Maximum Burnup†: - BPRAs, WABAs and vibration suppressors: 60 GWd/mtU - TPDs, NSAs, APSRs, RCCAs, CRAs, CEAs, water displacement guide tube plugs and orifice rod assemblies: 630 GWd/mtU - ITTRs: not applicable	N/A
Decay heat per fuel storage location	Regionalized Loading: See Table 1.2.3	Regionalized Loading: See Table 1.2.4

† Burnups for non-fuel hardware are to be determined based on the burnup and uranium mass of the fuel assemblies in which the component was inserted during reactor operation. Burnup not applicable for ITTRs since installed post-irradiation.

Table 2.1.1a (continued) MATERIAL TO BE STORED		
PARAMETER	**VALUE**	
	MPC-37	MPC-89
Fuel Assembly Nominal Length (in.)	Minimum: (1) All except 15x15I‡: 157 (with NFH); (2) 15x15I: 149 (with NFH)§ Reference: 167.2 (with NFH) Maximum: 199.2 (with NFH and DFC)	Minimum: 171 Reference: 176.5 Maximum: 181.5 (with DFC)
Fuel Assembly Width (in.)	≤ 8.54 (nominal design)	≤ 5.95 (nominal design)
Fuel Assembly Weight (lb)	Reference: 1600 (without NFH) 1750 (with NFH), 1850 (with NFH and DFC) Maximum: 2050 (including NFH and DFC)	Reference: 750 (without DFC), 850 (with DFC) Maximum: 850 (including DFC)

‡ See Table 2.1.2 for 15x15I fuel assembly array/class characteristics.
§ Minimum nominal fuel assembly length for 15x15I fuel assembly array/class is 149". The unique design of 15x15I fuel requires a 1" nominal fuel shim to properly support the assembly. Therefore the minimum MPC cavity height for 15x15I fuel is based on 150" fuel length.

Table 2.1.1a (continued)

MATERIAL TO BE STORED

PARAMETER	VALUE	
	MPC-37	MPC-89
Other Limitations	▪ Quantity is limited to 37 undamaged ZR clad PWR fuel assemblies with or without non-fuel hardware. Up to 12 damaged fuel containers containing PWR damaged fuel and/or fuel debris may be stored in the locations denoted in Figure 2.1.1 with the remaining basket cells containing undamaged ZR fuel assemblies, up to a total of 37. ▪ One NSA. ▪ Up to 30 BPRAs. ▪ BPRAs, TPDs, WABAs, water displacement guide tube plugs, orifice rod assemblies, and/or vibration suppressor inserts, with or without ITTRs, may be stored with fuel assemblies in any fuel cell location. ▪ CRAs, RCCAs, CEAs, NSAs, and/or APSRs may be stored with fuel assemblies in fuel cell locations specified in Figure 2.1.5.	▪ Quantity is limited to 89 undamaged ZR clad BWR fuel assemblies. Up to 16 damaged fuel containers containing BWR damaged fuel and/or fuel debris may be stored in locations denoted in Figure 2.1.2 with the remaining basket cells containing undamaged ZR fuel assemblies, up to a total of 89.

Table 2.1.1b

MATERIAL TO BE STORED

PARAMETER	VALUE	
	MPC-32ML	MPC-31C
Fuel Type	Uranium oxide undamaged fuel assemblies, damaged fuel assemblies, and fuel debris meeting the limits in Table 2.1.2 for the 16x16D array/class only.	Uranium oxide undamaged fuel assemblies, damaged fuel assemblies, and fuel debris meeting the limits in Table 2.1.2 for the V10A and V10B array/class only.
Cladding Type	ZR (see Glossary for definition)	ZR (see Glossary for definition)
Maximum Initial Rod Enrichment	Depending on soluble boron levels and assembly array/class as specified in Table 2.1.6.	≤ 5.0 wt. % U-235
Post-irradiation cooling time and average burnup per assembly	Minimum Cooling Time: 3 years Maximum Assembly Average Burnup: 68.2 GWd/mtU	Minimum Cooling Time: 3 years Maximum Assembly Average Burnup: 60 GWd/mtU
Non-fuel hardware post-irradiation cooling time and burnup†	Minimum Cooling Time: 3 years Maximum Burnup: - BPRAs, WABAs and vibration suppressors: 60 GWd/mtU - TPDs, NSAs, APSRs, RCCAs, CRAs, CEAs, water displacement guide tube plugs and orifice rod assemblies: 630 GWd/mtU - ITTRs: not applicable	Minimum Cooling Time: 3 years Maximum Burnup: - BPRAs: 60 GWd/mtU - NSAs: 630 GWd/mtU
Decay heat per fuel storage location	Uniform Loading per Table 1.2.3b.	Uniform Loading per Table 1.2.3c.

† Burnups for non-fuel hardware are to be determined based on the burnup and uranium mass of the fuel assemblies in which the component was inserted during reactor operation. Burnup not applicable for ITTRs since installed post-irradiation.

Table 2.1.1b (continued)

MATERIAL TO BE STORED

PARAMETER	VALUE	
	MPC-32ML	MPC-31C
Fuel Assembly Nominal Length (in)	≤ 193 (including NFH and DFC)	≤ 179.9 (including NFH and DFC)
Fuel Assembly Width (in)	≤ 9.04 (nominal design)	≤ 9.213 (nominal design)
Fuel Assembly Weight (lb)	≤ 1858 (including DFC and NFH)	≤ 1650 (including DFC and NFH)

Table 2.1.1b (continued)

MATERIAL TO BE STORED

PARAMETER	VALUE	
	MPC-32ML	MPC-31C
Other Limitations	▪ Quantity is limited to 32 undamaged ZR clad PWR class 16x16D fuel assemblies with or without non-fuel hardware. Up to 8 damaged fuel containers containing class 16x16D PWR damaged fuel and/or fuel debris may be stored in the locations denoted in Figure 2.1.1b with the remaining basket cells containing undamaged ZR fuel assemblies, up to a total of 32. ▪ One NSA. ▪ BPRAs, TPDs, WABAs, water displacement guide tube plugs, orifice rod assemblies, and/or vibration suppressor inserts, with or without ITTRs, may be stored with fuel assemblies in any fuel cell location. ▪ CRAs, RCCAs, CEAs, NSAs, and/or APSRs may be stored with fuel assemblies in fuel cell locations specified in Figure 2.1.5b.	▪ Quantity is limited to 31 undamaged ZR clad PWR class V10A or V10B fuel assemblies with or without non-fuel hardware. Up to 6 damaged fuel containers containing PWR class V10A or V10B damaged fuel may be stored in the locations denoted in Figure 2.1.1c with the remaining basket cells containing undamaged ZR fuel assemblies, up to a total of 31. ▪ Up to 6 damaged fuel containers containing PWR fuel debris may be stored in the locations denoted in Figure 2.1.1c with the remaining basket cells containing undamaged ZR fuel assemblies. Basket cells containing fuel debris within DFCs shall be accompanied by an adjacent empty cell in the locations denoted in Figure 2.1.1c. ▪ One NSA. ▪ BPRAs may be stored with fuel assemblies in any fuel cell location. ▪ A NSA may be stored with a fuel assembly in one of the fuel cell locations specified in Figure 2.1.5c.

Table 2.1.2 (continued)

PWR FUEL ASSEMBLY CHARACTERISTICS (Note 1)

Fuel Assembly Array and Class	**16x16 A**	**16x16B**	**16x16 C**	**16x16 D (MPC-32ML Only)**
No. of Fuel Rod Locations	236	236	235	236
Fuel Clad O.D. (in.)	≥ 0.382	≥ 0.374	≥ 0.374	≥ 0.423
Fuel Clad I.D. (in.)	≤ 0.3350	≤ 0.3290	≤ 0.3290	≤ 0.366
Fuel Pellet Dia. (in.) (Note 3)	≤ 0.3255	≤ 0.3225	≤ 0.3225	≤ 0.359
Fuel Rod Pitch (in.)	≤ 0.506	≤ 0.506	≤ 0.485	≤ 0.563
Active Fuel length (in.)	≤ 150	≤ 150	≤ 150	≤ 154.5
No. of Guide and/or Instrument Tubes	5 (Note 2)	5 (Note 2)	21	20
Guide/Instrument Tube Thickness (in.)	≥ 0.0350	≥ 0.04	≥ 0.0157	≥ 0.015

Table 2.1.2 (continued)

PWR FUEL ASSEMBLY CHARACTERISTICS (Note 1)

Fuel Assembly Array and Class	**V10A (MPC-31C Only)**	**V10B (MPC-31C Only)**
No. of Fuel Rod Locations	311	312
Fuel Clad O.D. (in.)	≥ 0.358	≥ 0.358
Fuel Clad I.D. (in.)	≤ 0.304	≤ 0.304
Fuel Pellet Dia. (in.) (Note 5)	≤ 0.298	≤ 0.299
Fuel Rod Pitch (in.)	≤ 0.502	≤ 0.502
Active Fuel length (in.)	≤ 138.98	Active Core with Blanket Rods: ≤ 138.98 Upper Blanket with Blanket Rods: ≤ 1.46 Lower Blanket with Blanket Rods: ≤ 4.45 Without Blankets: ≤ 144.88
No. of Guide and/or Instrument Tubes	20	19
Guide/Instrument Tube Thickness (in.)	≥ 0.0395	≥ 0.0395

Notes:

1. All dimensions are design nominal values. Maximum and minimum dimensions are specified to bound variations in design nominal values among fuel assemblies within a given array/class.
2. Each guide tube replaces four fuel rods.
3. Annular fuel pellets are allowed in the top and bottom 12” of the active fuel length.
4. Assemblies have one Instrument Tube and eight Guide Bars (Solid ZR). Some assemblies have up to 16 fuel rods removed or replaced by Guide Tubes.
5. Annular fuel pellets are allowed along the entire active fuel length for V10A and V10B.

Table 2.1.3

BWR FUEL ASSEMBLY CHARACTERISTICS (Note 1)

Fuel Assembly Array and Class	**7x7 B**	**8x8 B**	**8x8 C**	**8x8 D**	**8x8 E**
Maximum Planar-Average Initial Enrichment (wt.% ^{235}U) (Note 14)	≤ 4.8	≤ 4.8	≤ 4.8	≤ 4.8	≤ 4.8
Maximum Planar-Average Initial Enrichment with Gadolinium Credit (wt.% ^{235}U) (Note 15)	-	-	-	-	-
No. of Fuel Rod Locations	49	63 or 64	62	60 or 61	59
Fuel Clad O.D. (in.)	≥ 0.5630	≥ 0.4840	≥ 0.4830	≥ 0.4830	≥ 0.4930
Fuel Clad I.D. (in.)	≤ 0.4990	≤ 0.4295	≤ 0.4250	≤ 0.4230	≤ 0.4250
Fuel Pellet Dia. (in.)	≤ 0.4910	≤ 0.4195	≤ 0.4160	≤ 0.4140	≤ 0.4160
Fuel Rod Pitch (in.)	≤ 0.738	≤ 0.642	≤ 0.641	≤ 0.640	≤ 0.640
Design Active Fuel Length (in.)	≤ 150	≤ 150	≤ 150	≤ 150	≤ 150
No. of Water Rods (Note 10)	0	1 or 0	2	1 - 4 (Note 6)	5
Water Rod Thickness (in.)	N/A	≥ 0.034	> 0.00	> 0.00	≥ 0.034
Channel Thickness (in.)	≤ 0.120	≤ 0.120	≤ 0.120	≤ 0.120	≤ 0.100

Table 2.1.3 (continued)

BWR FUEL ASSEMBLY CHARACTERISTICS (Note 1)

Fuel Assembly Array and Class	**8x8F**	**9x9 A**	**9x9 B**	**9x9 C**	**9x9 D**
Maximum Planar-Average Initial Enrichment (wt.% ^{235}U) (Note 14)	≤ 4.5 (Note 12)	≤ 4.8	≤ 4.8	≤ 4.8	≤ 4.8
Maximum Planar-Average Initial Enrichment with Gadolinium Credit (wt.% ^{235}U) (Note 15)	-	-	-	-	-
No. of Fuel Rod Locations	64	74/66 (Note 4)	72	80	79
Fuel Clad O.D. (in.)	≥ 0.4576	≥ 0.4400	≥ 0.4330	≥ 0.4230	≥ 0.4240
Fuel Clad I.D. (in.)	≤ 0.3996	≤ 0.3840	≤ 0.3810	≤ 0.3640	≤ 0.3640
Fuel Pellet Dia. (in.)	≤ 0.3913	≤ 0.3760	≤ 0.3740	≤ 0.3565	≤ 0.3565
Fuel Rod Pitch (in.)	≤ 0.609	≤ 0.566	≤ 0.572	≤ 0.572	≤ 0.572
Design Active Fuel Length (in.)	≤ 150	≤ 150	≤ 150	≤ 150	≤ 150
No. of Water Rods (Note 10)	N/A (Note 2)	2	1 (Note 5)	1	2
Water Rod Thickness (in.)	≥ 0.0315	> 0.00	> 0.00	≥ 0.020	≥ 0.0300
Channel Thickness (in.)	≤ 0.055	≤ 0.120	≤ 0.120	≤ 0.100	≤ 0.100

Table 2.1.3 (continued)

BWR FUEL ASSEMBLY CHARACTERISTICS (Note 1)

Fuel Assembly Array and Class	**9x9 E (Note 3)**	**9x9 F (Note 3)**	**9x9 G**	**10x10 A**	**10x10 B**
Maximum Planar-Average Initial Enrichment (wt.% ^{235}U) (Note 14)	≤ 4.5 (Note 12)	≤ 4.5 (Note 12)	≤ 4.8	≤ 4.8	≤ 4.8
Maximum Planar-Average Initial Enrichment with Gadolinium Credit (wt.% ^{235}U) (Note 15)	-	-	-	≤ 5.0	≤ 5.0
No. of Fuel Rod Locations	76	76	72	92/78 (Note 7)	91/83 (Note 8)
Fuel Clad O.D. (in.)	≥ 0.4170	≥ 0.4430	≥ 0.4240	≥ 0.4040	≥ 0.3957
Fuel Clad I.D. (in.)	≤ 0.3640	≤ 0.3860	≤ 0.3640	≤ 0.3520	≤ 0.3480
Fuel Pellet Dia. (in.)	≤ 0.3530	≤ 0.3745	≤ 0.3565	≤ 0.3455	≤ 0.3420
Fuel Rod Pitch (in.)	≤ 0.572	≤ 0.572	≤ 0.572	≤ 0.510	≤ 0.510
Design Active Fuel Length (in.)	≤ 150	≤ 150	≤ 150	≤ 150	≤ 150
No. of Water Rods (Note 10)	5	5	1 (Note 5)	2	1 (Note 5)
Water Rod Thickness (in.)	≥ 0.0120	≥ 0.0120	≥ 0.0320	≥ 0.030	> 0.00
Channel Thickness (in.)	≤ 0.120	≤ 0.120	≤ 0.120	≤ 0.120	≤ 0.120

Table 2.1.3 (continued)

BWR FUEL ASSEMBLY CHARACTERISTICS (Note 1)

Fuel Assembly Array and Class	**10x10 C**	**10x10 F**	**10x10 G**
Maximum Planar-Average Initial Enrichment (wt.% ^{235}U) (Note 14)	≤ 4.8	≤ 4.7 (Note 13)	≤ 4.6 (Note 12)
Maximum Planar-Average Initial Enrichment with Gadolinium Credit (wt.% ^{235}U) (Note 15)	< 5.0	< 5.0	< 5.0
No. of Fuel Rod Locations	96	92/78 (Note 7)	96/84
Fuel Clad O.D. (in.)	≥ 0.3780	≥ 0.4035	≥ 0.387
Fuel Clad I.D. (in.)	≤ 0.3294	≤ 0.3570	≤ 0.340
Fuel Pellet Dia. (in.)	≤ 0.3224	≤ 0.3500	≤ 0.334
Fuel Rod Pitch (in.)	≤ 0.488	≤ 0.510	≤ 0.512
Design Active Fuel Length (in.)	≤ 150	≤ 150	≤ 150
No. of Water Rods (Note 10)	5 (Note 9)	2	5 (Note 9)
Water Rod Thickness (in.)	≥ 0.031	≥ 0.030	≥ 0.031
Channel Thickness (in.)	≤ 0.055	≤ 0.120	≤ 0.060

Table 2.1.3 (continued)

BWR FUEL ASSEMBLY CHARACTERISTICS

NOTES:

1. All dimensions are design nominal values. Maximum and minimum dimensions are specified to bound variations in design nominal values among fuel assemblies within a given array/class.

2. This assembly is known as "QUAD+." It has four rectangular water cross segments dividing the assembly into four quadrants.

3. For the SPC 9x9-5 fuel assembly, each fuel rod must meet either the 9x9E or the 9x9F set of limits or clad O.D., clad I.D., and pellet diameter

4. This assembly class contains 74 total rods; 66 full length rods and 8 partial length rods.

5. Square, replacing nine fuel rods.

6. Variable.

7. This assembly contains 92 total fuel rods; 78 full length rods and 14 partial length rods.

8. This assembly class contains 91 total fuel rods; 83 full length rods and 8 partial length rods.

9. One diamond-shaped water rod replacing the four center fuel rods and four rectangular water rods dividing the assembly into four quadrants.

10. These rods may also be sealed at both ends and contain ZR material in lieu of water.

11. Not Used

12. When loading fuel assemblies classified as damaged fuel assemblies, all assemblies in the MPC are limited to 4.0 wt.% U-235.

13. When loading fuel assemblies classified as damaged fuel assemblies, all assemblies in the MPC are limited to 4.6 wt.% U-235.

14. In accordance with the definition of undamaged fuel assembly, certain assemblies may be limited to 3.3 wt.% U-235. When loading these fuel assemblies, all assemblies in the MPC are limited to 3.3 wt.% U-235.

15. The restrictions in Table 2.1.9 apply.

Table 2.1.6

Soluble Boron Requirements for MPC-37 and MPC-32ML Wet Loading and Unloading Operations

MPC	Array/Class	All Undamaged Fuel Assemblies		One or More Damaged Fuel Assemblies and/or Fuel Debris	
		Maximum Initial Enrichment $\leq$ 4.0 wt% ^{235}U (ppmb)	Maximum Initial Enrichment 5.0 wt% ^{235}U (ppmb)	Maximum Initial Enrichment $\leq$ 4.0 wt% ^{235}U (ppmb)	Maximum Initial Enrichment 5.0 wt% ^{235}U (ppmb)
MPC-37	All 14x14 and 16x16A, B, C	1,000	1,600	1,300	1,800
	All 15x15 and 17x17	1,500	2,000	1,800	2,300
MPC-32ML	16x16D	1,500	2,000	1,600	2,100

Note:

1. For maximum initial enrichments between 4.0 wt% and 5.0 wt% ^{235}U, the minimum soluble boron concentration may be determined by linear interpolation between the minimum soluble boron concentrations at 4.0 wt% and 5.0 wt% ^{235}U.
2. If burnup credit is used (as described in Section 2.1.7), these soluble boron requirements do not apply.

TABLE 2.1.9

RESTRICTIONS FOR GADOLINIUM CREDIT

Fuel Assembly Array and Class	**Restriction**
All 10x10	The Gd rod loading is not less than 3.0 wt% Gd_2O_3;
All 10x10	The Gd rods located in the peripheral row of the fuel lattice cannot be credited
10x10A, 10x10B, and 10x10F	At least one Gd rod is required.
10x10C and 10x10G	Not less than two Gd rods are required.

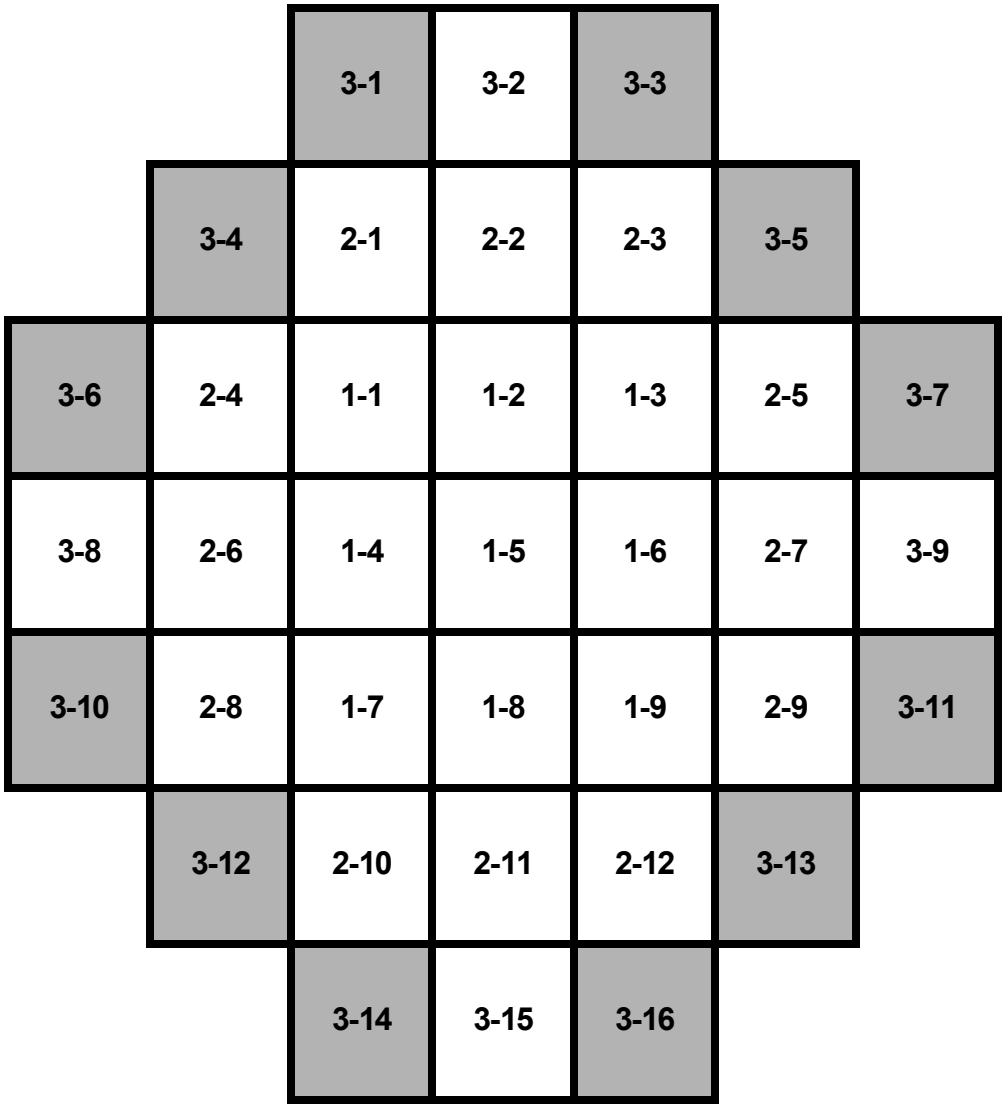

Figure 2.1.1a Location of DFCs for Damaged Fuel or Fuel Debris in the MPC-37(Shaded Cells)

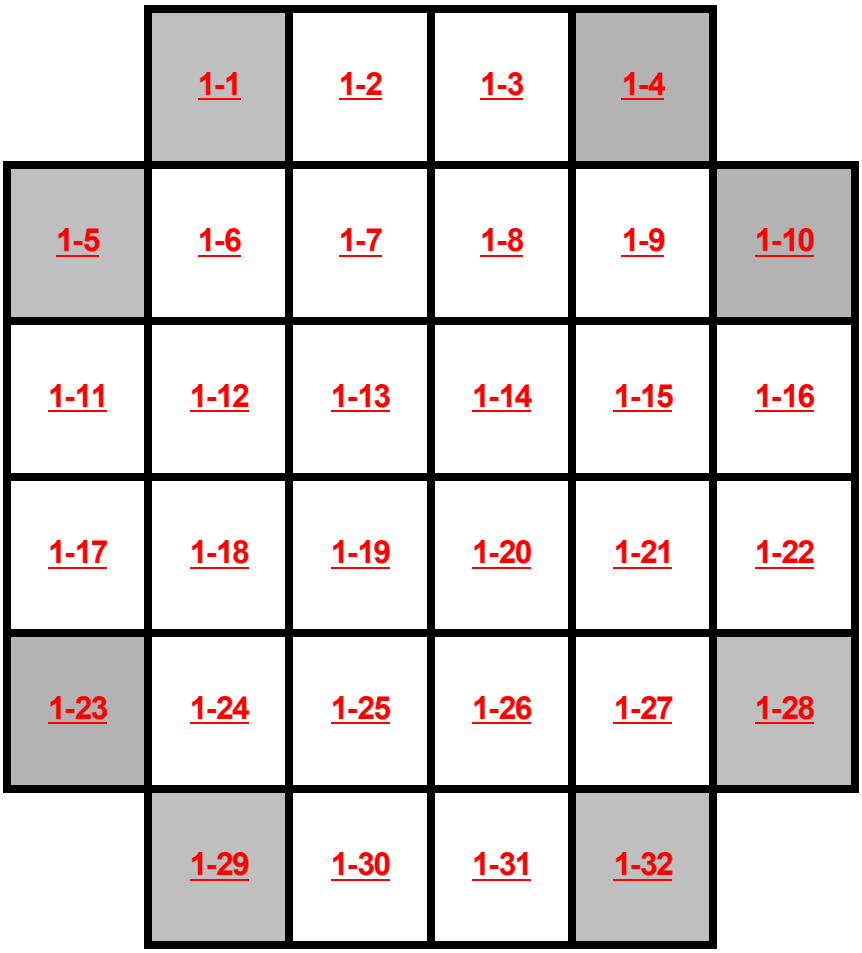

Figure 2.1.1b Location of DFCs for Damaged Fuel or Fuel Debris in the MPC-32ML (Shaded Cells)

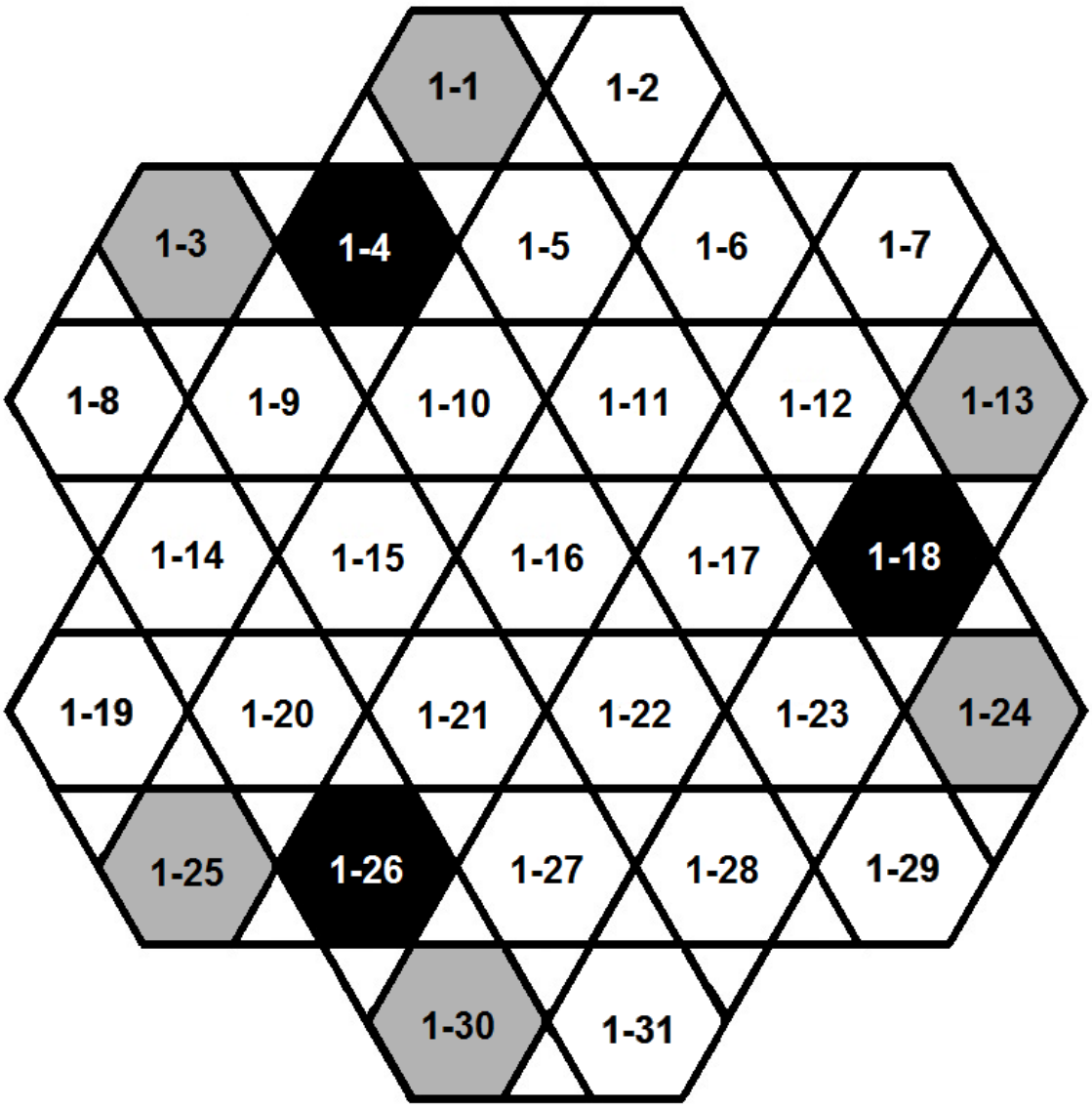

NOTE: Cells shaded in black must remain empty (i.e. are not permitted to store fuel) if an adjacent cell contains Fuel Debris.

Figure 2.1.1c Location of DFCs for Damaged Fuel or Fuel Debris in the MPC-31C (Gray Shaded Cells)

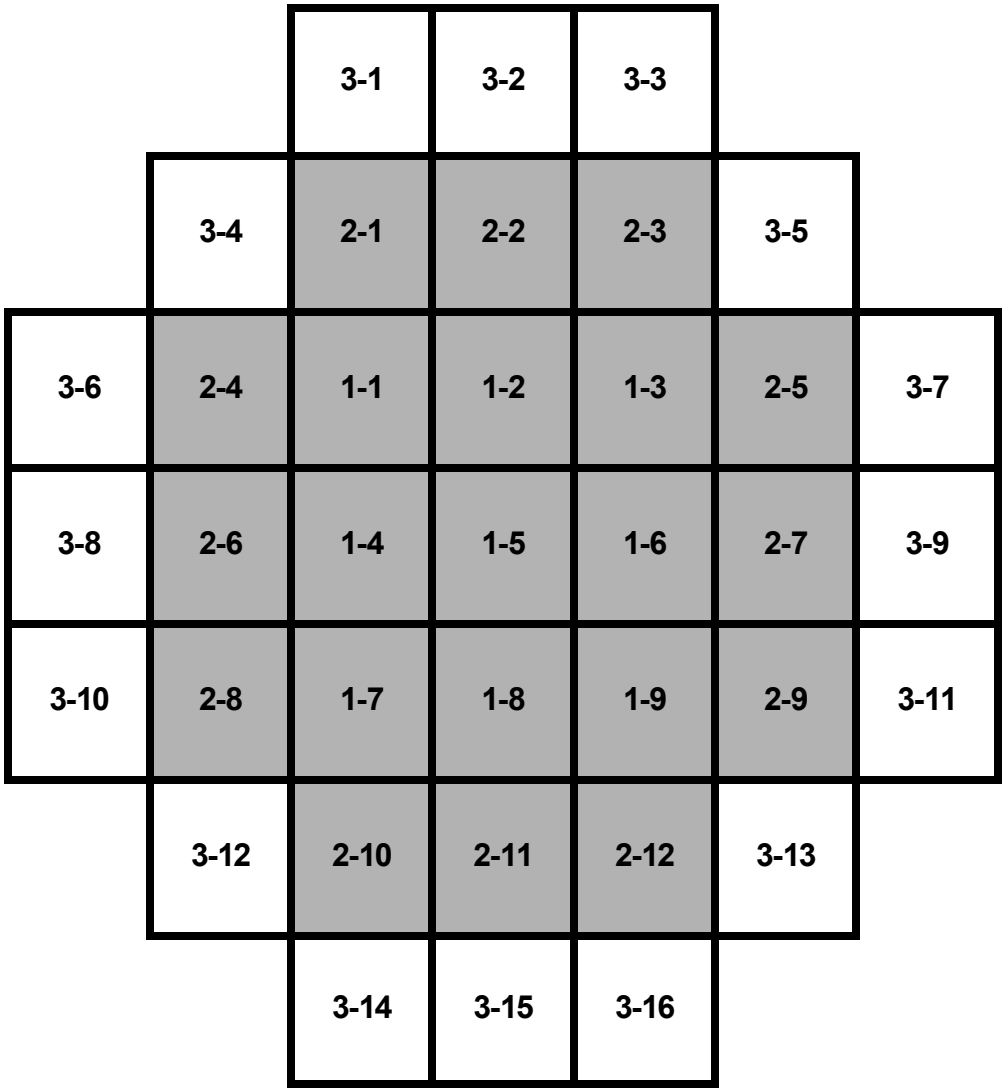

Figure 2.1.5a: Location of NSAs, APSRs, RCCAs, CEAs, and CRAs in the MPC-37 (Shaded Cells)

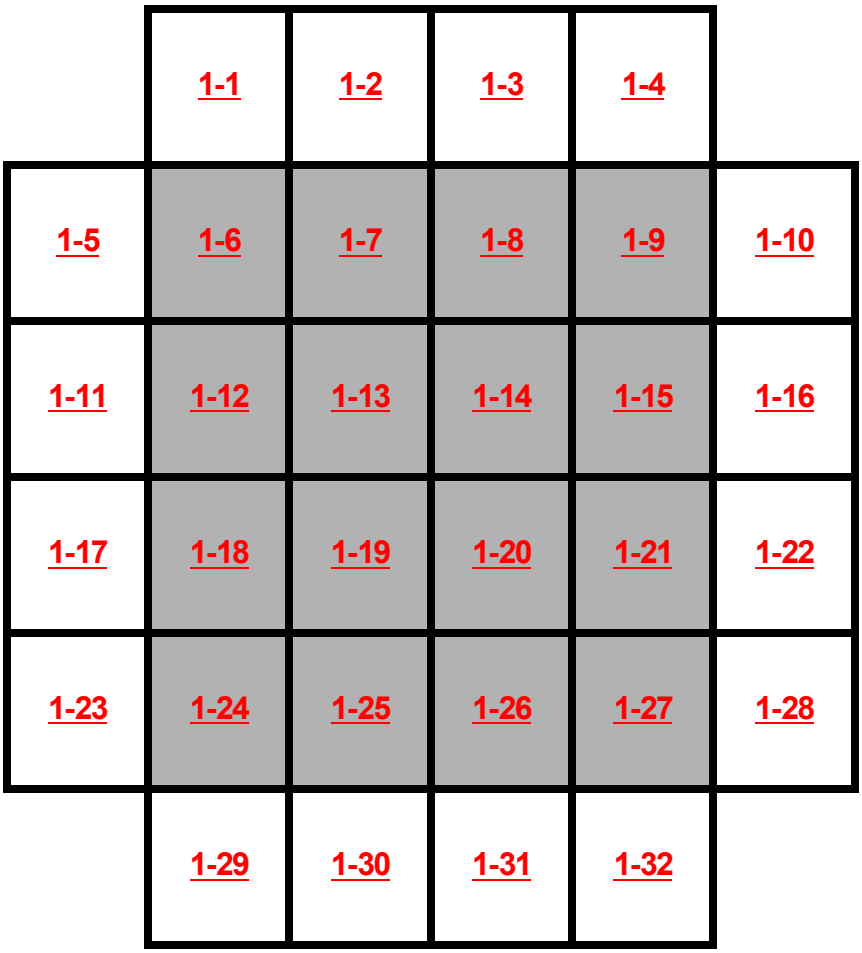

Figure 2.1.5b: Location of NSAs, APSRs, RCCAs, CEAs, and CRAs in the MPC-32ML (Shaded Cells)

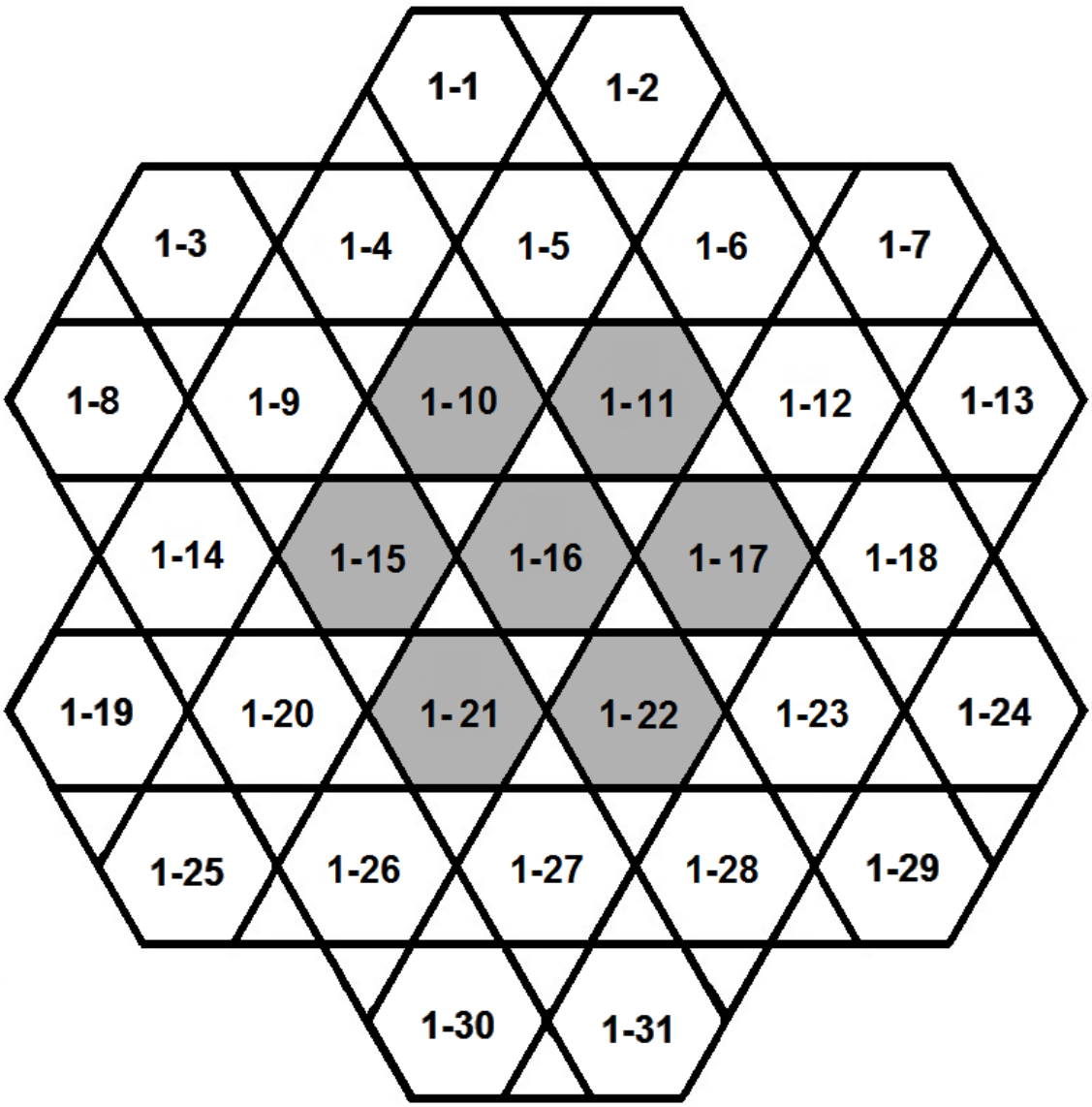

Figure 2.1.5c: Location of NSA in the MPC-31C (Shaded Cell)

Withheld in Accordance with 10 CFR 2.390

Figure 2.1.6: Damaged Fuel Container (Typical)

Table 2.2.1

DESIGN PRESSURES

Pressure Location	Condition	Pressure (psig)
MPC Internal Pressure	Normal	100
	Short-Term Operations	115
	Off-Normal~~/Short-Term~~	120
	Accident	200
MPC External Pressure	Normal	(0) Ambient
	Off-Normal/Short-Term	(0) Ambient
	Accident	55
HI-TRAC Water Jacket Internal Pressure	Accident	65
Overpack External Pressure	Normal	(0) Ambient
	Off-Normal/Short-Term	(0) Ambient
	Accident	See Paragraph 3.1.2.1.d

CHAPTER 3 CHANGED PAGES

- The MPC basket is separated from its lateral supports (basket shims) by a small, calibrated gap designed to prevent thermal stressing associated with the thermal expansion mismatches between the fuel basket and the basket support structure. The gap is designed to ensure that the basket remains unconstrained when subjected to the thermal heat generated by the spent nuclear fuel.

The MPC fuel basket maintains the spent nuclear fuel in a subcritical arrangement. Its safe operation is assured by maintaining the physical configuration of the storage cell cavities intact in the aftermath of a non-mechanistic tipover event. This requirement is satisfied if the MPC fuel basket plates undergo a minimal deflection (see Table 2.2.11). The fuel basket strains are shown in Subsection 3.4.4.1.4 to remain ~~essentially~~ largely elastic with only localized areas of plastic strain. Moreover, from the simulation results it is demonstrated that the cross-section of the storage cell, throughout the active fuel length, remains essentially unchanged. ~~, and, t~~Therefore, there is no impairment in the recoverability or retrievability of the fuel and the subcriticality of the stored fuel is unchallenged.

The MPC Confinement Boundary contains no valves or other pressure relief devices. In addition, the analyses presented in Subsections 3.4.3, 3.4.4.1.5, and 3.4.4.1.6 show that the MPC Enclosure Vessel meets the stress intensity criteria of the ASME Code, Section III, Subsection NB for all service conditions. Therefore, the demonstration that the MPC Enclosure Vessel meets Subsection NB stress limits ensures that there will be no discernible release of radioactive materials from the MPC.

(ii) Storage Overpack

The HI-STORM FW storage overpack is a steel cylindrical structure consisting of inner and outer low carbon steel shells, a lid, and a baseplate. Between the two shells is a thick cylinder of un-reinforced (plain) concrete. Plain concrete is also installed in the lid to minimize skyshine. The storage overpack serves as a missile and radiation barrier, provides flow paths for natural convection, provides kinematic stability to the system, and acts as a shock absorber for the MPC in the event of a postulated tipover accident. The storage overpack is not a pressure vessel since it contains cooling vents. The structural steel weldment of the HI-STORM FW overpack is designed to meet the stress limits of the ASME Code, Section III, Subsection NF, Class 3 for normal and off-normal loading conditions and Regulatory Guide 3.61 for handling conditions.

As discussed in Chapters 1 and 2, the principal shielding material utilized in the HI-STORM FW overpack is plain concrete. The plain concrete in the HI-STORM FW serves a structural function only to the extent that it may participate in supporting direct compressive or punching loads. The allowable compression/bearing resistance is defined and quantified in ACI-318-05 [3.3.5]. Strength analyses of the HI-STORM FW overpack and its confined concrete have been carried out in Subsections 3.4.4.1.3 and 3.4.4.1.4 to show that the concrete is able to perform its radiation protection function and that retrievability of the MPC subsequent to any postulated accident condition of storage or handling is maintained.

bottom edges are assumed to be pinned and the lateral edges are assumed to be free to minimize the permissible buckling load (a particularly severe modeling artifice to minimize buckling strength). The Euler buckling load for this geometry is given by (see Timoshenko et al., "Theory of Elastic Stability", 2nd Edition):

$$P_{cr} = \frac{\pi^2 EI}{h^2} = 125.2lbf$$

where E = Young's Modulus of Metamic-HT at 500ºC = 3,300 ksi,
I = moment of inertia of 8.94" wide by 0.59" thick plate = 0.153 in^4,
h = maximum height of fuel basket = 199.5"

The corresponding compressive axial stress is given by:

$$\sigma_{cr} = \frac{P_{cr}}{A} = \frac{125.2lbf}{(8.94in)(0.59in)} = 23.7psi$$

The factor of safety against buckling is given by (where σ_b is the compressive stress in the basket due to ~~self-weight~~self-weight):

$$SF = \frac{\sigma_{cr}}{\sigma_b} = \frac{23.7psi}{19.5psi} = 1.21$$

Thus, even with an exceedingly conservative model, the safety margin against buckling is more than 20%.

Therefore, buckling is ruled out as a credible failure mechanism in the HI-STORM FW system components. Nevertheless, a Design Basis Load consisting of external pressure is specified in Table 2.2.1 with the (evidently, non-mechanistic) conservative assumption that the internal pressure, which will counteract buckling behavior, is zero psig. (In reality, internal pressure cannot be zero because of the positive helium fill pressure established at the time of canister backfill.)

3.1.2.7 Consideration of Manufacturing and Material Deviations

Departure from the assumed values of material properties in the safety analyses clearly can have a significant effect on the computed margins. Likewise, the presence of deviations in manufacturing that inevitably occur in custom fabrication of capital equipment may detract from the safety factors reported in this chapter. In what follows, the method and measures adopted to insure that deviations in material properties or in the fabricated hardware will not undermine the structural safety conclusions are summarized.

That the yield and ultimate strengths of materials used in manufacturing the HI-STORM FW

archived in the Calculation Packages [3.4.11, 3.4.13] within the Company's Configuration Control System. Essential portions of the results for each loading case necessary to draw safety conclusions are extracted from the Calculation Packages and reported in this FSAR. Specifically, the results summarized from the finite element solutions in this chapter are self-contained to enable an independent assessment of the system's safety. Input data is provided in tabular form as suggested in ISG-21. For consistency, the following units are employed to document input data throughout this chapter:

- Time: second
- Mass: pound
- Length: inch

3.1.3.1 HI-STORM FW Overpack

The physical geometry and materials of construction of the HI-STORM FW overpack are provided in Sections 1.1 and 1.2 and the drawings in Section 1.5. The finite element simulation of the overpack consists of two discrete models, one for the overpack body and the other for the top lid.

The models are initially developed using the finite element code ANSYS [3.4.1], and then, depending on the load case, numerical simulations are performed either in ANSYS or in LS-DYNA [3.1.8]. For example, the handling loads (Load Case 9) and the snow load (Load Case 10) are simulated in ANSYS, and the non-mechanistic tipover event (Load Case 4) is simulated in LS-DYNA. For the non-mechanistic tipover analysis, ~~two~~ four distinct finite element models are ~~created~~developed with HI-STORM FW overpack carrying the maximum length MPC-37 (see Figure 3.4.10A) and the maximum length MPC-89 (see Figure 3.4.10B), as well as the MPC-32ML and the MPC-31C. The overpack FE model for the MPC-32ML and the MPC-31C is same as that for the MPC-37. This conservatively maximizes the weight and the angular velocity of the overpack for the non-mechanistic tipover analysis.
~~: one for the HI-STORM FW overpack carrying the maximum length MPC-37 and one for the HI-STORM FW overpack carrying the maximum length MPC-89 (Figures 3.4.10A and 3.4.10B).~~

The key attributes of the HI-STORM FW overpack models (implemented in ANSYS) are:

i. The finite element discretization of the overpack is sufficiently detailed to accurately articulate the primary membrane and bending stresses as well as the secondary stresses at locations of gross structural discontinuity. The finite element layout of the HI-STORM FW overpack body and the top lid are pictorially illustrated in Figures 3.4.3 and 3.4.5, respectively. The overpack model consists of over 70,000 nodes and 50,000 elements, which exceed the number of nodes and elements in the HI-STORM 100 tipover model utilized in [3.1.4]. Table 3.1.11 summarizes the key input data that is used to create the finite element models of the HI-STORM FW overpack body and top lid.

ii. The overpack baseplate, anchor blocks, and the lid studs are modeled with SOLID45 elements. The overpack inner and outer shells, bottom vent shells, and the lifting ribs are modeled with SHELL63 elements. A combination of SOLID45, SHELL63, and SOLSH190 elements is used to model the steel components in the HI-STORM FW lid. These element types are well suited for the overpack geometry and loading conditions, and they have been used successfully in previous cask licensing applications [3.1.10, 3.3.2].

iii. All overpack steel members are represented by their linear elastic material properties (at 300ºF) based on the data provided in Section 3.3. The concrete material in the overpack body is not explicitly modeled. Its mass, however, is accounted for by applying a uniformly distributed pressure on the baseplate annular area between the inner and outer shells (see Figure 3.4.26). The plain concrete in the HI-STORM FW lid is explicitly modeled in ANSYS using SOLID65 elements along with the input parameters listed in Table 3.1.12.

iv. To implement the ANSYS finite element model in LS-DYNA, the SOLID45, SHELL63, and SOLSH190 elements are converted to solid, shell, and thick shell elements, respectively, in LS-DYNA. The SOLID65 elements used to model the plain concrete in the HI-STORM FW lid are replaced by MAT_PSEUDO_TENSOR (or MAT_016) elements in LS-DYNA. The plain concrete in the overpack body is also modeled in LS-DYNA using MAT_PSEUDO_TENSOR elements.

v. In LS-DYNA, all overpack steel members are represented by their applicable nonlinear elastic-plastic true stress-strain relationships. The methodology used for obtaining a true stress-strain curve from a set of engineering stress-strain data (e.g., strength properties from [3.3.1]) is provided in [3.1.9], which utilizes the following power law relation to represent the flow curve of metal in the plastic deformation region:

$$\sigma = K\varepsilon^{n}$$

where n is the strain-hardening exponent and K is the strength coefficient. Table 3.1.13 provides the values of K and n ~~that~~ which are subsequently used to model the behavior of the overpack steel materials in LS-DYNA. Further details of the development of the true stress-strain relations for these materials are found in [3.4.11]. The concrete material is modeled in LS-DYNA using a non-linear material model (i.e., MAT_PSEUDO_TENSOR or MAT_016) based on the properties listed in Section 3.3.

3.1.3.2 Multi-Purpose Canister (MPC)

The two constituent parts of the MPC, namely (i) the Enclosure Vessel and (ii) the Fuel Basket, are modeled separately. The model for the Enclosure Vessel is focused to quantify its stress and strain field under the various loading conditions. The model for the Fuel Basket is focused on characterizing its strain and displacement behavior during a non-mechanistic tipover event. For the non-mechanistic tipover analysis, ~~two~~ four distinct finite element models are created: one for the maximum length MPC-37 ~~and~~ , one for the maximum length MPC-89, one for the MPC-32ML, and

one for the MPC-31C. The finite element models for the MPC-37 and MPC-89 enclosure vessels are shown in Figures 3.4.11A and 3.4.11B, respectively. ~~(Figures 3.4.11 and 3.4.12).~~Note that the MPC-32ML and MPC-31C enclosure vessels, carrying the PWR fuel types, are identical to the MPC-37 except for the length. The finite element models for the fuel baskets, the fuel assemblies and the basket shims, for all four basket types are shown in Figures 3.4.12, 3.4.13 and 3.4.14, respectively.

The key attributes of the MPC finite element models (implemented in ANSYS) are:

i. The finite element layout of the Enclosure Vessel is pictorially illustrated in Figure 3.4.1. The finite element discretization of the Enclosure Vessel is sufficiently detailed to accurately articulate the primary membrane and bending stresses as well as the secondary stresses at locations of gross structural discontinuity, particularly at the MPC shell to baseplate juncture. This has been confirmed by comparing the ANSYS stress results with the analytical solution provided in [3.4.16] (specifically Cases 4a and 4b of Table 31) for the discontinuity stress at the junction between a cylindrical shell and a flat circular plate under internal pressure (100 psig). The two solutions agree within 3% indicating that the finite element mesh for the Enclosure Vessel is adequately sized. Table 3.1.14 summarizes the key input data that is used to create the finite element model of the Enclosure Vessel.

ii. The Enclosure Vessel shell, baseplate, and upper and lower lids are meshed using SOLID185 elements. The MPC lid-to-shell weld and the reinforcing fillet weld at the shell-to-baseplate juncture are also explicitly modeled using SOLID185 elements (see Figure 3.4.1).

iii. Consistent with the drawings in Section 1.5, the MPC lid is modeled as two separate plates, which are joined together along their perimeter edge. The upper lid is conservatively modeled as 4.5" thick, which is less than the minimum thickness specified on the licensing drawing (see Section 1.5). "Surface-to-surface" contact is defined over the interior interface between the two lid plates using CONTA173 and TARGE170 contact elements.

iv. The materials used to represent the Enclosure Vessel are assumed to be isotropic and are assigned linear elastic material properties based on the Alloy X material data provided in Section 3.3. The Young's modulus value varies throughout the model based on the applied temperature distribution, which is shown in Figure 3.4.27 and conservatively bounds the normal operating temperature distribution for the maximum length MPC-37 as determined by the thermal analyses in Chapter 4.

v. The fuel basket models (Figures 3.4.12A ~~and~~ , 3.4.12B, 3.4.12C and 3.4.12D), which are implemented in LS-DYNA, are assembled from intersecting plates per the licensing drawings in Section 1.5, include all potential contacts and allow for relative rotations between intersecting plates. ~~For conservatism, a bounding gap is assumed at contact interfaces between any two perpendicular basket plates to allow for impacts and, therefore, maximize the stress and deformation of the fuel basket plate.~~ The fuel basket plates are modeled in LS-DYNA using thick shell elements, which behave like solid elements in contact, but can also accurately simulate the bending behavior of the fuel basket plates. To ensure numerical

accuracy, full integration thick shell elements with 10 through-thickness integration points are used. This modeling approach is consistent with the approach taken in [3.1.10] to qualify the F-32 and F-37 fuel baskets.

vi. In LS-DYNA, the fuel basket plates are represented by their applicable nonlinear elastic-plastic true stress-strain relationships in the same manner as the steel members of the HI-STORM FW overpack (see Subsection 3.1.3.1). Table 3.1.13 provides the values of K and n ~~that~~ which are subsequently used to model the behavior of the fuel basket plates in LS-DYNA. Details of the development of the true stress-strain relations are found in [3.4.11].

3.1.3.3 HI-TRAC VW Transfer Cask

The stress analysis of the transfer cask addresses three performance features that are of safety consequence. They are:

i. Performance of the water jacket as a pressure retaining enclosure under an accident condition leading to overheating of water.
ii. Performance of the threaded anchor locations in the HI-TRAC VW top flange under the maximum lifted load.
iii. Performance of the HI-TRAC VW bottom lid under its own self weight plus the weight of the heaviest MPC.

The above HI-TRAC VW components are analyzed separately using strength of materials formula, the details of which are provided in Subsections 3.4.3 and 3.4.4.

Table 3.1.1

GOVERNING CASES AND AFFECTED COMPONENTS

Case	Loading Case I.D. from Tables 2.2.6, 2.2.7 and 2.2.13	Loading Event	Affected Components			Objective of the Analysis	For additional discussion, refer to Subsection
			HI-STORM	MPC	HI-TRAC		
1	AD	Moving Flood Moving Floodwater with loaded HI-STORM on the pad.	X	—	—	Determine the flood velocity that will not overturn the overpack.	2.2.3
2.	AE	Design Basis Earthquake (DBE) Loaded HI-STORMs arrayed on the ISFSI pad subject to ISFSI's DBE	X	X	—	Determine the maximum magnitude of the earthquake that meets the acceptance criteria of 2.2.3(g).	2.2.3
3	AC	Tornado Missile A large, medium or small tornado missile strikes a loaded HI-STORM on the ISFSI pad or HI-TRAC.	X	X	X	Demonstrate that the acceptance criteria of 2.2.3(e) will be met.	2.2.3
4	AA	Non-Mechanistic Tip-Over A loaded HI-STORM is assumed to tip over and strike the pad.	X	X	—	Satisfy the acceptance criteria of 2.2.3(b).	2.2.3
5	NB	Design Internal Pressure MPC under the normal condition Design Internal Pressure	—	X	—	Demonstrate that the MPC meets "NB" stress intensity limits.	2.2.1
6	NB	Maximum Internal Pressure Under the Accident Condition MPC under the accident condition internal pressure (from Table 2.2.1)	—	X	—	Demonstrate that the Level D stress intensity limits are met.	2.2.1

Table 3.1.1 (continued)

GOVERNING CASES AND AFFECTED COMPONENTS

Case	Loading Case I.D. from Tables 2.2.6, 2.2.7 and 2.2.13	Loading Event	Affected Components			Objective of the Analysis	For additional discussion, refer to Subsection
7	AH	Design External Pressure MPC under the accident condition external pressure (from Table 2.2.1)	—	X	—	The Enclosure Vessel must not buckle.	2.2.3
8	AJ	HI-TRAC Non-Mechanistic Heat-Up Postulate the water jacket's internal pressure reaches the Design Pressure (defined in Table 2.2.1)	—	—	X	Demonstrate that the stresses in the water jacket meet the ASME Code Section III Subsection Class 3 limits for the Design Condition.	2.2.1
9.	HA, HB, and HC	Handling of Components	X	X	X	Demonstrate that the tapped anchor locations (TALs) meet the Regulatory Guide 3.61 and NUREG-0612 stress limits (as applicable).	2.2.1
10.	NA	Snow Load	X	—	—	Demonstrate that the top lid's steel structure meets "NF" stress limit for normal condition.	2.2.1
11.	NA	MPC Reflood Event	—	X	—	Demonstrate that there is no breach of the fuel rod cladding.	12.3.1

3.2 WEIGHTS AND CENTERS OF GRAVITY

As stated in Chapter 1, while the diameters of the MPC, HI-STORM FW, and HI-TRAC VW are fixed, their height is dependent on the length of the fuel assembly. The MPC cavity height (which determines the external height of the MPC) is set equal to the nominal fuel length (along with control components, if any) plus Δ, where Δ is between 1.5" (minimum), 2.0" (maximum), Δ is increased above 1.5" so that the MPC cavity height is a full inch or half-inch number. Thus, for the PWR reference fuel (Table 1.0.4), whose length including control components is 167.2" (Table 2.1.1), Δ = 1.8" so that the MPC cavity height, c, becomes 169". Δ is provided to account for irradiation and thermal growth of the fuel in the reactor. Table 3.2.1 provides the height of the internal cavities and bottom-to-top external dimension of all system components. Table 3.2.2 provides the parameters that affect the weight of cask components and their range of values assumed in this FSAR.

The cavity heights of the HI-STORM FW overpack and the HI-TRAC VW transfer cask are set greater than the MPC height by fixed amounts to account for differential thermal expansion and manufacturing tolerances. Table 3.2.1 provides the height data on HI-STORM FW, HI-TRAC VW, and the MPC as the adder to the MPC cavity length.

Table 3.2.5 provides the reference weight of the HI-STORM FW overpack for storing MPC-37 and MPC-89 containing reference PWR and BWR fuel, respectively. Conservatively, the HI-STORM FW overpack storing MPC-32ML and MPC-31C, both carrying PWR fuel, use the same PWR reference weights listed in Table 3.2.5. The weight of the HI-STORM FW overpack body is provided for two discrete concrete densities and for two discrete heights for PWR and BWR fuel. The weight at any other density and any other height can be obtained by linear interpolation. Similarly the weight of the HI-STORM FW lid is provided for two discrete values of concrete density. The weight corresponding to any other density can be computed by linear interpolation.

As discussed in Section 1.2, the weight of the HI-TRAC VW transfer cask is maximized for a particular site to take full advantage of the plant's crane capacity within the architectural limitations of the Fuel Building. Accordingly, the thickness of the lead shield and outer diameter of the water jacket can be increased to maximize shielding. The weight of the empty HI-TRAC VW cask in Table 3.2.4 is provided for three lengths corresponding to PWR fuel. Using the data for three lengths, the transfer cask's weight corresponding to any other length can be obtained by linear interpolation (or extrapolation). For MPC-89, the weight data is provided for the minimum and reference fuel lengths, as well as the reference fuel assembly with a DFC and therefore likewise the transfer cask's weight corresponding to any other length can be obtained by linear interpolation (or extrapolation).

The approximate change in the empty weight of HI-TRAC VW (in kilo pounds) of a certain height, h (inch), by virtue of changing the thickness of the lead by an amount, δ (inch), is given by the formula:

$$\Delta W_{lead} = 0.1128(h - 13.5)\,\delta$$

Table 3.2.3

MPC WEIGHT DATA (COMPUTED NOMINAL VALUES)

Item	BWR Fuel Based on length below			PWR Fuel Based on length below (see Note 2)		
	Reference	Shortest from Table 3.2.2	Longest from Table 3.2.2	Reference	Shortest from Table 3.2.2	Longest from Table 3.2.2
Enclosure Vessel	27,500	27,100	27,800	28,600	25,600	31,100
Fuel Basket	8,600	8,300	8,800	7,900	7,000	9,400
Water in the MPC @ SG = 1 (See Note 1)	16,700	16,200	18,900	15,400	14,000	18,700
Water mass displaced by a closed MPC Enclosure Vessel (SG = 1)	30,800	29,900	31,600	29,300	26,600	34,500

SG = Specific Gravity

Notes 1: Water weight in the MPC assumes that water volume displaced by the fuel is equal to the fuel weight divided by an average fuel assembly density of 0.396 lb/in^3. The fuel weights used for calculating the fuel volumes for Reference/Shortest/Longest PWR and BWR fuel assemblies are 1750/1450/2050 and 750/700/850 pounds respectively.

2: Weight data for the MPC-32ML and the MPC-31C are bounded by values for the longest PWR fuel.

Table 3.2.4

HI-TRAC VW WEIGHT DATA (COMPUTED NOMINAL VALUES)

Item	BWR Fuel Based on length below			PWR Fuel Based on length below (see Note 1)		
	Reference	Shortest from Table 3.2.2	Longest from Table 3.2.2	Reference	Shortest from Table 3.2.2	Longest from Table 3.2.2
HI-TRAC VW Body (no Bottom Lid, water jacket empty)	84,000	81,700	86,200	85,200	78,000	99,600
HI-TRAC VW Bottom Lid	11,300	11,300	11,300	11,300	11,300	11,300
MPC with Basket	36,100	35,400	36,600	36,500	32,600	40,500
Fuel Weight (assume 50% with control components or channels, as applicable)	66,800 (750 lb per assembly average)	64,600 (725 lb per assembly average)	71,200 (800 lb per assembly average)	62,000 (1,675 lb per assembly average)	53,700 (1,450 lb per assembly average)	69,400 (1,875 lb per assembly average)
Water in the Annulus	600	600	600	600	600	700
Water in the Water Jacket	8,800	8,500	9,000	8,400	7,600	9,900
Displaced Water Mass by the Cask in the Pool (Excludes MPC)	18,900	18,400	19,400	18,600	17,500	21,600

Notes: 1: HI-TRAC VW weight data for the longest PWR fuel is bounding for the HI-TRAC carrying the MPC-32ML and MPC-31C.

~~Two~~ Four LS-DYNA finite element models are developed to simulate the postulated tipover event of HI-STORM FW storage cask with loaded MPC-37, ~~and~~ MPC-89, MPC-32ML and MPC-31C, respectively. The ~~two~~ four LS-DYNA models are constructed according to the dimensions specified in the licensing drawings included in Section 1.5; the tallest configuration for each MPC enclosure type is considered to ensure a bounding tipover analysis. Because of geometric and loading symmetries, a half model of the loaded cask and impact target (i.e., the ISFSI pad) is considered in the analysis. The LS-DYNA models of the HI-STORM FW overpack and the MPC are described in Subsections 3.1.3.1 and 3.1.3.2, respectively.

The ISFSI pad LS-DYNA model, which consists of a 320"×100"×36" concrete pad and the underlying subgrade (800"×275"×470" in size) with non-reflective lateral and bottom surface boundaries, is identical to that used in the HI-STORM 100 tipover analysis documented in the HI-STORM 100 FSAR [3.1.4]. All structural members of the loaded cask are explicitly modeled so that any violation of the acceptance criteria can be found by examining the LS-DYNA simulation results (note: the fuel assembly, which is not expected to fail in a tipover event, is modeled as an elastic rectangular body). This is an improvement compared with the approach taken in the HI-STORM 100 tipover analysis, where the loaded MPC was modeled as a cylinder and therefore the structural integrity of the MPC and fuel basket had to be analyzed separately based on the rigid body deceleration result of the cask. Except for the fuel basket, which is divided into four parts based on the temperature distribution of the basket, each structural member of the cask is modeled as an independent part in the LS-DYNA model. Note that the critical weld connection between the MPC shell and the MPC lid is treated as a separate part and modeled with solid elements. Each of the two LS-DYNA models consists of forty-two parts, which are discretized with sufficiently high mesh density; very fine grids are used in modeling the MPC enclosure vessel, especially in the areas where high stress gradients are expected (e.g., initial impact location with the overpack). To ensure numerical accuracy, full integration thin shell and thick shell elements with 10 though-thickness integration points or multi-layer solid elements are used. The LS-DYNA tipover model consists of over 470,000 nodes and 255,000 elements for HI-STORM FW with loaded MPC-37, and the model for the cask with loaded MPC-89 consists of over 689,000 nodes and 350,000 elements. The tipover model with loaded MPC-32ML consists of 464,200 nodes and 280,500 elements, and the model MPC-31C consists of over 346,900 nodes and 199,000 elements.

The same ISFSI concrete pad material model used for the HI-STORM 100 tipover analysis reported in [3.1.4] is repeated for the HI-STORM FW tipover analysis. Specifically, the concrete pad behavior is characterized using the same LS-DYNA material model (i.e., MAT_PSEUDO_TENSOR or MAT_016) as for the end drop and tipover analyses of the HI-STORM 100 storage cask (the only difference between the HI-STORM FW reference ISFSI concrete pad model and the model of the HI-STORM 100 Set B ISFSI concrete pad is thickness). Moreover, the subgrade is also conservatively modeled as an elastic material as before. Note that this ISFSI pad material modeling approach was originally taken in the USNRC approved storage cask tipover and end drop LS-DYNA analyses [3.4.5] where a good correlation was obtained between the analysis results and the test results.

To assess the potential damage of the cask caused by the tipover accident, an LS-DYNA nonlinear

material model with strain rate effect is used to model the responses of all HI-STORM FW cask structural members based on the true stress-strain curves of the corresponding materials. Note that the strain rate effect for the fuel basket material, i.e., Metamic HT, is not considered for conservatism.

Figures 3.4.9A throughe 3.4.9D14 depict the fourtwe finite-element tipover analysis models developed for the bounding HI-STORM FW cask configurations with loaded MPC-37, and MPC-89, MPC-32ML and MPC-31C, respectively.

As shown in Figure 3.4.15, the fuel basket does not experience significant plastic deformation in the active fuel region to exceed the acceptable limits; plastic deformation is essentially limited locally in cells near the top of the basket beyond the active fuel region for the both MPCMPC-37 and, MPC-89, MPC-32ML and MPC-31C baskets. Note that the basket corner welds are not considered in the tip-over analysis for conservatism.. The fuel basket is considered to be structurally safe since it can continue maintaining appropriate spacing between fuel assemblies after the tipover event. The MPC enclosure vessel experiences minor plastic deformation at the impact locations with the overpack guide tubes; the maximum local plastic strain (9.910.9%, see Figure 3.4.16) is well below the failure strain of the material and smaller than the plastic strain limit (i.e., at least 0.2 for stainless steel) recommended by [3.4.6] for ASME NB components. Similarly, local plastic deformation occurs in the overpack shear ring near the cask-to-pad impact location as shown in Figure 3.4.17. However, the shielding capacity of overpack will not be compromised by the tipover accident and there is no gross plastic deformation in the overpack inner shell to affect the retrievablilty of the MPC. In addition, the cask closure lid bolts are demonstrated to be structurally safe after the tipover event, only a negligibly small plastic strain is observed in the bolt near the impact location (see Figure 3.4.18). Therefore, the cask lid will not dislodge after the tipover event. Finally, Figures 3.4.19 and 3.4.20 present the deceleration time history results of the cask lid predicted by LS-DYNA. The peak rigid body decelerations, measured for the HI-STORM FW lid concrete, are shown to be 65.41.75 g's in the vertical direction and 19.316.71 g's in the horizontal direction, respectively. Note that the deceleration time histories are filtered using the LS-DYNA built-in Butterworth filter with a cut-off frequency of 350 Hz; the same filter was used for the HI-STORM 100 non-mechanistic tipover analysis [3.1.4].

The structural integrity of the HI-STORM FW lid cannot be ascertained from the LS-DYNA tipover analyses since some components of the lid, namely the lid outer shell and the lid gussets,gussets are defined as rigid members in order to simplify the modeling effort and maintain proper connectivity. Therefore, a separate tipover analysis has been performed for the HI-STORM FW lid using ANSYS, wherein a bounding peak rigid body deceleration established based on LS-DYNA tipover analysis results is statically applied to the lid. The finite element model is identical to the one used in Subsection 3.4.3 to simulate a vertical lift of the HI-STORM FW lid (Figure 3.4.5), except that the eight circumferential gussets are conservatively neglected (i.e., deleted from the finite element model).

The resulting stress distribution in the HI-STORM FW lid is shown in Figure 3.4.21. Per Subsection 2.2.3, the HI-STORM FW lid should not suffer any gross loss of shielding as a result of the non-

mechanistic tipover event. To satisfy this criterion, the primary membrane stresses in the lid components are compared against the material yield strength. The most heavily loaded component is the upper shim plate closest to the point of impact (Figure 3.4.21). In order to determine the primary membrane stress in the upper shim plate, the stresses are linearized along a path that follows the outside vertical edge of the upper shim plate (see Figure 3.4.21 for path definition). Figure 3.4.22 shows the linearized stress results. Since the membrane stress is less than the yield strength of the material at 300ºF (Table 3.3.6), it is concluded that the lid will not suffer any gross loss of shielding as a result of the non-mechanistic tipover event. The complete details of the lid tipover analysis are provided in [3.4.13].

Finally, to evaluate the potential for crack propagation and growth for the MPC fuel baskets under the non-mechanistic tipover event, a conservative crack propagation analysis is carried out for ~~both MPC-37 and MPC-89~~all of the fuel baskets using the same methodology utilized in Attachment D of [1.2.6] to evaluate the HI-STAR 180 F-37 fuel basket in support of the HI-STAR 180 SAR [3.1.10]. The crack propagation analysis is bounding since the maximum tensile strength of the basket material (28.2 ksi) documented in Table 1.2.8 is conservatively considered as the maximum tensile stress experienced by the Metamic fuel baskets in the tip-over accident and used as input to the following crack propagation analysis.

Per [1.2.6] the critical stress intensity factor of Metamic-HT panels is estimated to be

$$K_{IC} = 30ksi\sqrt{in}$$

based on Charpy V-notch absorbed energy (CVE) correlations for steels. The estimated value is consistent with the range for aluminum alloys, which is 20 to 50 $MPa\sqrt{m}$ or 18.2 to 45 $ksi\sqrt{in}$ per Table 3 of [3.4.19]. Next the minimum crack size, a_{min}, for crack propagation to occur is calculated below using the formula for a through-thickness edge crack given in [3.1.5]. Although the formula is derived for a straight-edge specimen, the use of the maximum tensile strength of the fuel basket material as the maximum tensile stress experienced by the basket well compensates for the geometric difference between the basket panel and the specimen. Moreover, the maximum size of a pre-existing crack (1/16") in the fuel basket panel is less than 1/5~~9~~th of the minimum basket panel thickness (0.~~59~~35"). Thus, the assumption of a through-thickness edge crack is very conservative. The result is

$$a_{\min} = \frac{\left(\frac{K_{IC}}{1.12\sigma_{\max}}\right)^2}{\pi} = \frac{\left[\frac{30ksi\sqrt{in}}{1.12(28.2ksi)}\right]^2}{\pi} = 0.287in$$

And the safety factor against crack propagation (based on a 1/16" minimum detectable flaw size) is

$$SF = \frac{a_{\min}}{a_{\det}} = \frac{0.287in}{0.0625in} = 4.595$$

3.4.4.1.11 Load Case 11: MPC Reflood Event

During a MPC reflood event, water is introduced to the MPC cavity through the lid drain line to cooldown the MPC internals and support fuel unloading. This quenching operation induces thermal stresses and strains in the fuel rod cladding, which are maximum at the boundary interface between the rising water and the dry (gaseous) cavity. The following analysis demonstrates that the maximum total strain in the fuel cladding due to the reflood event is well below the failure strain limit of the material. Thus, the fuel rod cladding will not be breached due to the MPC reflood event.

The analysis is carried out using the finite element code ANSYS [3.4.1]. The model, which is shown in Figure 3.4.37, is constructed using 4-node plastic large strain elements (SHELL43) based on the cladding dimensions of the PWR reference fuel type. The overall length of the model is equal to 30 times the outside diameter of the fuel cladding. As seen in Figure 3.4.37, the mesh size is reduced at the boundary between the wetted fuel rod and the dry fuel rod, where the highest stresses and strains occur. To account for the gas pressure inside the fuel rod, the top end of the fuel rod is fixed in the vertical direction, and an equivalent axial force is applied at the bottom end. A radial pressure is also applied to the inside surface of the fuel cladding (see Figure 3.4.38). The fuel cladding material is modeled as a bi-linear isotropic hardening material with temperature dependent properties. The key input data used to develop the finite element model are summarized in Table 3.4.14A.

The MPC reflood pressure, which is restricted to below the normal condition pressure limit, is too low to have anyd adverse effect on the fuel cladding. Moreover,~~,~~ the reflood water pressure acts to produce compressive hoop stresses which help reduce the tensile hoop stress (albeit by a small amount) from the internal gas pressure in the rods. Therefore, the MPC flooding pressure has no ~~harmful~~ adverse consequence to the fuel cladding and is neglected in the analysis.

At t = 0 sec, the uniform temperature throughout the entire fuel rod is set at 752ºF (400ºC), which equals the fuel cladding temperature limit under normal operating conditions. At t = 0.1 sec, the temperature assigned to the lower half of the fuel rod model is suddenly reduced to 80ºF to simulate the water quenching (see Figure 3.4.39). The resulting stress and strain distributions in the fuel rod are shown in Figures 3.4.40 and 3.4.41, respectively. The maximum stress and strain values are summarized in Table 3.4.15A. The maximum total strain in the fuel rod is well below the failure strain limit of 1.7% for the cladding material per [3.4.20]. In fact, the maximum stress and strain in the fuel rod remain in the elastic range.

The analysis described above makes a number of assumptions that significantly overstate the computed thru-wall strain in the fuel cladding. The major assumptions are:

1. Even though the peak cladding temperature occurs at a localized location, the fuel rod is modeled as a pressurized tube with closed ends at a uniform temperature that is greater than the maximum peak cladding temperature value reported in Chapter 4 when the MPC is in the HI-TRAC under the Design Basis heat load condition.
2. The rapid thermal straining of the pressurized tube (fuel rod) due to the quenching effect of water is simulated as a step transient wherein the temperature of the quenched portion of the

tube is assumed to drop down to the injected water temperature (assumed to be 80ºF) causing a step change in the cladding wall temperature in the longitudinal direction at its interface with the "dry" portion of the tube. This assumption is extremely conservative because in actuality the immersed portion of the fuel rod is blanketed by vapor which acts to retard the severity of the thermal transient.

3. Even though, as the rod is gradually immersed in water, the axial heat conduction will tend to cool the un-immersed portion of the tube thus reducing the ΔT at the quenched/dry interface, no credit for axial conduction is taken.
4. The cooling of the fuel rod by gradual immersion in the water has the beneficial effect of reducing the internal pressure (per the ideal gas law) and thus the magnitude of pressure induced stress in the fuel cladding. As the peak cladding temperature in the MPC is reached in the upper half of the fuel rods (see Chapter 4), a substantial amount of rod is cooled by water (as its level gradually rises inside the MPC) before the vulnerable zone (where the peak cladding temperature exists) is subjected to the thermal transient from quenching. No credit for this amelioration of the pressure stresses due to the gradual cooling of the rod is taken in the analysis.

The same analysis approach is repeated for the MPC-32ML and MPC-31C to reflect fuel rod geometries specific to these PWR fuel types. The geometric data, used in the re-flooding analysis, for these two fuel types is summarized in Table 3.4.14B. The governing results for the fuel types used in MPC-32ML and MPC-31C are presented in 3.4.15B. The governing stress and strains for the governing fuel rods are presented in Figures 3.4.42 and 3.4.43.

In summary, even though the analysis presented above is highly conservative, the maximum stress and strain in the fuel rod remain elastic. Moreover, the maximum strain is less than the failure strain limit by a factor of 6. Thus, the MPC reflood event will not cause a breach of the fuel rod cladding.

3.4.5 Cold

A discussion of the resistance to failure due to brittle fracture is provided in Subsection 3.1.2.

The value of the ambient temperature has two principal effects on the HI-STORM FW system, namely:

i. The steady-state temperature of all material points in the cask system will go up or down by the amount of change in the ambient temperature.

ii. As the ambient temperature drops, the absolute temperature of the contained helium will drop accordingly, producing a proportional reduction in the internal pressure in accordance with the Ideal Gas Law.

In other words, the temperature gradients in the system under steady-state conditions will remain the same regardless of the value of the ambient temperature. The internal pressure, on the other hand, will decline with the lowering of the ambient temperature. Since the stresses under normal storage

Assurance program assures competent compliance with the fabrication requirements.

- Use of materials with known characteristics, verified through rigorous inspection and testing, as described in Chapter 10, assures component compliance with design requirements.

- Use of welding procedures in full compliance with Section III of the ASME Code ensures high-quality weld joints.

Technical Specifications, as defined in Chapter 13, have been developed and imposed on the MPC that assure that the integrity of the MPC and the contained SNF assemblies are maintained throughout the 60-year design life of the MPC.

The principal design considerations bearing on the adequacy of the MPC for the service life are summarized below.

Corrosion

All MPC materials are fabricated from corrosion-resistant austenitic stainless steel and passivated aluminum. The corrosion-resistant characteristics of such materials for dry SNF storage canister applications, as well as the protection offered by these materials against other material degradation effects, are well established in the nuclear industry. The moisture in the MPC is removed to eliminate all oxidizing liquids and gases and the MPC cavity is backfilled with dry inert helium at the time of closure to maintain an atmosphere in the MPC that provides corrosion protection for the SNF cladding throughout the dry storage period. The preservation of this non-corrosive atmosphere is assured by the inherent sealworthiness of the MPC Confinement Boundary integrity (there are no gasketed joints in the MPC).

Structural Fatigue

The passive non-cyclic nature of dry storage conditions does not subject the MPC to conditions that might lead to structural fatigue failure. Ambient temperature and insolation cycling during normal dry storage conditions and the resulting fluctuations in MPC thermal gradients and internal pressure ~~is~~ are the only mechanism for fatigue. ~~These low-stress~~These low-stress, high-cycle conditions cannot lead to a fatigue failure of the MPC that is made from stainless alloy stock (endurance limit well in excess of 20,000 psi). All other off-normal or postulated accident conditions are infrequent or one-time occurrences, which cannot produce fatigue failures. Finally, the MPC uses materials that are not susceptible to brittle fracture.

Maintenance of Helium Atmosphere

The inert helium atmosphere in the MPC provides a non-oxidizing environment for the SNF cladding to assure its integrity during long-term storage. The preservation of the helium atmosphere in the MPC is assured by the robust design of the MPC Confinement Boundary described in Section 7.1. Maintaining an inert environment in the MPC mitigates conditions that might otherwise lead to

SNF cladding failures. The required mass quantity of helium backfilled into the canister at the time of closure and the associated fabrication and closure requirements for the canister are specifically set down to assure that an inert helium atmosphere is maintained in the canister throughout the 60-year design life.

Allowable Fuel Cladding Temperatures

The helium atmosphere in the MPC promotes heat removal and thus reduces SNF cladding temperatures during dry storage. In addition, the SNF decay heat will substantially attenuate over a 60-year dry storage period. Maintaining the fuel cladding temperatures below allowable levels during long-term dry storage mitigates the damage mechanism that might otherwise lead to SNF cladding failures. The allowable long-term SNF cladding temperatures used for thermal acceptance of the MPC design are conservatively determined, as discussed in Section 4.3.

Neutron Absorber Boron Depletion

The effectiveness of the fixed borated neutron absorbing material used in the MPC fuel basket design requires that sufficient concentrations of boron be present to assure criticality safety during worst case design basis conditions over the 60-year design life of the MPC. Information on the characteristics of the borated neutron absorbing material used in the MPC fuel basket is provided in Subsection 1.2.1 and Chapter 8. The relatively low neutron flux, to which this borated material is subjected and will continue to decay over time, does not result in significant depletion of the material's available boron to perform its intended safety function. In addition, the boron content of the material used in the criticality safety analysis is conservatively based on the minimum specified boron areal density (rather than the nominal), which is further reduced by 25% for analysis purposes, as described in Section 6.1. Analysis discussed in Section ~~6.3 demonstrates~~6.3 demonstrates that the boron depletion in the neutron absorber material is negligible over a 60-year duration. Thus, sufficient levels of boron are present in the fuel basket neutron absorbing material to maintain criticality safety functions over the 60-year design life of the MPC.

The above findings are consistent with those of the NRC's Waste Confidence Decision Review, which concluded that dry storage systems designed, fabricated, inspected, and operated in the manner of the requirements set down in this document are adequate for a 100-year service life, while satisfying the requirements of 10CFR72.

3.4.9 Design and Service Life

The discussion in the preceding sections seeks to provide the logical underpinnings for setting the design life of the storage overpacks, the HI-TRAC VW transfer cask, and the MPCs as sixty years. Design life, as stated earlier, is a lower bound value for the expected performance life of a component (service life). If operated and maintained in accordance with this Safety Analysis Report, Holtec International expects the service life of HI-STORM FW casks to substantially exceed their design life values.

Table 3.4.11

INPUT DATA USED FOR CALCULATING ANGULAR VELOCITY OF OVERPACK DURING NON-MECHANISTIC TIPOVER (LOAD CASE 4)

Item	Value
Maximum weight of loaded HI-STORM FW (W)	426,300 lbf[†]
Mid-height of maximum length HI-STORM FW (h)	119.75 in
Outer diameter of HI-STORM FW (d)	140 in
Distance between cask pivot point and cask center (r)	138.709 in
Mass moment of inertia of loaded HI-STORM FW about cask pivot point (I_A)	1.076×10^{10} lb-in^2
Note: The bounding parameters defined above are only used for computing the maximum angular velocity imparted during a tip over event involving the HI-STORM FW overpack along with its contents. Also, the term "h" represents the nominal height of the maximum length of the HI-STORM FW.	

[†] Bounds value in Table 3.2.8.

Table 3.4.14A

KEY INPUT DATA FOR FUEL ROD INTEGRITY ANALYSIS DURING MPC REFLOOD EVENT (LOAD CASE 11)

Item	Input Value	Source
Cladding Thickness (for reference PWR fuel), in	0.022	SAR Tables 1.0.4 and 2.1.2
Cladding OD (for reference PWR fuel), in	0.377	SAR Tables 1.0.4 and 2.1.2
Fuel Rod Pressure, psi	2,000	Ref. [3.4.24] (upper bound value)
Yield Strength of Zircaloy, psi	100,000 (at 80°F) 50,500 (at 750°F)	Ref. [3.4.21]
Tensile Strength of Zircaloy, psi	112,100 (at 80°F) 68,200 (at 750°F)	Ref. [3.4.21]
Elastic Modulus of Zircaloy, × 10^6 psi	13.42 (at 80°F) 10.4 (at 750°F)	Ref. [3.4.21]
Coefficient of Thermal Expansion of Zircaloy, × 10^{-6} in/in/°F	3.3 (at 80°F) 4.5 (at 750°F)	Ref. [3.4.22]
Poisson's Ratio of Zircaloy	0.4	Appendix C of Ref. [3.4.23]

Table 3.4.14B†

KEY INPUT DATA FOR MPC-32ML AND MPC-31C FUEL TYPES

Item	MPC-32ML	MPC-31C
Cladding Thickness, in	0.0285	0.027
Cladding OD, in	0.423	0.358

† The other input parameters such as the pressure loading, the fuel cladding thermal expansion coefficient and the cladding strength properties remain identical to that defined in Table 3.4.14A. These bounding parameters ensure that a conservative analysis is performed for these MPC-32ML and MPC-31C fuel types.

The fuel geometric information is obtained from Table 2.1.2 of this SAR.

Table 3.4.15A

MAXIMUM RESULTS FOR FUEL ROD INTEGRITY ANALYSIS
DURING MPC REFLOOD EVENT (LOAD CASE 11)

Result	Value
Maximum Stress in Fuel Rod Cladding	29,995 psi
Maximum Strain in Fuel Rod Cladding	2.66×10^{-3}

Table 3.4.15B

MAXIMUM RESULTS FOR FUEL ROD INTEGRITY ANALYSIS
DURING MPC REFLOOD EVENT (LOAD CASE 11) – FOR MPC-32ML AND MPC-31C†

Result	Value
Maximum Stress in Fuel Rod Cladding	28,349 psi
Maximum Strain in Fuel Rod Cladding	2.54×10^{-3}

†Only the results for the bounding fuel rod (i.e. Fuel used in MPC-32ML) are summarized here.

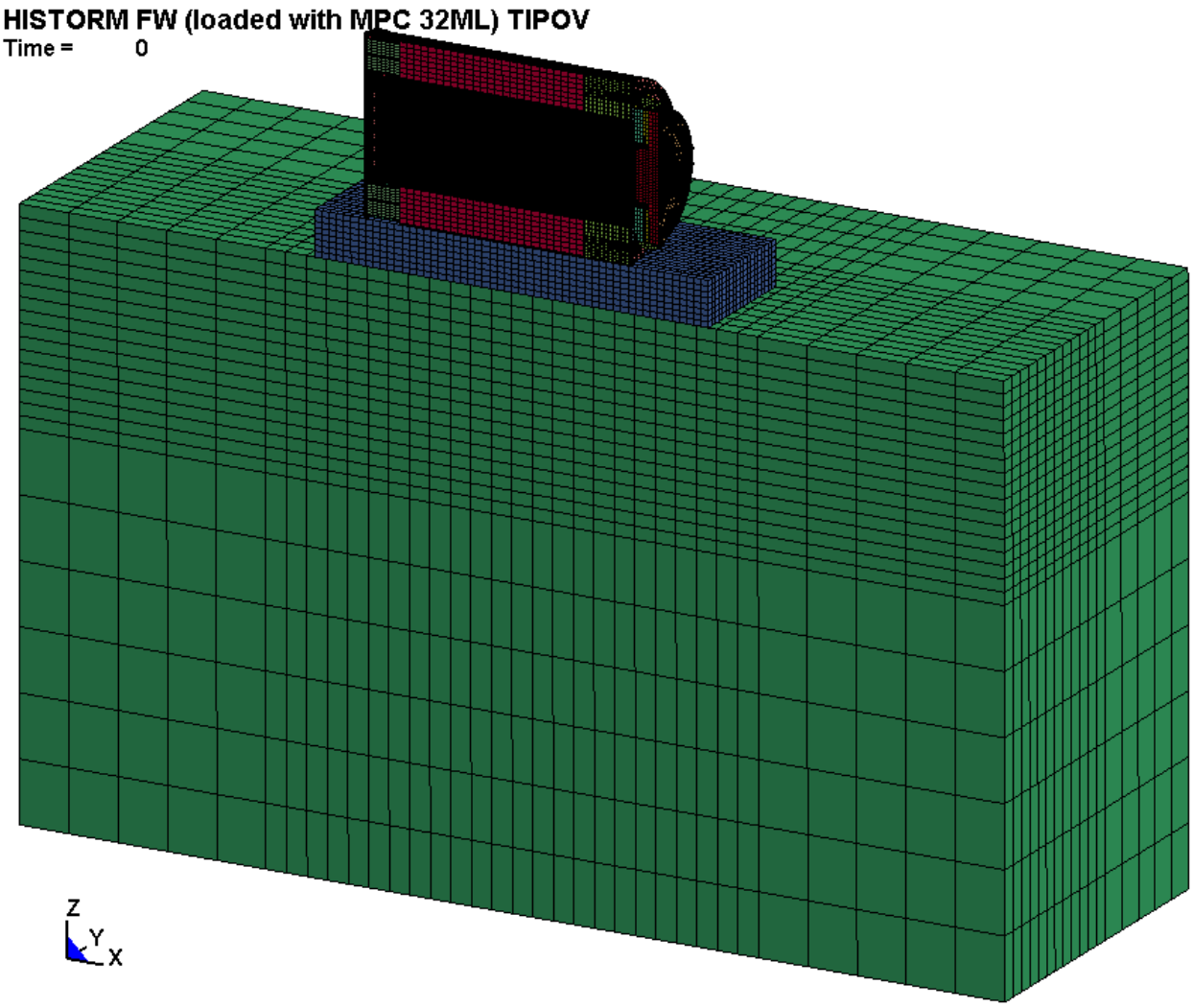

Figure 3.4.9C: LS-DYNA Tipover Model – HI-STORM FW Loaded with MPC-32ML

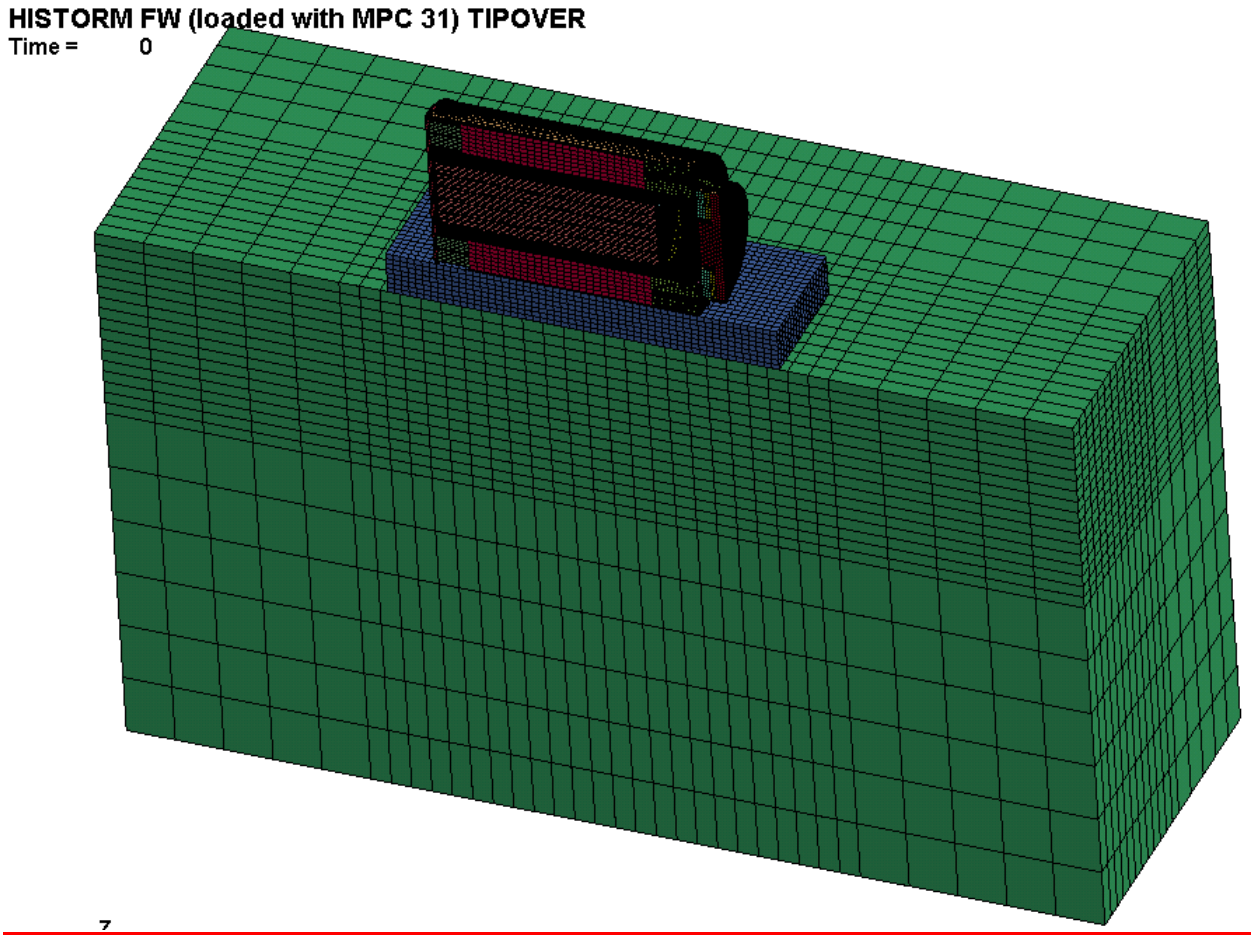

Figure 3.4.9D: LS-DYNA Tipover Model – HI-STORM FW Loaded with MPC-31C

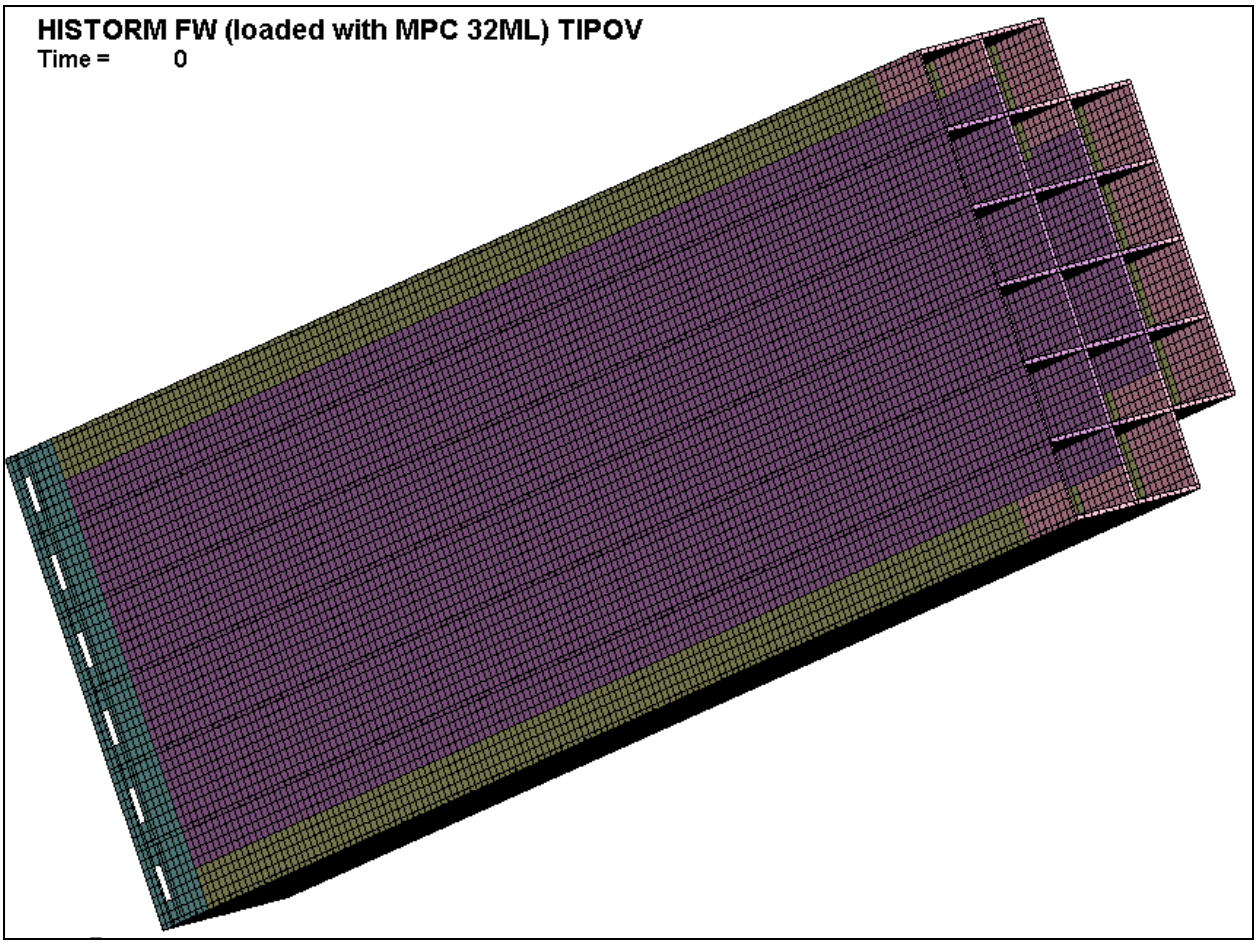

Figure 3.4.12C: LS-DYNA Model – MPC-32ML Fuel Basket
(note: the different colors represent regions with bounding temperatures of 350°C, 325°C and 200°C, respectively)

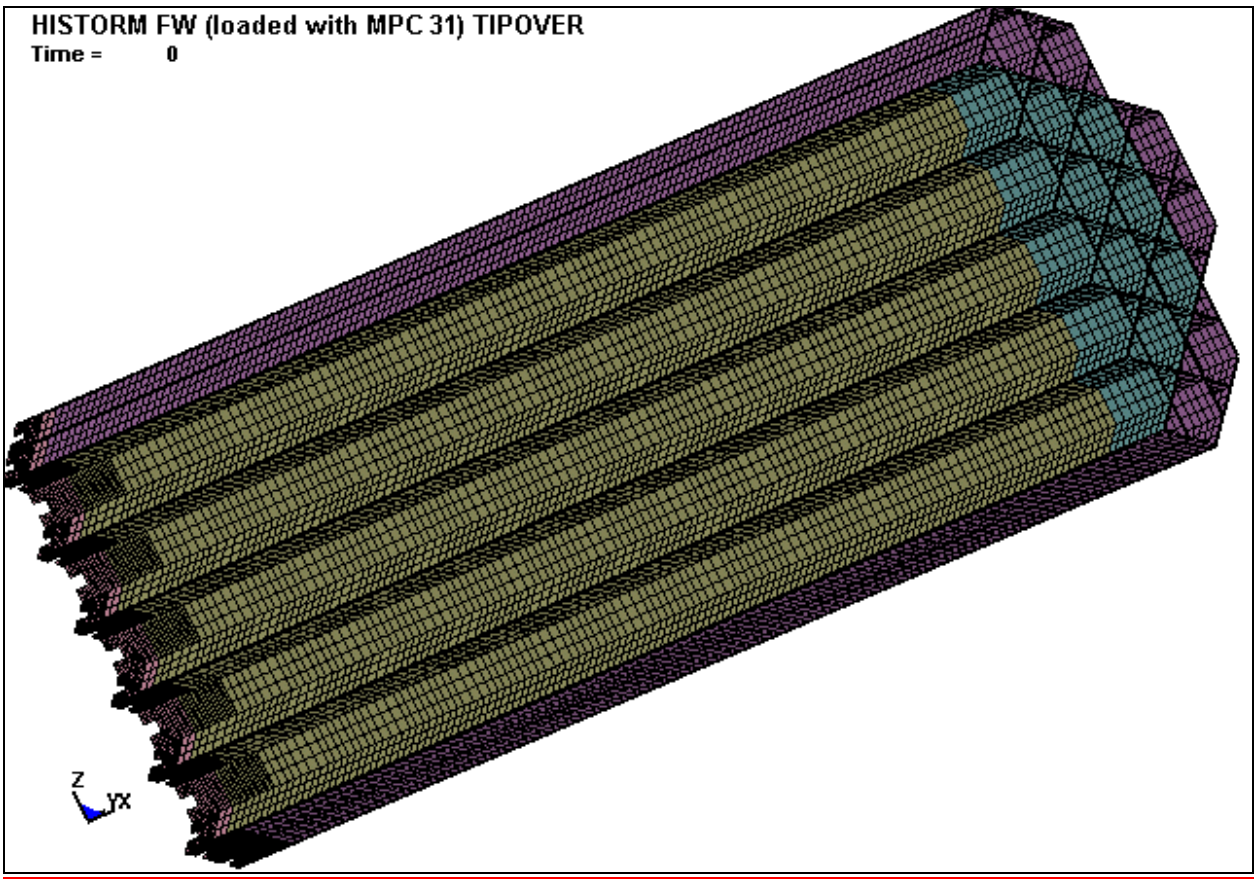

Figure 3.4.12B: LS-DYNA Model – MPC-31C Fuel Basket
(note: the different colors represent regions with bounding temperatures of 295°C, 255°C and 200°C, respectively)

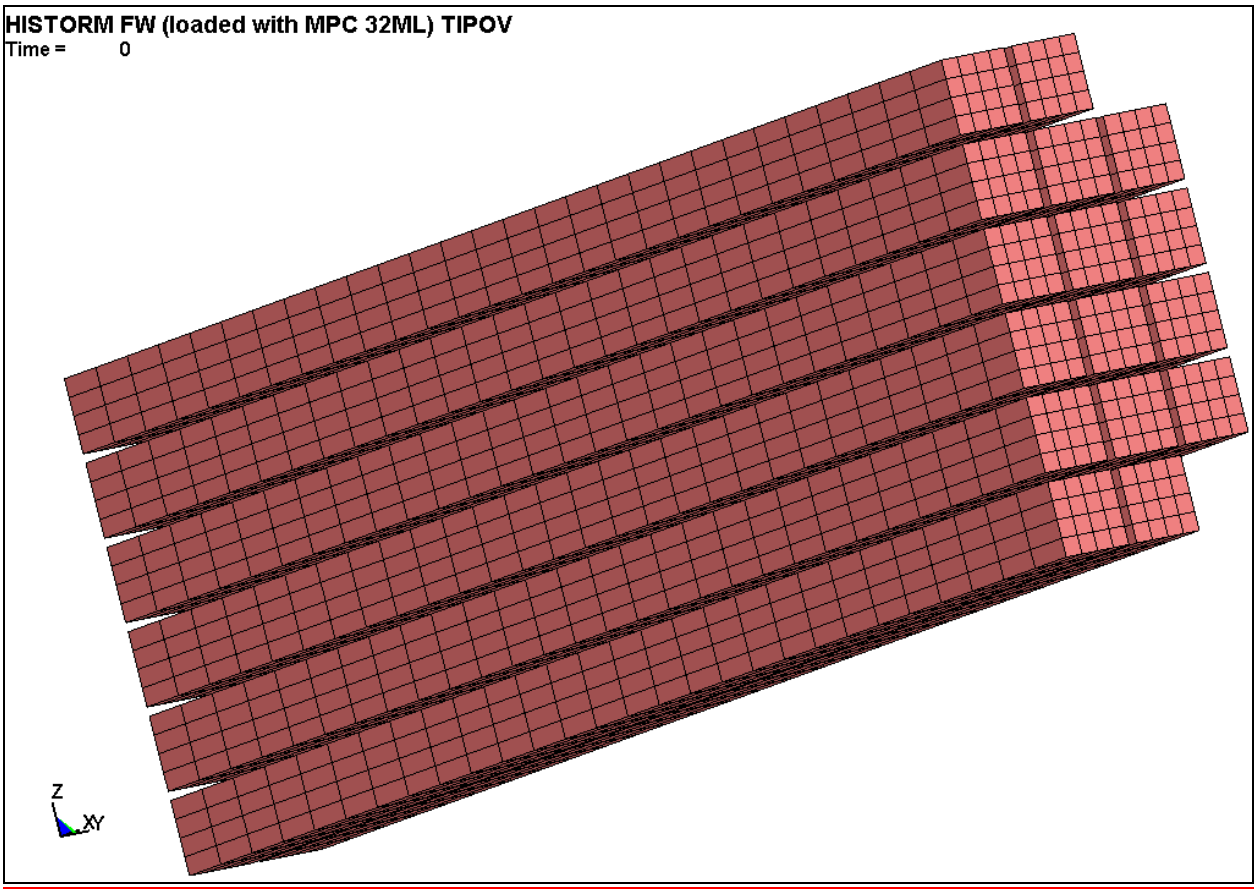

Figure 3.4.13C: LS-DYNA Model – PWR Fuel Assemblies Fuel Assemblies Loaded into MPC-32ML

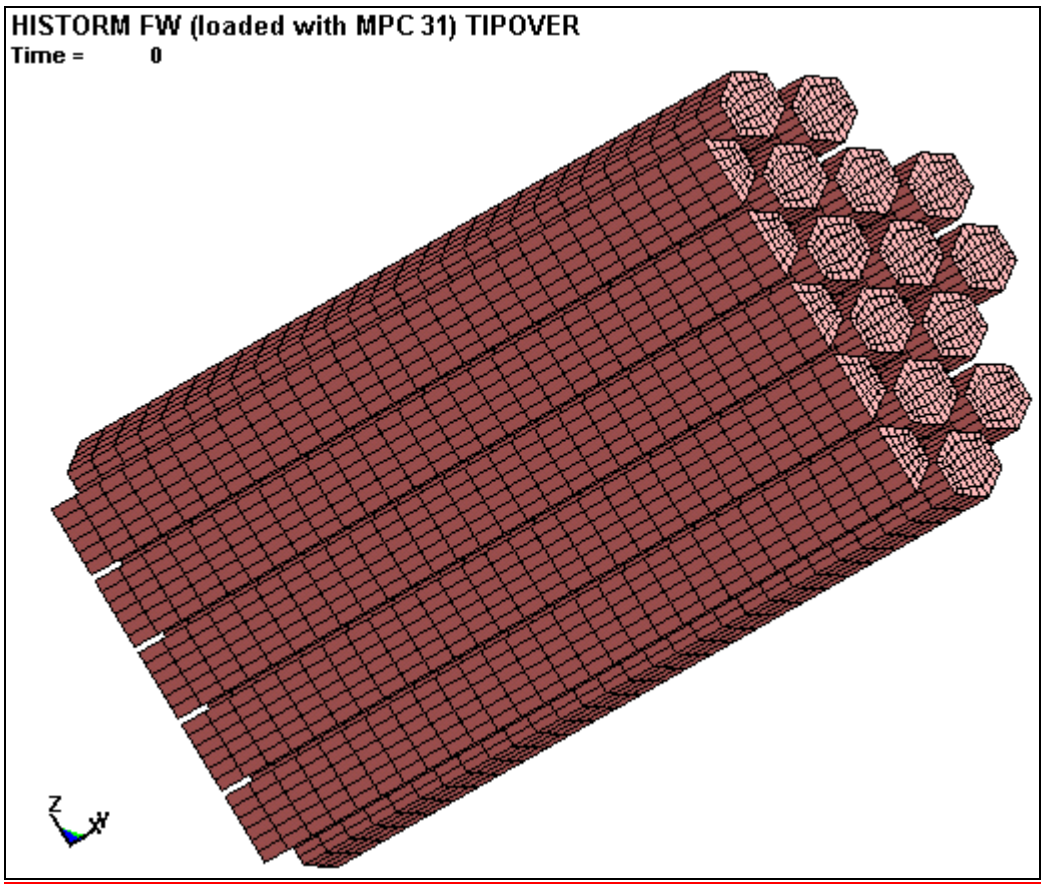

Figure 3.4.13D: LS-DYNA Model – PWR Fuel Assemblies Fuel Assemblies Loaded into MPC-31C

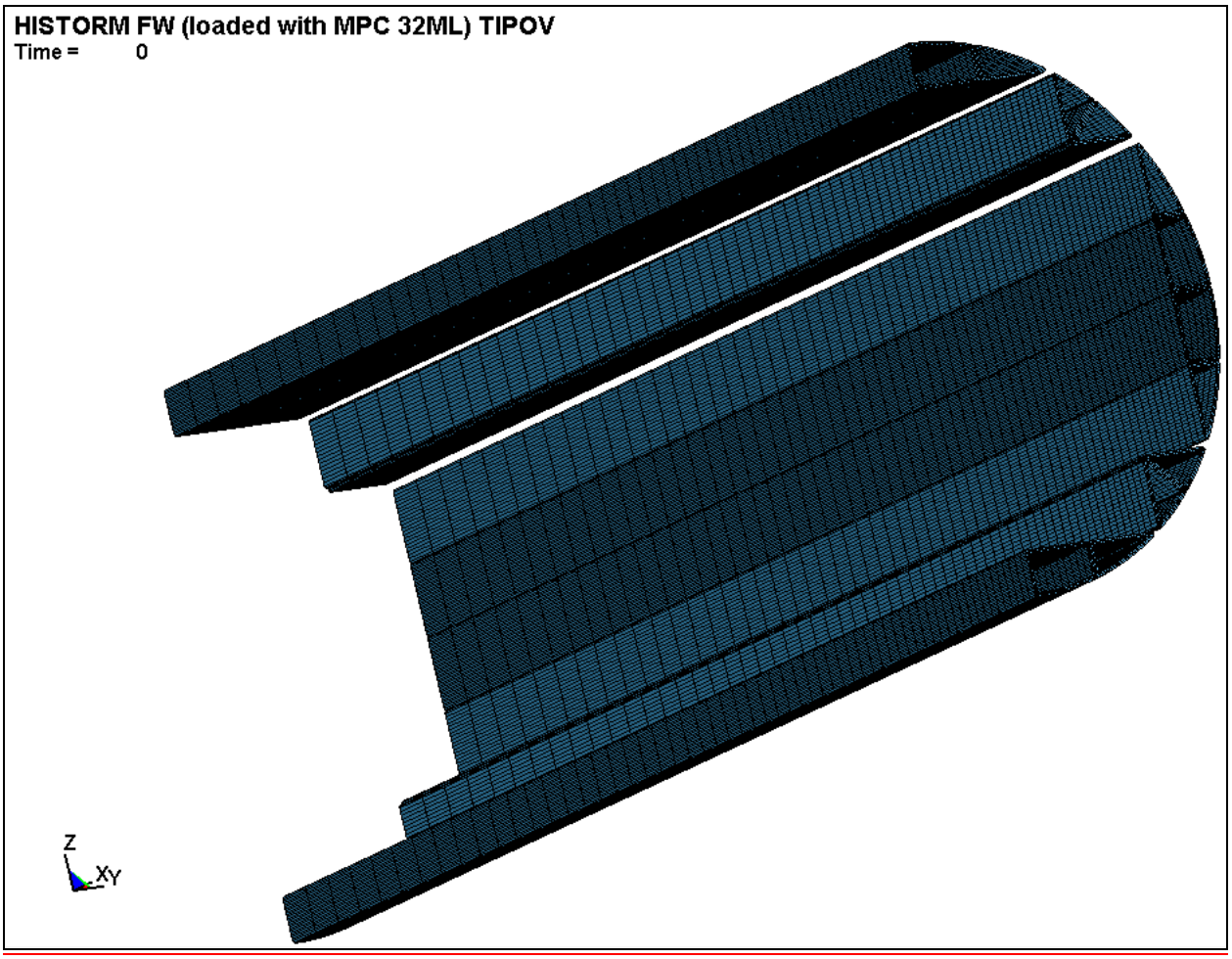

Figure 3.4.14C: LS-DYNA Model – MPC-32ML Fuel Basket Shims

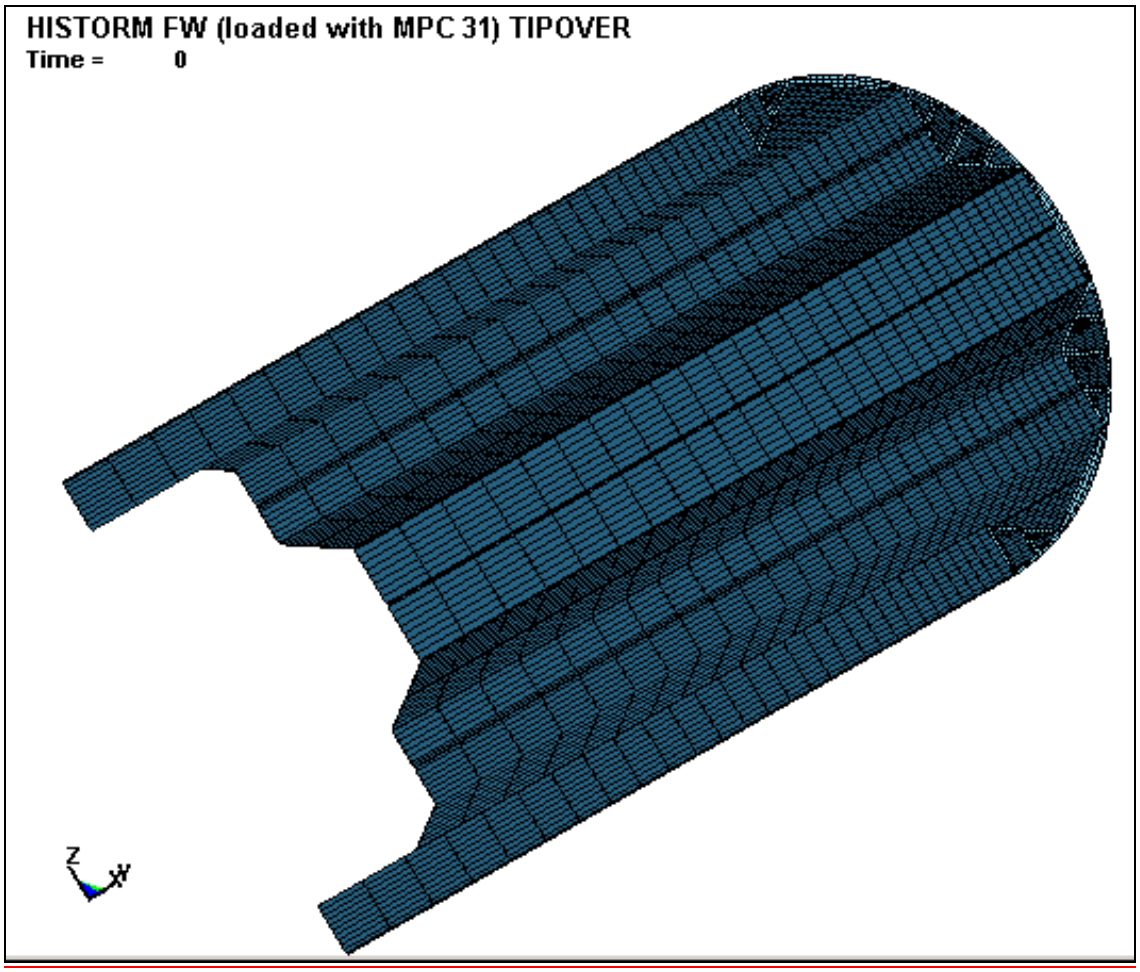

Figure 3.4.14D: LS-DYNA Model – MPC-31C Fuel Basket Shims

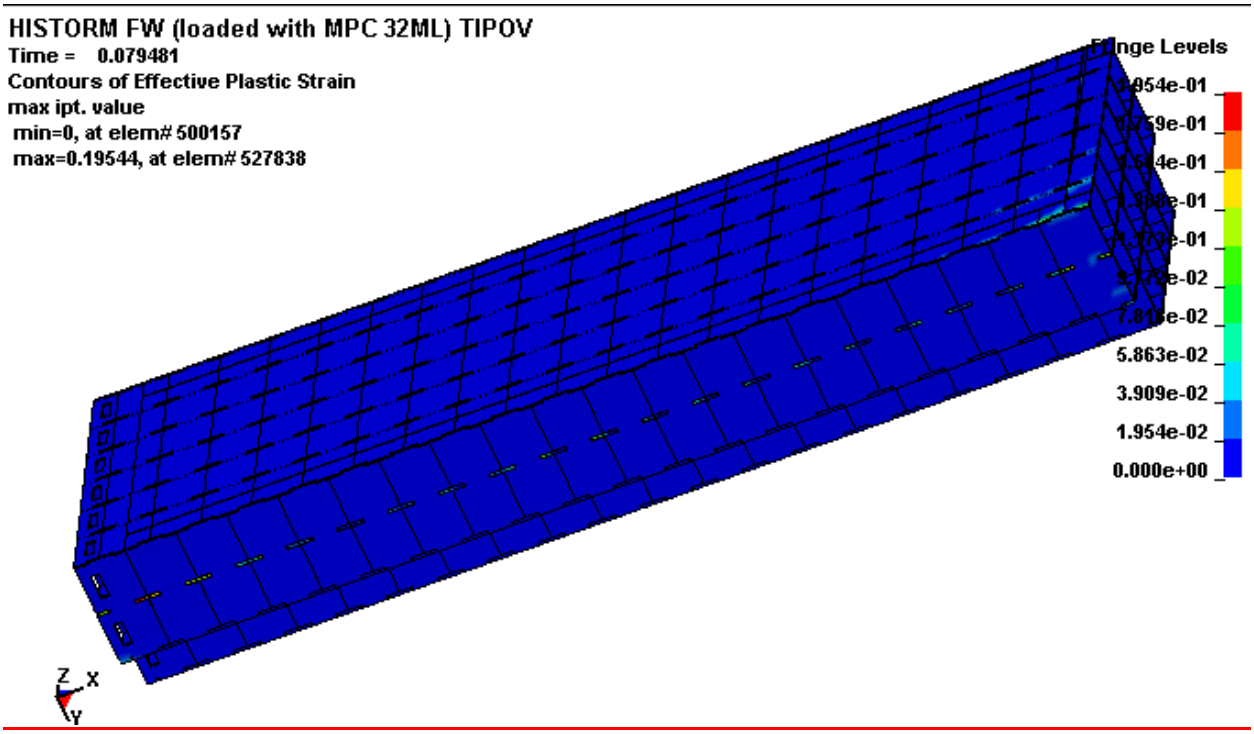

Figure 3.4.15C: Maximum Plastic Strain – MPC-32ML Fuel Basket

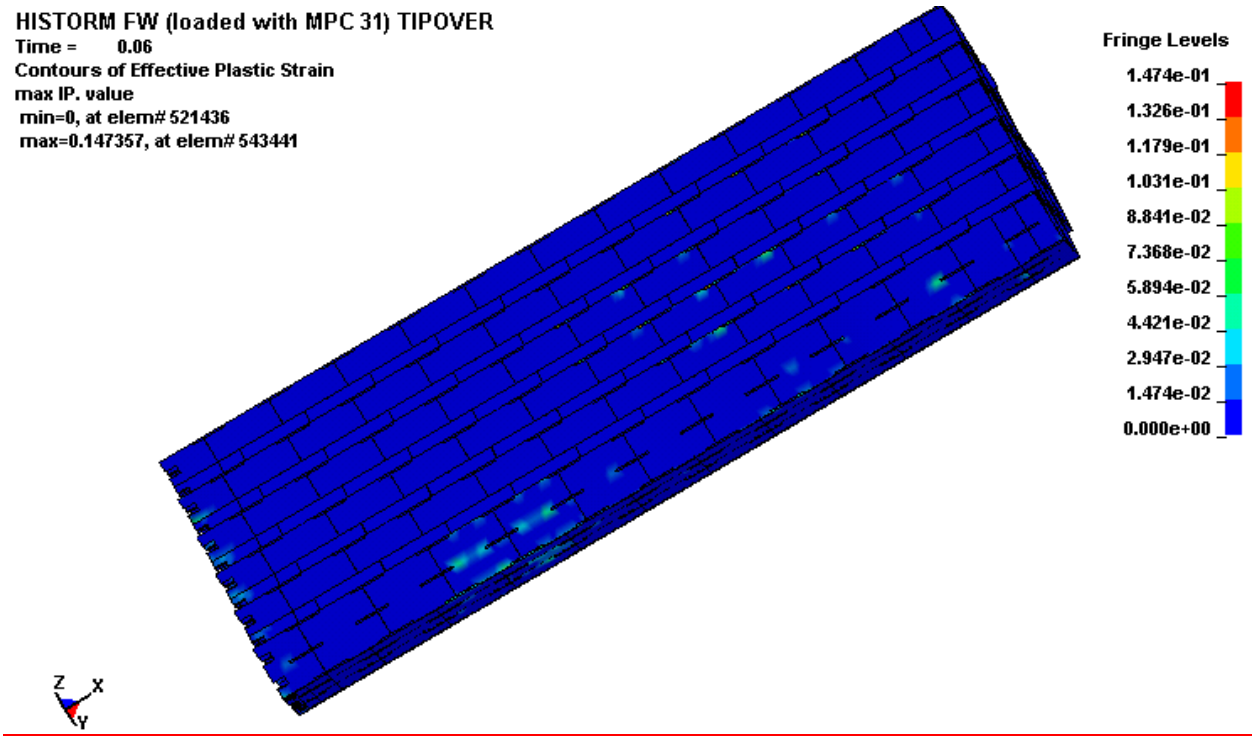

Figure 3.4.15D: Maximum Plastic Strain – MPC-31C Fuel Basket

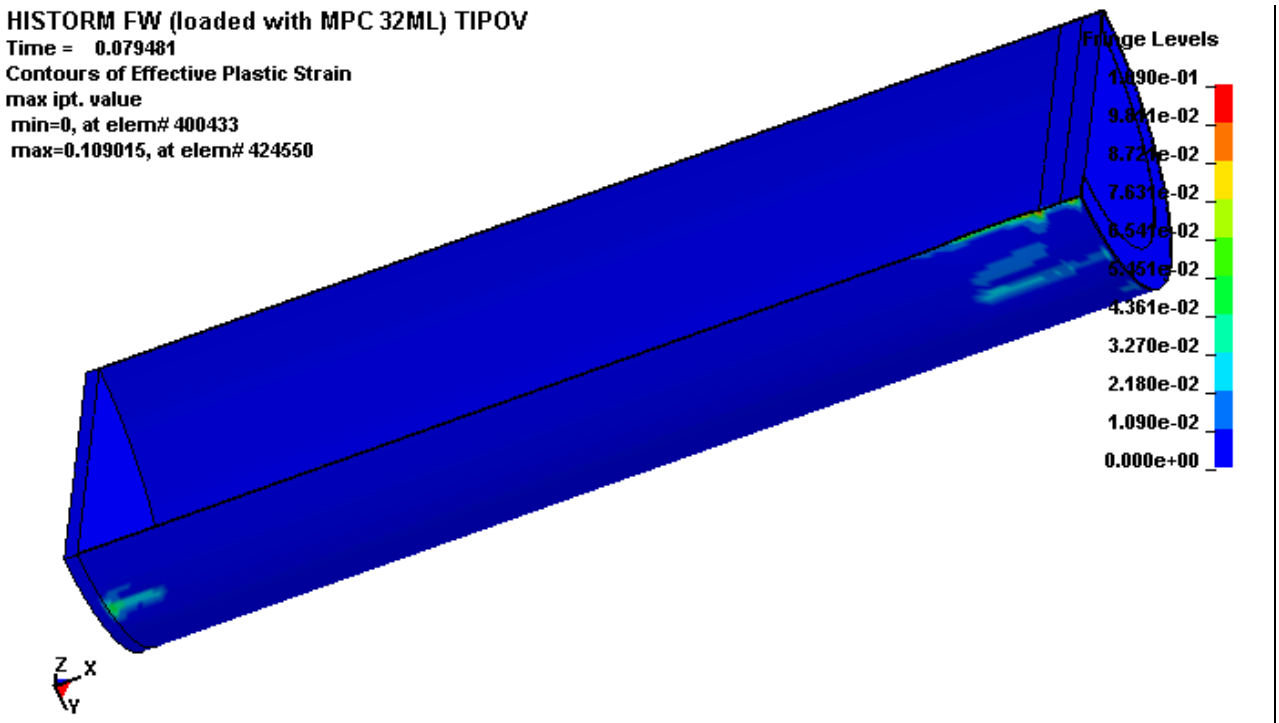

Figure 3.4.16C: Maximum Plastic Strain – MPC-32ML Enclosure Vessel

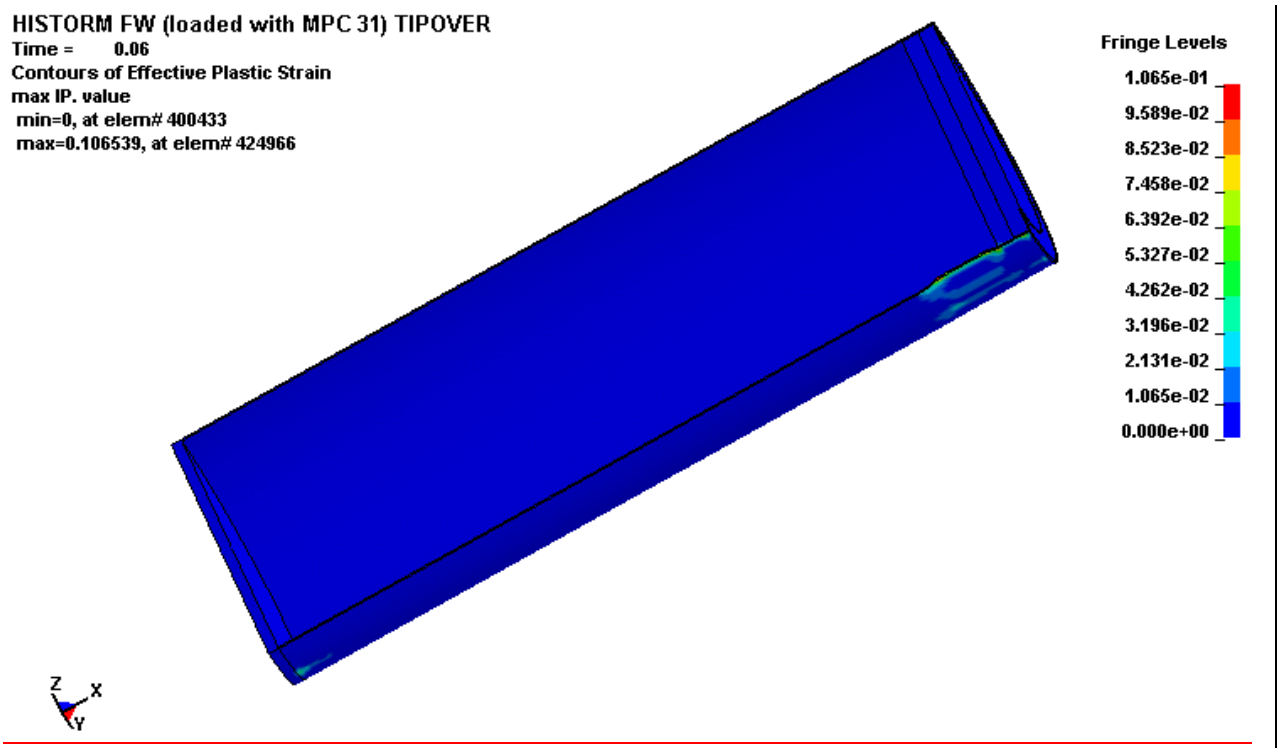

Figure 3.4.16D: Maximum Plastic Strain – MPC-31C Enclosure Vessel

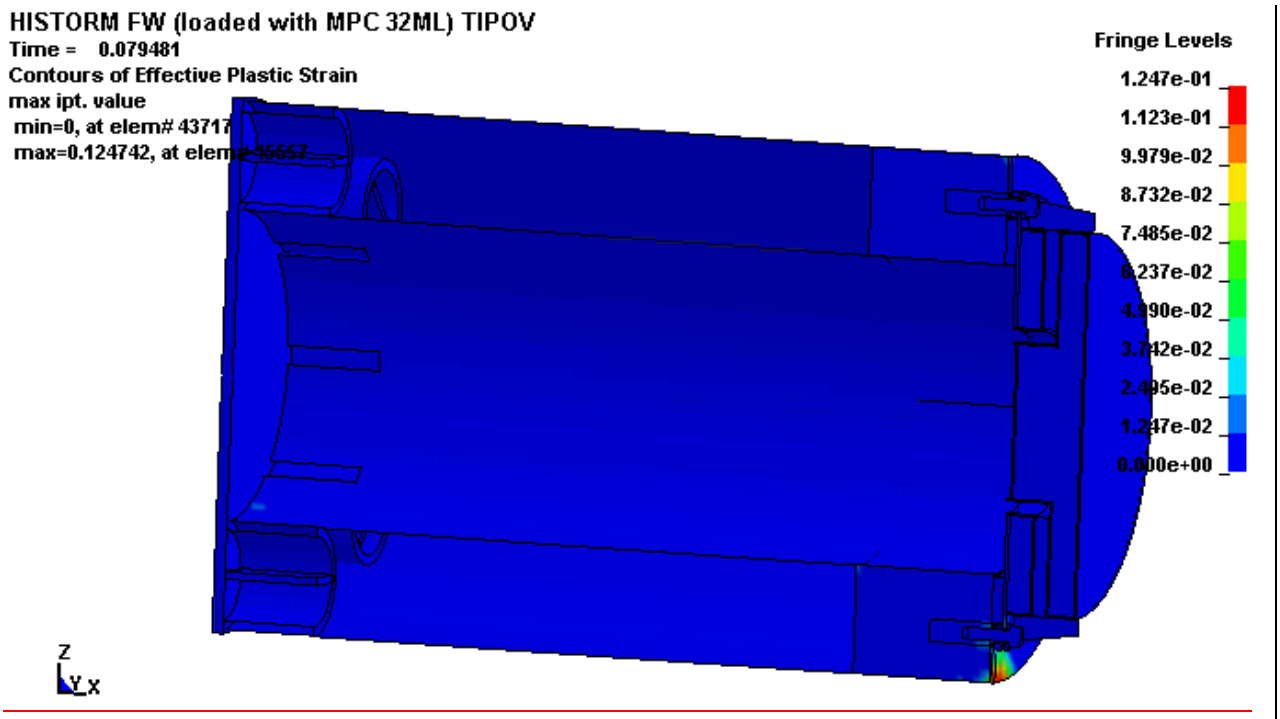

Figure 3.4.17C: Maximum Plastic Strain – HI-STORM FW Overpack (for MPC-32ML, Excluding MPC Guide Tubes)

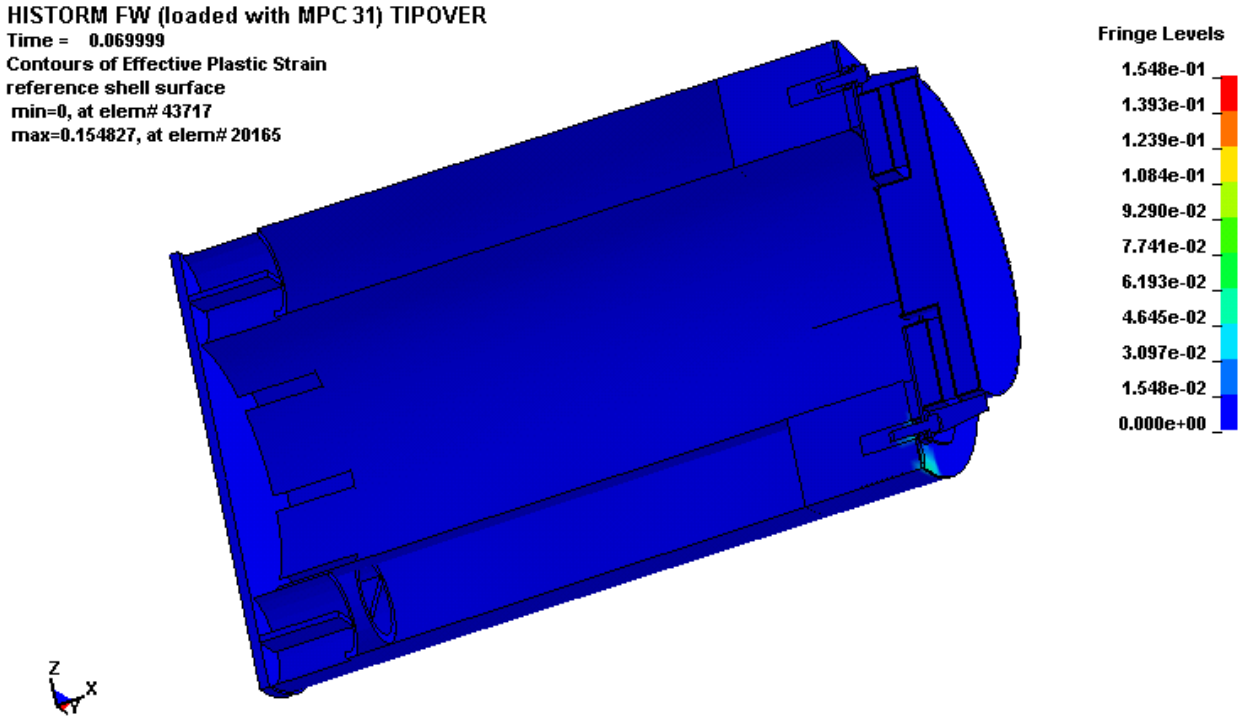

Figure 3.4.17D: Maximum Plastic Strain – HI-STORM FW Overpack (for MPC-31C, Excluding MPC Guide Tubes)

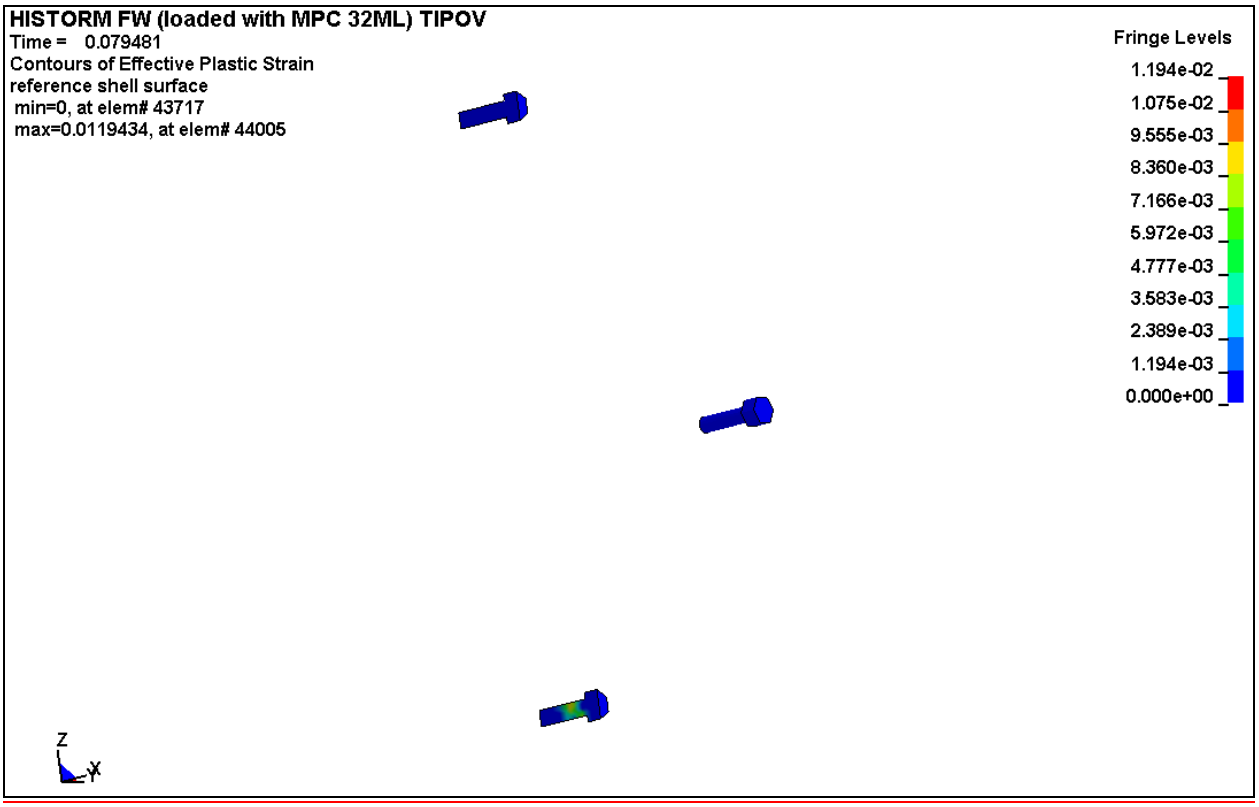

Figure 3.4.18C: Maximum Plastic Strain –
HI-STORM FW Overpack (for MPC-32ML) Closure Lid Bolts

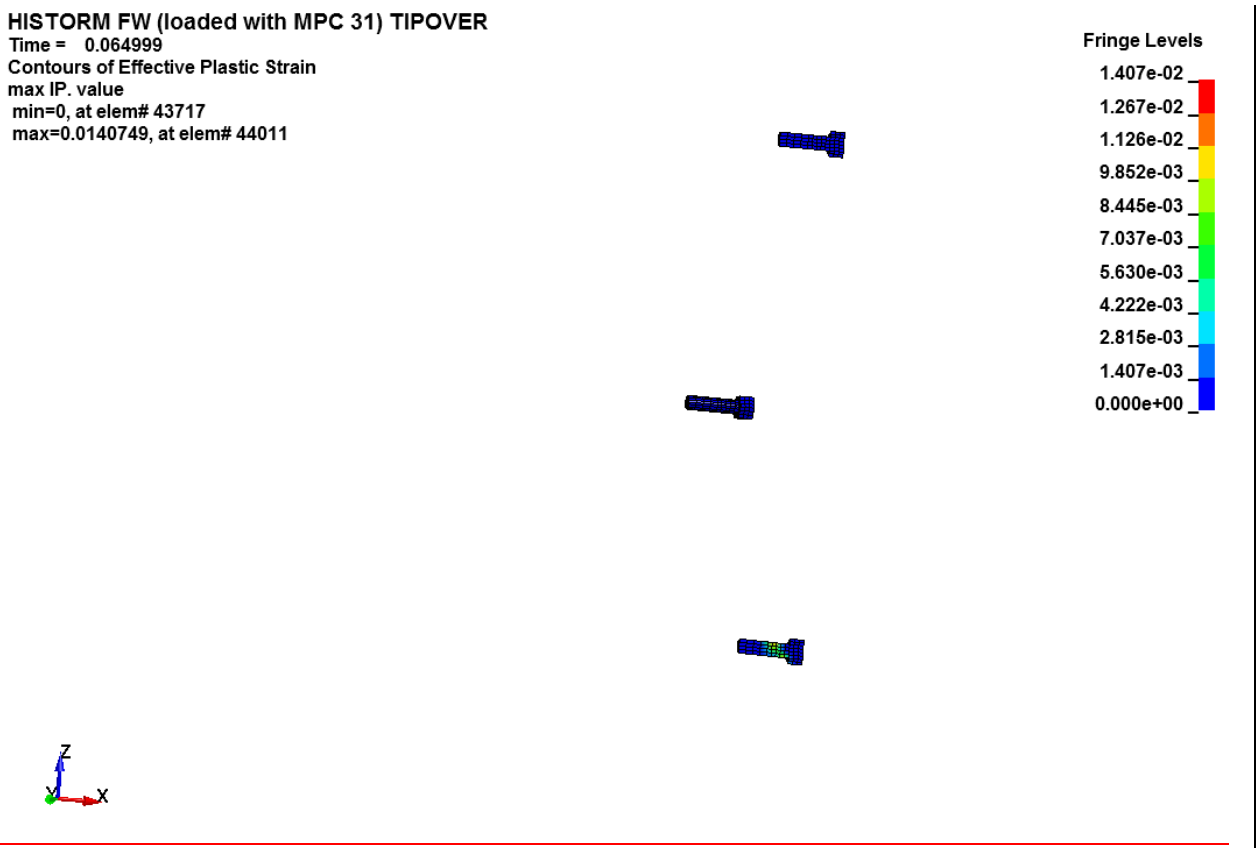

Figure 3.4.18D: Maximum Plastic Strain –
HI-STORM FW Overpack (for MPC-31C) Closure Lid Bolts

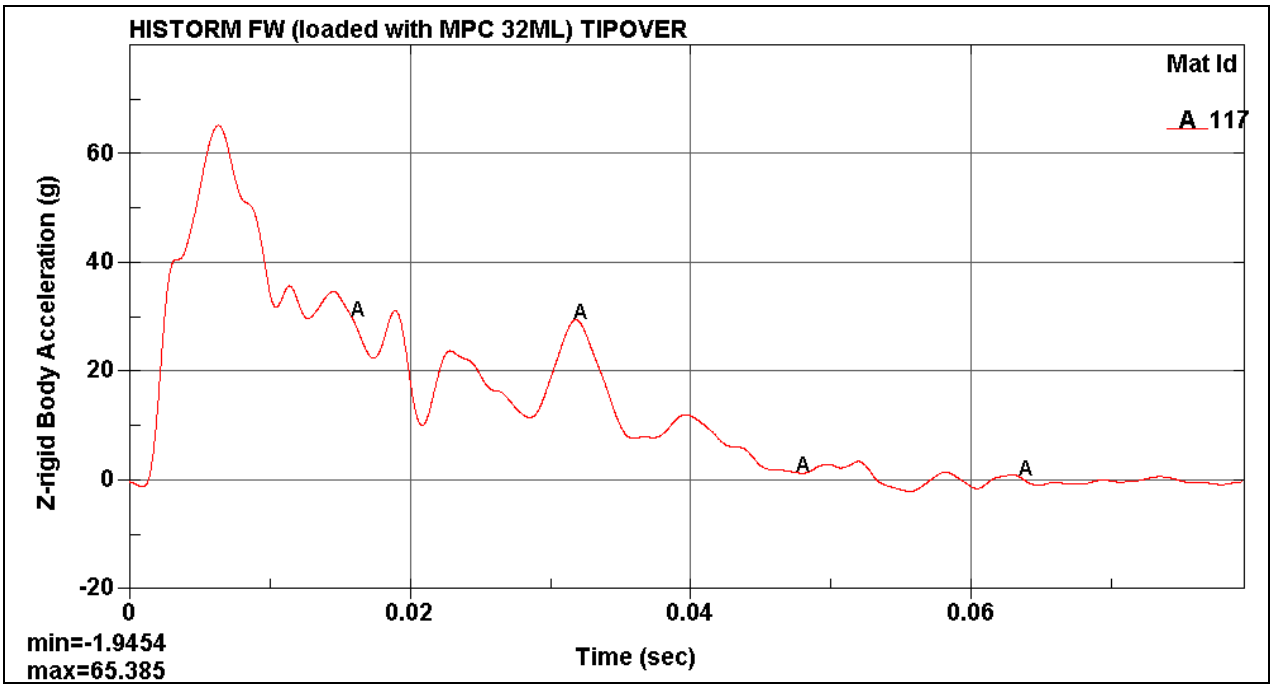

Figure 3.4.19C: Vertical Rigid Body Deceleration Time History – Cask Lid Concrete (for HI-STORM FW Loaded with MPC-32ML)

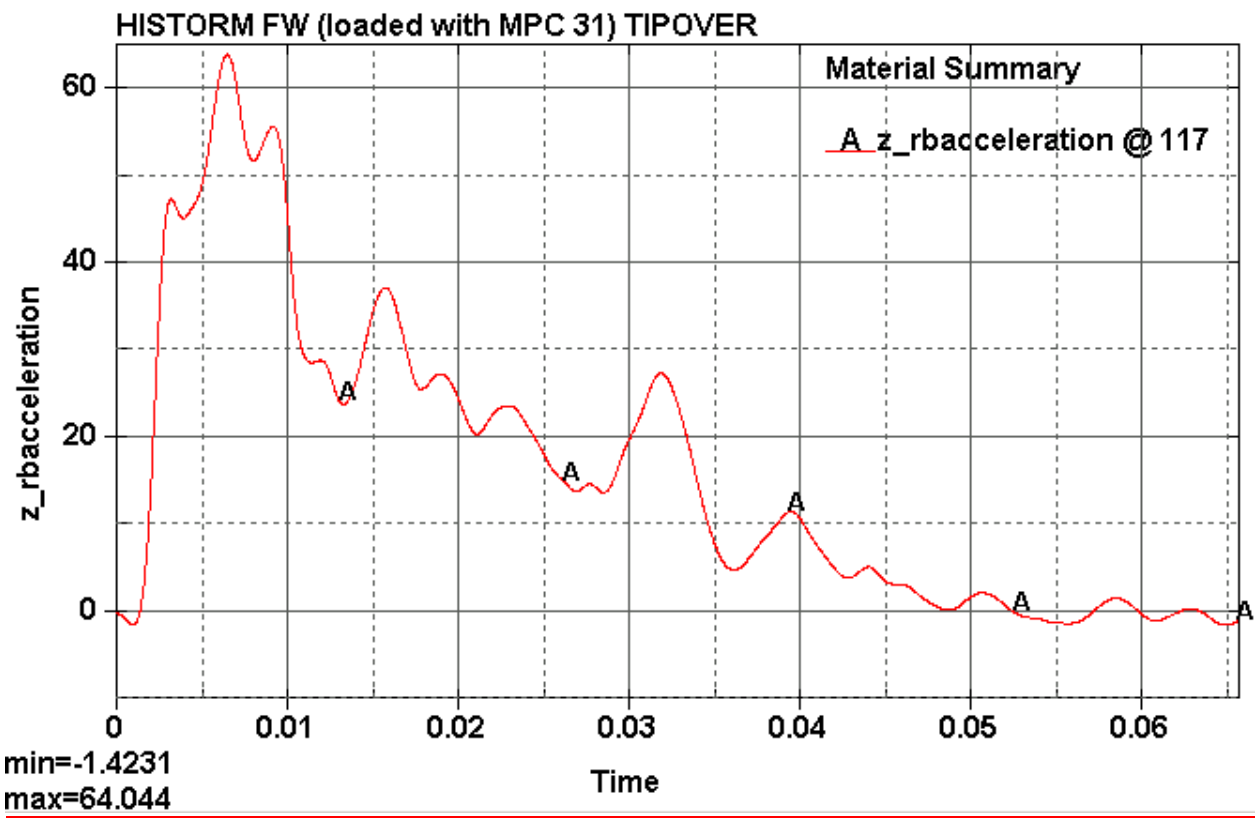

Figure 3.4.19D: Vertical Rigid Body Deceleration Time History – Cask Lid Concrete (for HI-STORM FW Loaded with MPC-31C)

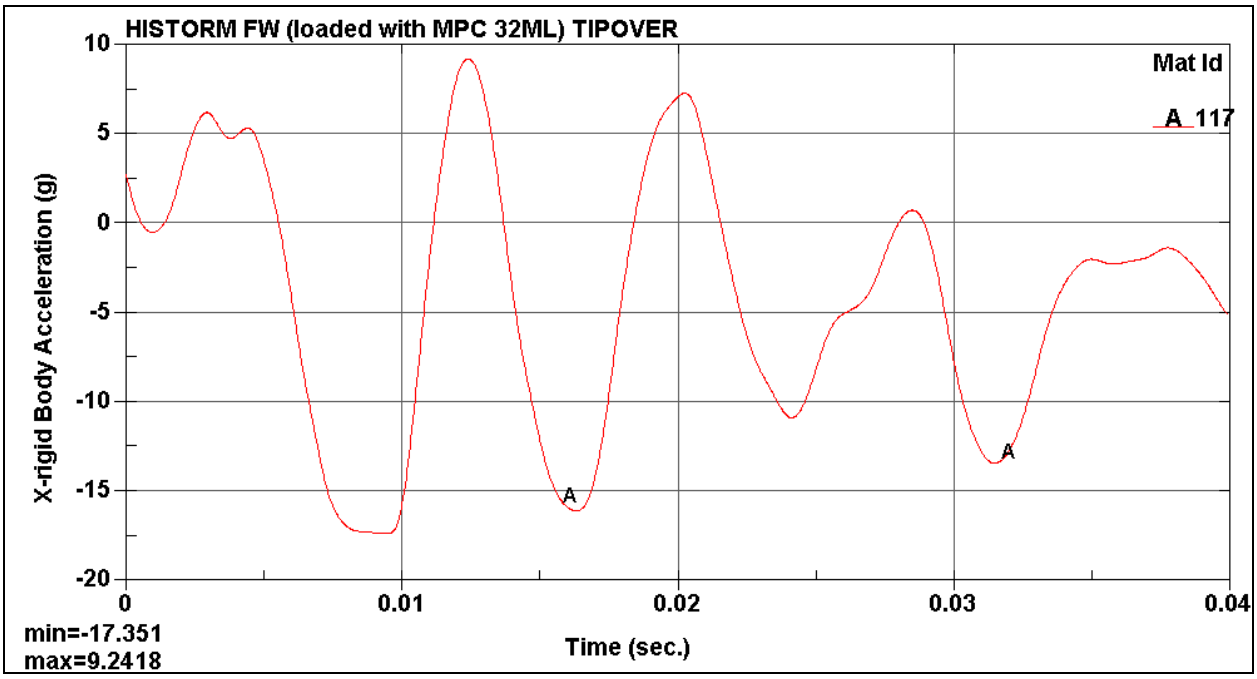

Figure 3.4.20C: Horizontal Rigid Body Deceleration Time History – Cask Lid Concrete (for HI-STORM FW Loaded with MPC-32ML)

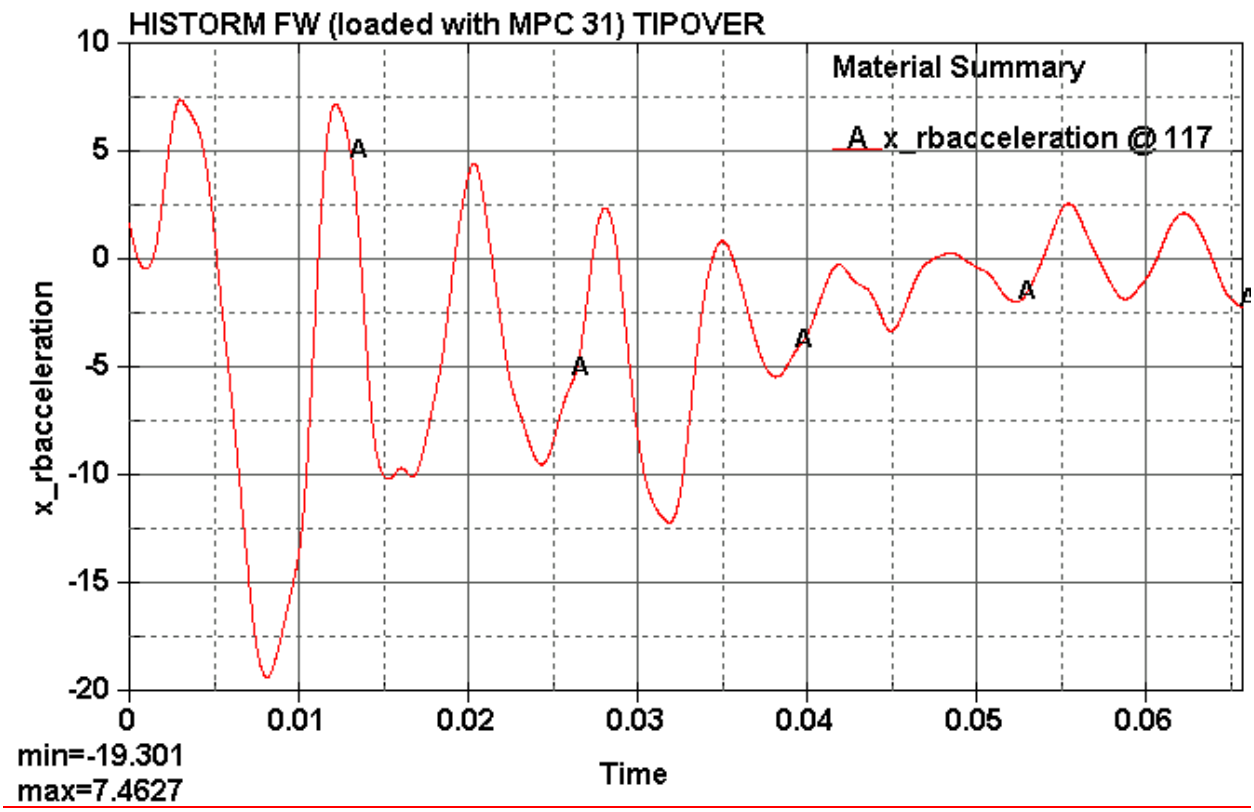

Figure 3.4.20D: Horizontal Rigid Body Deceleration Time History – Cask Lid Concrete (for HI-STORM FW Loaded with MPC-31C)

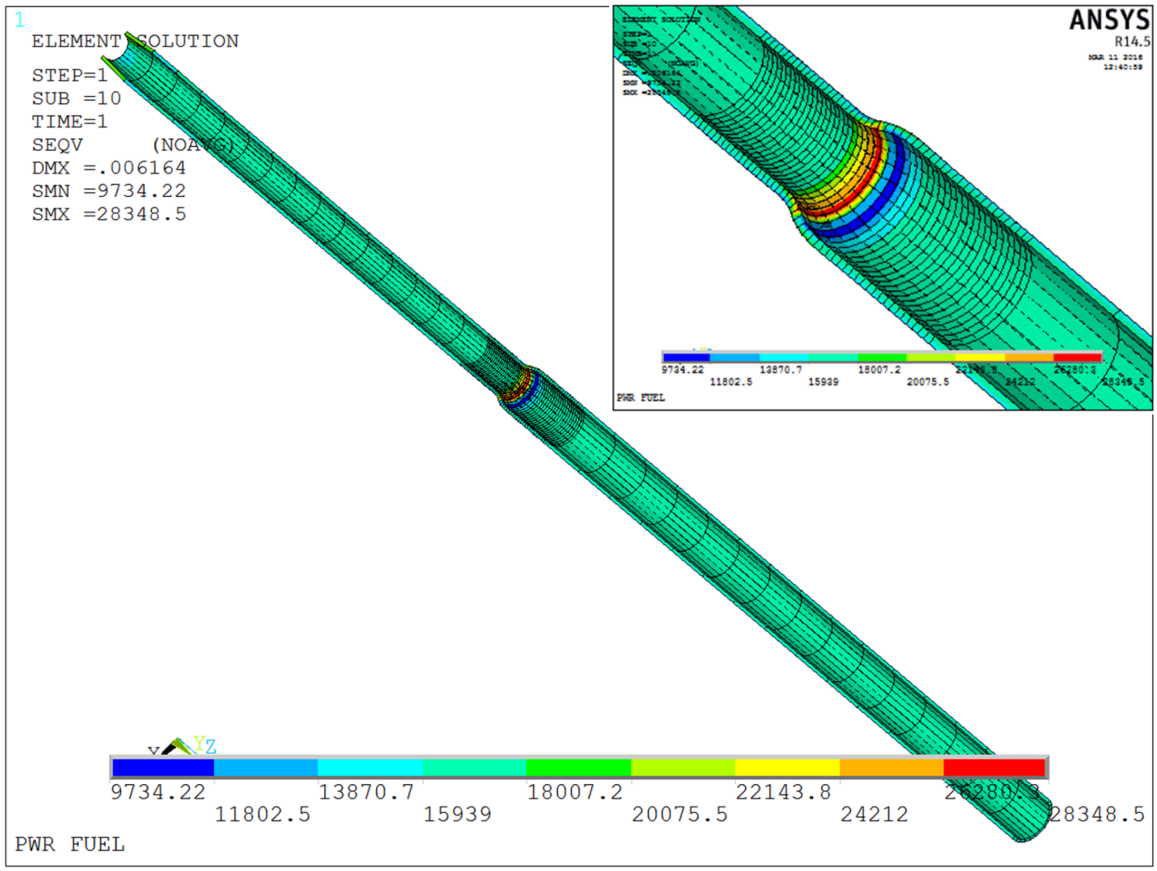

Figure 3.4.42: Stress Distribution in Fuel Rod Due to MPC Reflood (Load Case 11) – For MPC-32ML Fuel Type

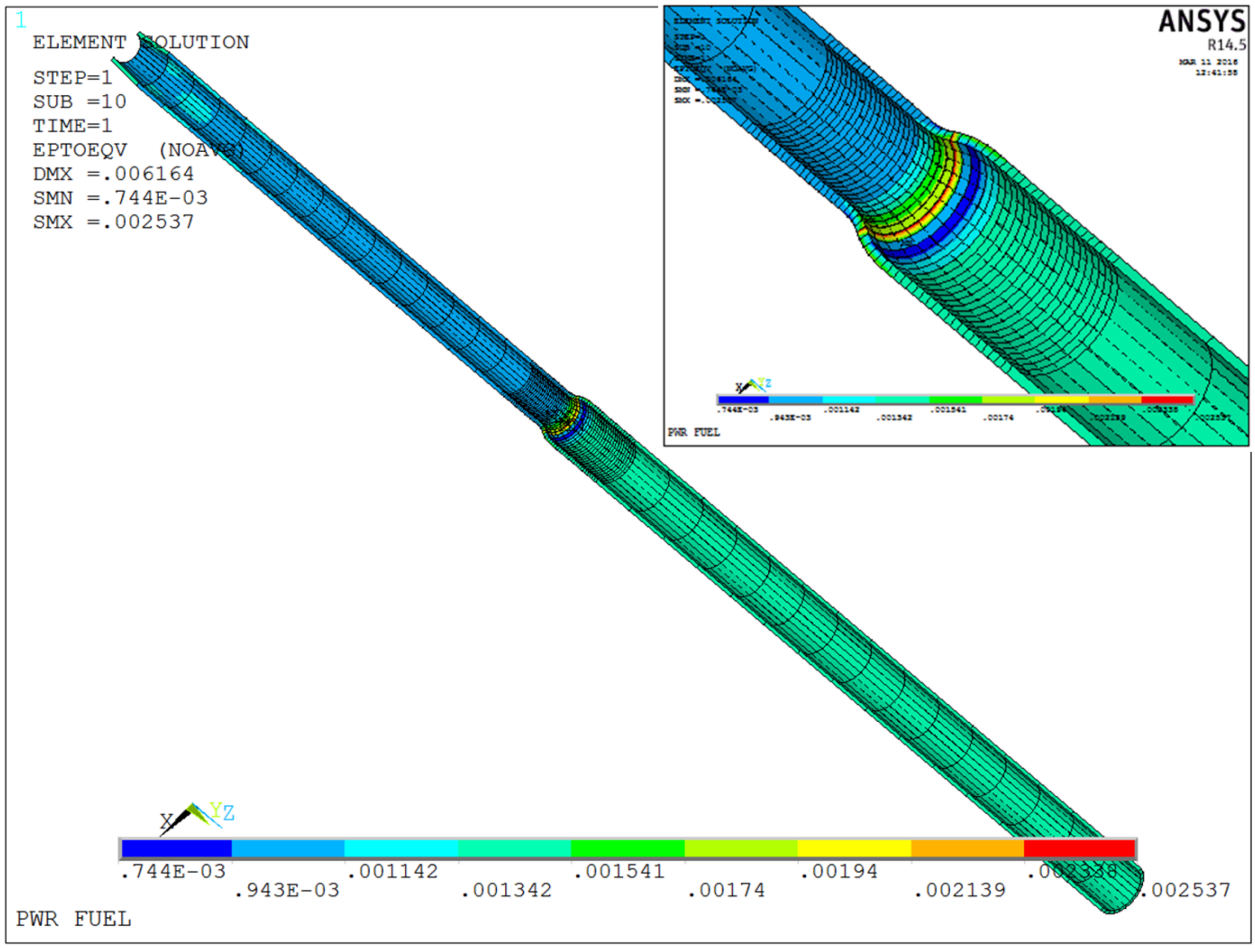

Figure 3.4.43: Strain Distribution in Fuel Rod Due to MPC Reflood (Load Case 11) – For MPC-32ML Fuel Type

[3.4.11] Holtec Proprietary Report HI-2094353, "Analysis of the Non-Mechanistic Tipover Event of the Loaded HI-STORM FW Storage Cask", Latest Revision.

[3.4.12] Oberg, E. et. al., Machinery's Handbook, Industrial Press Inc., 27th Edition.

[3.4.13] Holtec Proprietary Report HI-2094418, "Structural Calculation Package for HI-STORM FW System", Latest Revision.

[3.4.14] EPRI NP-440, Full Scale Tornado Missile Impact Tests, 1977.

[3.4.15] Holtec Proprietary Report HI-2094392, "Tornado Missile Analysis for HI-STORM FW System", Latest Revision.

[3.4.16] Young, W., Roark's Formulas for Stress & Strain, McGraw Hill Book Company, 6th Edition.

[3.4.17] Interim Staff Guidance - 15, "Materials Evaluation", Revision 0.

[3.4.18] Timoshenko, S., Strength of Materials (Part II), Third Edition, 1958.

[3.4.19] "Mechanical Testing and Evaluation", ASM Handbook, Volume 8, 2000.

[3.4.20] Adkins, H.E., Koeppel, B.J., Tang, D.T., "Spent Nuclear Fuel Structural Response When Subject to an End Drop Impact Accident," Proceedings ASME/JSME Pressure Vessels and Piping Conference, PVP-Vol. 483, American Society of Mechanical Engineers, New York, New York, 2004.

[3.4.21] Chun, R., Witte, M., Schwartz, M., "Dynamic Impact Effects on Spent Fuel Assemblies", Lawrence Livermore National Laboratory, Report UCID-21246, 1987.

[3.4.22] Rust, J.H., Nuclear Power Plant Engineering, Haralson Publishing Company, 1979.

[3.4.23] NUREG/CR-1864, "A Pilot Probabilistic Risk Assessment of a Dry Cask Storage System at a Nuclear Power Plant", USNRC, Washington D.C., 2007.

[3.4.24] EPRI TR-103949, "Temperature Limit Determination for the Inert Dry Storage of Spent Nuclear Fuel", May 1994.

[3.4.25] Holtec Proprietary Report HI-2166998, "Analysis of the Non-Mechanistic Tipover Event of the Loaded HI-STORM FW Storage Cask Loaded with MPC-32ML and MPC-31C", Latest Revision.

CHAPTER 4 CHANGED PAGES

compliance with ISG-11 and with NUREG-1536 guidelines, subject to the exceptions and clarifications discussed in Chapter 1, Table 1.0.3.

As explained in Section 1.2, the storage of SNF in the fuel baskets in the HI-STORM FW system is configured for a three-region storage system under regionalized storage and uniform storage. Figures 1.2.1a, 1.2.1b, 1.2.1c and 1.2.2 provide the information on the location of the regions and Tables 1.2.3a, 1.2.3b, 1.2.3c and 1.2.4 provide the permissible specific heat load (heat load per fuel assembly) in each region for the PWR and BWR MPCs, respectively. The Specific Heat Load (SHL) values under regionalized storage are defined for two patterns that in one case maximizes ALARA (Table 1.2.3a, Pattern A and Table 1.2.4) and in the other case maximizes heat dissipation (Table 1.2.3a, Pattern B). The ALARA maximized fuel loading is guided by the following considerations:

- Region 1: Located in the core region of the basket is permitted to store fuel with medium specific heat load.
- Region 2: This is the intermediate region flanked by the core region (Region I) from the inside and the peripheral region (Region III) on the outside. This region has the maximum SHL in the basket.
- Region 3: Located in the peripheral region of the basket, this region has the smallest SHL. Because a low SHL means a low radiation dose emitted by the fuel, the low heat emitting fuel around the periphery of the basket serves to block the radiation from the Region II fuel, thus reducing the total quantity of radiation emanating from the MPC in the lateral direction.

Thus, the 3-region arrangement defined above serves to minimize radiation dose from the MPC and peak cladding temperatures mitigated by avoiding placement of hot fuel in the basket core.

To address the needs of cask users having high heat load fuel inventories, fuel loading Pattern B is defined in Table 1.2.3a to maximize heat dissipation by locating hotter fuel in the cold peripheral Region 3 and in this manner minimize cladding temperatures. This has the salutary effect of minimizing core temperature gradients in the radial direction and thermal stresses in the fuel and fuel basket.

The salutary consequences of all regionalized loading arrangements become evident from the computed peak cladding temperatures in this chapter, which show margin to the ISG-11 limit discussed earlier.

The safety analyses summarized in this chapter demonstrate acceptable margins to the allowable limits under all design basis loading conditions and operational modes. Minor changes to the design parameters that inevitably occur during the product's life cycle which are treated within the purview of 10CFR72.48 and are ascertained to have an insignificant effect on the computed safety factors may not prompt a formal reanalysis and revision of the results and associated data in the tables of this chapter unless the cumulative effect of all such unquantified changes on the reduction of any of the computed safety margins cannot be deemed to be insignificant. For purposes of this determination, an insignificant loss of safety margin with reference to an

stresses due to restraint on basket periphery thermal growth is eliminated by providing adequate basket-to-canister shell gaps to allow for basket thermal growth during all operational modes.

[

Withheld in Accordance with 10 CFR 2.390

]

The MPCs uniform & regionalized fuel storage scenarios are defined in Figures 1.2.1a, 1.2.1b, 1.2.1c and 1.2.2 in Chapter 1 and design maximum decay heat loads for storage of zircaloy clad fuel are listed in Tables 1.2.3a, 1.2.3b, 1.2.3c and 1.2.4. The axial heat distribution in each fuel assembly is conservatively assumed to be non-uniformly distributed with peaking in the active fuel mid-height region (see axial burnup profiles in Figures 2.1.3 and 2.1.4). Table 4.1.1 summarizes the principal operating parameters of the HI-STORM FW system.

The fuel cladding temperature limits that the HI-STORM FW system is required to meet are discussed in Section 4.3 and given in Table 2.2.3. Additionally, when the MPCs are deployed for storing High Burnup Fuel (HBF) further restrictions during certain fuel loading operations (vacuum drying) are set forth herein to preclude fuel temperatures from exceeding the normal temperature limits. To ensure explicit compliance, a specific term “short-term operations” is defined in Chapter 2 to cover all fuel loading activities. ISG-11 fuel cladding temperature limits are applied for short-term operations.

The HI-STORM FW system (i.e., HI-STORM FW overpack, HI-TRAC VW transfer cask and MPC) is evaluated under normal storage (HI-STORM FW overpack), during off-normal and accident events and during short-term operations in a HI-TRAC VW. Results of HI-STORM FW thermal analysis during normal (long-term) storage are obtained and reported in Section 4.4. Results of HI-TRAC VW short-term operations (fuel loading, on-site transfer and vacuum drying) are reported in Section 4.5. Results of off-normal and accident events are reported in Section 4.6.

Table 4.1.1

HI-STORM FW OPERATING CONDITION PARAMETERS

Condition	**Value**
MPC Decay Heat, max.	Tables 1.2.3a, 1.2.3b, 1.2.3c and 1.2.4
MPC Operating Pressure	Note 1
Normal Ambient Temperature	Table 2.2.2
Helium Backfill Pressure	Table 4.4.8
Note 1: The MPC operating pressure used in the thermal analysis is based on the minimum helium backfill pressure specified in Table 4.4.8 and MPC cavity average temperature.	

Table 4.2.1

SUMMARY OF HI-STORM FW SYSTEM MATERIALS
THERMAL PROPERTY REFERENCES

Material	Emissivity	Conductivity	Density	Heat Capacity
Helium	N/A	Handbook [4.2.2]	Ideal Gas Law	Handbook [4.2.2]
Air	N/A	Handbook [4.2.2]	Ideal Gas Law	Handbook [4.2.2]
Zircaloy	[4.2.3], [4.2.17], [4.2.18], [4.2.7]	NUREG [4.2.17]	Rust [4.2.4]	Rust [4.2.4]
UO_2	Note 1	NUREG [4.2.17]	Rust [4.2.4]	Rust [4.2.4]
Stainless Steel (machined forgings)[Note 2]	Kern [4.2.5]	ASME [4.2.8]	Marks' [4.2.1]	Marks' [4.2.1]
Stainless Steel Plates[Note 3]	ORNL [4.2.11], [4.2.12]	ASME [4.2.8]	Marks' [4.2.1]	Marks' [4.2.1]
Carbon Steel	Kern [4.2.5]	ASME [4.2.8]	Marks' [4.2.1]	Marks' [4.2.1]
Concrete	Note 1	Marks' [4.2.1]	Appendix 1.D of HI-STORM 100 FSAR [4.1.8]	Handbook [4.2.2]
Lead	Note 1	Handbook [4.2.2]	Handbook [4.2.2]	Handbook [4.2.2]
Water	Note 1	ASME [4.2.10]	ASME [4.2.10]	ASME [4.2.10]
Metamic-HT	Test Data Table 1.2.8	Test Data Table 1.2.8	Test Data Table 1.2.8	Test Data Table 1.2.8
Aluminum Alloy 2219	~~Test Data Table 1.2.8~~Note 4	ASM [4.2.19]	ASM [4.2.19]	ASM [4.2.19]

Note 1: Emissivity not reported as radiation heat dissipation from these surfaces is conservatively neglected.
Note 2: Used in the MPC lid.
Note 3: Used in the MPC shell and baseplate.
Note 4: **[Withheld in Accordance with 10 CFR 2.390]**

Table 4.2.4

SUMMARY OF MATERIALS SURFACE EMISSIVITY DATA*

Material	**Emissivity**
Zircaloy	0.80
Painted surfaces	0.85
Stainless steel (machined forgings)	0.36
Stainless Steel Plates	0.587**
Carbon Steel	0.66
Metamic-HT***	Table 1.2.8
Extruded Shims (Aluminum Alloy 2219)‡	Table 1.2.9 **[Withheld in Accordance with 10 CFR 2.390]**
Solid Shims (Aluminum Alloy)‡	Table 1.2.9

* See Table 4.2.1 for cited references.

** Lower bound value from the cited references in Table 4.2.1.

*** [

Withheld in Accordance with 10 CFR 2.390

]

4.4 THERMAL EVALUATION FOR NORMAL CONDITIONS OF STORAGE

The HI-STORM FW Storage System (i.e., HI-STORM FW overpack and MPC) and HI-TRAC VW transfer cask thermal evaluation is performed in accordance with the guidelines of NUREG-1536 [4.4.1] and ISG-11 [4.1.4]. To ensure a high level of confidence in the thermal evaluation, 3-dimensional models of the MPC, HI-STORM FW overpack and HI-TRAC VW transfer cask are constructed to evaluate fuel integrity under normal (long-term storage), off-normal and accident conditions and in the HI-TRAC VW transfer cask under short-term operation and hypothetical accidents. The principal features of the thermal models are described in this section for HI-STORM FW and Section 4.5 for HI-TRAC VW. Thermal analyses results for the long-term storage scenarios are obtained and reported in this section. The evaluation addresses the design basis thermal loadings defined in Chapter 1, Tables 1.2.3a (MPC-37, Patterns A and B) 1.2.3b (MPC-32ML), 1.2.3c (MPC-31C) and 1.2.4 (MPC-89). Based on these evaluations the limiting thermal loading condition is defined in Subsection 4.4.4 and adopted for evaluation of on-site transfer in the HI-TRAC (Section 4.5) and off-normal and accident events defined in Section 4.6.

4.4.1 Overview of the Thermal Model

As illustrated in the drawings in Section 1.5, the basket is a matrix of interconnected square compartments designed to hold the fuel assemblies in a vertical position under long term storage conditions. The basket is a honeycomb structure of Metamic-HT plates that are slotted and arrayed in an orthogonal configuration to form an integral basket structure. **[**

Withheld in Accordance with 10 CFR 2.390

]

Thermal analysis of the HI-STORM FW System is performed for all heat load scenarios defined in Chapter 1 for regionalized storage (Figures 1.2.1a and 1.2.2) and uniform storage (Figures 1.2.1b and 1.2.1c). Each fuel assembly is *assumed to be generating heat at the maximum permissible rate (Tables 1.2.3a, 1.2.3b, 1.2.3c and 1.2.4)*. While the assumption of limiting heat generation in each storage cell imputes a certain symmetry to the cask thermal problem, it grossly overstates the total heat duty of the system in most cases because it is unlikely that any basket would be loaded with fuel emitting heat at their limiting values in *each* storage cell. Thus, the thermal model for the HI-STORM FW system is inherently conservative for real life applications. Other noteworthy features of the thermal analyses are:

i. While the rate of heat conduction through metals is a relatively weak function of temperature, radiation heat exchange increases rapidly as the fourth power of absolute temperature.

ii. Heat generation in the MPC is axially non-uniform due to non-uniform axial burnup

profiles in the fuel assemblies.

iii. Inasmuch as the transfer of heat occurs from inside the basket region to the outside, the temperature field in the MPC is spatially distributed with the lowest values reached at the periphery of the basket.

As noted in Chapter 1 and in Section 3.2, the height of the PWR MPC cavity can vary within a rather large range to accommodate spent nuclear fuel of different lengths in the MPC-37 and MPC-89[1]. The heat load limits in Table 1.2.3 (PWR MPC) and Table 1.2.4 (BWR MPC) for regionalized storage are, however, fixed regardless of the fuel (and hence MPC cavity) length. Because it is not a'priori obvious whether the shortest or the longest fuel case will govern, thermal analyses are performed for the minimum[2], reference and maximum height MPCs. Table 2.1.1 allows two different fuel assembly lengths under "minimum" category for PWR fuel. Unless specified in this chapter, the term "minimum" or "short" is used for all short fuel assembly arrays except 15x15I short fuel defined in Chapter 2.

4.4.1.1 Description of the 3-D Thermal Model

i. Overview

The HI-STORM FW System is equipped with fourtwo MPC designs, MPC-37, MPC-32ML, MPC-31C and MPC-89 engineered to store 37, 32, 31 PWR and 89 PWR and BWR fuel assemblies respectively. The interior of the MPC is a 3-D array of square/hexagonal shaped cells inside an irregularly shaped basket outline confined inside the cylindrical space of the MPC cavity. To ensure an adequate representation of these features, a 3-D geometric model of the MPC is constructed using the FLUENT CFD code pre-processor [4.1.2]. Because the fuel basket is made of a single isotropic material (Metamic-HT), the 3-D thermal model requires no idealizations of the fuel basket structure. However, since it is impractical to model every fuel rod in every stored fuel assembly explicitly, the cross-section bounded by the inside of the storage cell (inside of the fuel channel in the case of BWR MPCs), which surrounds the assemblage of fuel rods and the interstitial helium gas (also called the "rodded region"), is replaced with an "equivalent" square or hexagonal (MPC-31C) homogeneous section characterized by an effective thermal conductivity. Homogenization of the cell cross-section is discussed under item (ii) below. For thermal-hydraulic simulation, each fuel assembly in its storage cell is represented by an equivalent porous medium. For BWR fuel, the presence of the fuel channel divides the storage cell space into two distinct axial flow regions, namely, the in-channel (rodded) region and the square prismatic annulus region (in the case of PWR fuel this modeling complication does not exist). The methodology to represent the spent fuel storage space as a homogeneous region with equivalent conductivities is identical to that used in the HI-STORM 100 Docket No. 72-1014 [4.1.8].

1 MPC-32ML and MPC-31C are fixed fuel length canisters for storing a specific fuel defined in Table 2.1.1b.

2 Both allowable PWR fuel assembly lengths under "minimum" category as shown in Table 2.1.1 are evaluated in this chapter.

ii. Details of the 3-D Model

The HI-STORM FW fuel basket is modeled in the same manner as the model described in the HI-STAR 180 SAR (NRC Docket No. 71-9325) [4.1.11]. Modeling details are provided in the following:

Fuel Basket 3D Model

The MPC-37, MPC-32ML and MPC-89 fuel baskets are essentially an array of square cells and MPC-31C hexagonal cells within an irregularly shaped basket outline. The fuel basket is confined inside a cylindrical cavity of the MPC shell. Between the fuel basket-to-shell spaces, thick Aluminum basket shims are installed to facilitate heat dissipation. To ensure an adequate representation of the fuel basket a geometrically accurate 3D model of the array of square cells and Metamic-HT plates is constructed using the FLUENT pre-processor. Other than the representation of fuel assemblies inside the storage cell spaces as porous region with effective thermal-hydraulic properties as described in the next paragraph, the 3D model includes an explicit articulation of other canister parts. The basket shims are explicitly modeled in the peripheral spaces. The fuel basket is surrounded by the MPC shell and outfitted with a solid welded lid above and a baseplate below. All of these physical details are explicitly articulated in a quarter-symmetric 3D thermal model of the HI-STORM FW as shown in Figures 4.4.2a, 4.4.2b, 4.4.2c and 4.4.3.

Fuel Region Effective Planar Conductivity

In the HI-STORM FW thermal modeling, the cross section bounded by the inside of a PWR storage cell and the channeled area of a BWR storage cell is replaced with an "equivalent" square section characterized by an effective thermal conductivity in the planar and axial directions. Figure 4.4.1 pictorially illustrates this concept. The two conductivities are unequal because while in the planar direction heat dissipation is interrupted by inter-rod gaps; in the axial direction heat is dissipated through a continuous medium (fuel cladding). The equivalent planar conductivity of the storage cell space is obtained using a 2D conduction-radiation model of the bounding PWR and BWR fuel storage scenarios defined in the table below. The fuel geometry, consisting of an array of fuel rods with helium gaps between them residing in a storage cell, is constructed using QA validated computer codes~~the~~ (ANSYS code [4.1.1] and FLUENT[1] [4.1.2]) and lowerbound conductivities under the assumed condition of stagnant helium (no-helium-flow-condition) are obtained. In the axial direction, an area-weighted average of the cladding and helium conductivities is computed. Axial heat conduction in the fuel pellets is conservatively ignored.

The effective fuel conductivity is computed under four bounding fuel storage configurations for PWR fueled MPC-37, one each MPC-32ML and MPC-31C for specific PWR fuel and one bounding scenario for BWR fueled MPC-89. The fuel storage configurations are defined below:

[1] NRC has accepted FLUENT code for evaluation of fuel conductivities in the HI-STAR 180D licensing (Docket No. 71-9367).

Storage Scenario	MPC	Fuel
PWR: 15x15I Short Fuel	Minimum Height MPC-37 for 15x15I fuel assembly array	15x15I in Table 2.1.2
PWR: Short Fuel	Minimum Height MPC-37 for all fuel assembly arrays except 15x15I	14x14 Ft. Calhoun
PWR: Standard Fuel	Reference Height MPC-37	W-17x17
PWR: XL Fuel	Maximum Height MPC-37	AP1000
PWR: 16x16D	MPC-32ML	16x16D
PWR: V10A/V10B	MPC-31C	VVER 1000
BWR	MPC-89	GE-10x10

The fuel region effective conductivity is defined as the calculated equivalent conductivity of the fuel storage cell due to the combined effect of conduction and radiation heat transfer in the manner of the approach used in the HI-STORM 100 system (Docket No. 72-1014). Because radiation is proportional to the fourth power of absolute temperature, the effective conductivity is a strong function of temperature. ~~The~~ ANSYS and FLUENT computer codes~~finite element model~~ have been~~is~~ used to characterize fuel resistance at several representative storage cell temperatures and the effective thermal conductivity as a function of temperature obtained for all storage configurations defined above and tabulated in Table 4.4.1.

Heat Rejection from External Surfaces

The exposed surfaces of the HI-STORM FW dissipate heat by radiation and external natural convection heat transfer. Radiation is modeled using classical equations for radiation heat transfer (Rohsenow & Hartnett [4.2.2]). Jakob and Hawkins [4.2.9] recommend the following correlations for natural convection heat transfer to air from heated vertical and horizontal surfaces:

Turbulent range:

$$h = 0.19\,(\Delta T)^{1/3}\ (\text{Vertical}, \text{GrPr} > 10^9)$$

$$h = 0.18\,(\Delta T)^{1/3}\ (\text{Horizontal Cylinder}, \text{GrPr} > 10^9)$$

$$(\text{in conventional U.S. units})$$

Laminar range:

$$h = 0.29\,(\frac{\Delta T}{L})^{1/4}\ (\text{Vertical}, \text{GrPr} < 10^9)$$

$$h = 0.27\,(\frac{\Delta T}{D})^{1/4}\ (\text{Horizontal Cylinder}, \text{GrPr} < 10^9)$$

HI-STAR 180 in docket 71-9325. This model has the following key attributes:

a) The fuel storage spaces are modeled as porous media having effective thermal-hydraulic properties.

b) In the case of BWR MPC-89, the fuel bundle and the small surrounding spaces inside the fuel "channel" are replaced by an equivalent porous media having the flow impedance properties computed using a conservatively articulated 3-D CFD model [4.4.2]. The space between the BWR fuel channel and the storage cell is represented as an open flow annulus. The fuel channel is also explicitly modeled. The channeled space within is also referred to as the "rodded region" that is modeled as a porous medium. The fuel assembly is assumed to be positioned coaxially with respect to its storage cell. The MPC-89 storage cell occupied with channeled BWR fuel is shown in Figure 4.4.4.

   In the case of the PWR CSF, the porous medium extends to the entire cross-section of the storage cell. As described in [4.4.2], the CFD models for both the BWR and PWR storage geometries are constructed for the Design Basis fuel defined in Table 2.1.4. The model contains comprehensive details of the fuel which includes grid straps, BWR water rods and PWR guide and instrument tubes (assumed to be plugged for conservatism).

c) The effective conductivities of the MPC storage spaces are computed for bounding fuel storage configurations defined in Paragraph 4.4.1.1(ii). The in-plane thermal conductivities are obtained using ANSYS [4.1.1] and FLUENT [4.4.2] computer~~finite element~~ models of an array of fuel rods enclosed by a square box. Radiation heat transfer from solid surfaces (cladding and box walls) is enabled in these models. Using these models the effective conduction-radiation conductivities are obtained and reported in Table 4.4.1. For heat transfer in the axial direction an area weighted mean of cladding and helium conductivities are computed (see Table 4.4.1). Axial conduction heat transfer in the fuel pellets and radiation heat dissipation in the axial direction are conservatively ignored. Thus, the thermal conductivity of the rodded region, like the porous media simulation for helium flow, is represented by a 3-D continuum having effective planar and axial conductivities. In the interest of conservatism, thermal analysis of normal storage condition in HI-STORM FW and normal onsite transfer condition in HI-TRAC VW (Section 4.5) are performed with a 10% reduced effective thermal conductivity of fuel region.

d) The internals of the MPC, including the basket cross-section, aluminum shims, bottom flow holes, top plenum, and circumferentially irregular downcomer formed by the annulus gap in the aluminum shims are modeled explicitly. For simplicity, the flow holes are modeled as rectangular openings with an understated flow area.

e) The inlet and outlet vents in the HI-STORM FW overpack are modeled explicitly to incorporate any effects of non-axisymmetry of inlet air passages on the system's thermal performance.

f) The air flow in the HI-STORM FW/MPC annulus is simulated by the k-ω turbulence model with the transitional option enabled. The adequacy of this turbulence model is confirmed in the Holtec benchmarking report [4.1.6]. The annulus grid size is selected to ensure a converged solution.(See Section 4.4.1.6).

g) A limited number of fuel assemblies defined in Table 1.2.1 ~~(upto 12 in MPC-37 and upto 16 in MPC-89)~~ classified as damaged fuel are permitted to be stored in the MPC inside Damaged Fuel Containers (DFCs). A DFC can be stored in the outer peripheral locations of ~~both~~ MPC-37, MPC-32ML, MPC-31C and MPC-89 as shown in Figures 2.1.1a, 2.1.1b, 2.1.1c and 2.1.2, respectively. DFC emplaced fuel assemblies have a higher resistance to helium flow because of the debris screens. However, DFC fuel storage does not affect temperature of hot fuel stored in the core of the basket because DFC storage is limited by Technical Specifications for placement in the peripheral storage locations away from hot fuel. For this reason the thermal modeling of the fuel basket under the assumption of all storage spaces populated with intact fuel is justified.

h) As shown in HI-STORM FW drawings in Section 1.5 the HI-STORM FW overpack is equipped with an optional heat shield to protect the inner shell and concrete from radiation heating by the emplaced MPC. The inner and outer shells and concrete are explicitly modeled. All the licensing basis thermal analyses explicitly include the heat shields. A sensitivity study is performed as described in paragraph 4.4.1.9 to evaluate the absence of heat shield on the overpack inner shell and overpack lid.

i) To maximize lateral resistance to heat dissipation in the fuel basket, 0.8 mm full length inter- panel gaps are conservatively assumed to exist at all intersections. This approach is identical to that used in the thermal analysis of the HI-STAR 180 Package in Docket 71-9325. The shims installed in the MPC peripheral spaces (See MPC-37, MPC-32ML, MPC-31C and MPC-89 drawings in Section 1.5) are explicitly modeled. For conservatism bounding as-built gaps (3 mm basket-to-shims and 3 mm shims-to-shell) are assumed to exist and incorporated in the thermal models.

j) The thermal models incorporate all modes of heat transfer (conduction, convection and radiation) in a conservative manner.

k) The Discrete Ordinates (DO) model, previously utilized in the HI-STAR 180 docket (Docket 71-9325), is deployed to compute radiation heat transfer.

l) Laminar flow conditions are applied in the MPC internal spaces to obtain a lowerbound rate of heat dissipation.

The 3-D model described above is illustrated in the cross-section for the MPC-89, MPC-32ML, MPC-31C and MPC-37 in Figures 4.4.2a, 4.4.2b, 4.4.2c and 4.4.3, respectively. A closeup of the fuel cell spaces which explicitly include the channel-to-cell gap in the 3-D model applicable to BWR fueled basket (MPC-89) is shown in Figure 4.4.4. The principal 3-D modeling conservatisms are listed below:

1) The storage cell spaces are loaded with high flow resistance design basis fuel assemblies (See Table 2.1.4).
2) Each storage cell is generating heat at its limiting value under the regionalized storage scenarios defined in Chapter 2, Section 2.1.
3) Axial dissipation of heat by conduction in the fuel pellets is neglected.
4) Dissipation of heat from the fuel rods by radiation in the axial direction is neglected.
5) The fuel assembly channel length for BWR fuel is overstated.
6) The most severe environmental factors for long-term normal storage – ambient temperature of 80°F and 10CFR71 insolation levels – were coincidentally imposed on the system.
7) Reasonably bounding solar absorbtivity of HI-STORM FW overpack external surfaces is applied to the thermal models.
8) To understate MPC internal convection heat transfer, the helium pressure is understated.
9) No credit is taken for contact between fuel assemblies and the MPC basket wall or between the MPC basket and the basket supports.
10) Heat dissipation by fuel basket peripheral supports is neglected.
11) Lowerbound fuel basket emissivity function defined in the Metamic-HT Sourcebook [4.2.6] is adopted in the thermal analysis.
12) Lowerbound stainless steel emissivity obtained from cited references (See Table 4.2.1) are applied to MPC shell.
13) The k-ω model used for simulating the HI-STORM FW annulus flow yields uniformly conservative results [4.1.6].
14) Fuel assembly length is conservatively modeled equal to the height of the fuel basket.

The effect of crud resistance on fuel cladding surfaces has been evaluated and found to be negligible [4.1.8]. The evaluation assumes a thick crud layer (130 μm) with a bounding low conductivity (conductivity of helium). The crud resistance increases the clad temperature by a very small amount (~0.1°F) [4.1.8]. Accordingly this effect is neglected in the thermal evaluations.

4.4.1.2 Fuel Assembly 3-Zone Flow Resistance Model[1]

[1] This Sub- section duplicates the methodology used in the HI-STORM FSAR, Rev. 7, supporting CoC Amendment

Figure 4.4.4. The channeled space occupied by the GE-10x10 fuel assembly is modeled as a porous region with effective flow resistance properties computed by deploying an independent 3D FLUENT model of the array of fuel rods and grid spacers.

In the PWR fuel resistance modeling case physical reasoning suggests that the flow resistance of a fuel assembly placed in the larger MPC-37 storage cell will be less than that computed using the (smaller) counterpart cells cavities in the MPC-32. However to provide numerical substantiation FLUENT calculations are performed for the case of W-17x17 fuel placed inside the MPC-32 cell opening of 8.79" and the enlarged MPC-37 cell opening of 8.94". The FLUENT results for the cell pressure drops under the baseline (MPC-32) and enlarged cell opening (MPC-37) scenarios are shown plotted in Figure 4-4-7. The plot shows that, as expected, the larger cell cross section case (MPC-37) yields a smaller pressure loss. Therefore, the MPC-37 flow resistance is bounded by the MPC-32 flow resistance used in the FLUENT simulations in the SAR. This evaluation is significant because the MPC-37 basket is determined as the limiting MPC and therefore the licensing basis HI-STORM FW temperatures by use of higher-than-actual resistance are overstated.

However, as mentioned in Sub-section 4.4.1.2, a flow resistance of $1x10^6$ m^{-2} through PWR fuel assemblies is used in the thermal analysis.

4.4.1.5 Screening Calculations to Ascertain Limiting Storage Scenario

To define the thermally most limiting HI-STORM FW storage scenario the following cases are evaluated under the limiting heat load patterns defined in Tables ~~1.2.3a, 1.2.3b,~~ 1.2.3a~~e~~[1], 1.2.3b, 1.2.3c and 1.2.4:

(i) MPC-89
(ii) Minimum height MPC-37
(iii) Reference height MPC-37
(iv) Maximum height MPC-37
(v) MPC-32ML
(vi) MPC-31C

To evaluate the above scenarios, 3D FLUENT screening models of the HI-STORM FW cask are constructed, Peak Cladding Temperatures (PCT) computed and tabulated in Table 4.4.2. The results of the calculations yield the following:

(a) Fuel storage in MPC-37 produces a higher peak cladding temperature than that in MPC-89
(b) Fuel storage in the minimum height MPC-37 is limiting (produces the highest peak cladding temperature).

[1] Pattern A defined in Table 1.2.3a is the limiting fuel storage pattern (See Subsection 4.4.4.1).

Table 1.2.9 since it results in the most limiting PCT and MPC pressure (see supporting evaluations in Section 4.5).

4.4.1.9 Evaluation of Overpack Heat Shields

HI-STORM FW overpack is equipped with a heat shield on the overpack inner shell and underneath the overpack lid concrete. They are optional features engineered to protect the overpack body concrete and overpack lid concrete from excessive temperature rise due to radiant heat from the MPC. Absence of the heat shields will have an adverse impact on the overpack temperatures. To quantify the impact, a thermal evaluation is performed for a HI-STORM overpack without the heat shields. The thermal model is exactly the same as the converged mesh discussed above in paragraph 4.4.1.6 except that heat shields are removed from the thermal model. The results of this thermal evaluation are discussed in paragraph 4.4.4.4.

4.4.1.10 Evaluation of 16x16D and VVER-1000 Fuel Assembly

(a) 16x16D
This fuel type is defined in Table 2.1.1b for storage in MPC-32ML. As the number of rods in this fuel type is bounded by W-17x17 fuel physical reasoning will suggest flow resistance would be bounded by it. As a due diligence measure the methodology defined in Para 4.4.1.7 is adopted to evaluate 16x16D flow resistance. The flow resistance computes ~50% of the reference W-17x17 fuel [4.1.9]. However, in the interest of conservatism a robustly bounding value of $1x10^{6}$ m^{-2} is adopted in the thermal analysis.

(b) VVER-1000 fuel
This is a unique fuel type that features a triangular rods pitch and a hexagonal cross-section that renders it not suitable for referencing to W-17x17 fuel. As an over-arching measure of conservatism axial flow of helium in VVER-1000 fuel assemblies situated in MPC-31C is conservatively neglected.

4.4.2 Effect of Neighboring Casks

HI-STORM FW casks are typically stored on an ISFSI pad in regularly spaced arrays (See Section 1.4, Figures 1.4.1 and 1.4.2). Relative to an isolated HI-STORM FW the heat dissipation from a HI-STORM FW cask placed in an array is somewhat disadvantaged. However, as the analysis in this Sub-section shows, the effect of the neighboring casks on the peak cladding temperature in the "surrounded" cask is insignificant.

(i) Effect of Insolation
The HI-STORM FW casks are subject to insolation heating during daytime hours. Presence of surrounding casks has the salutary effect of partially blocking insolation flux. This effect, results in lower temperatures and in the interest of conservatism is ignored in the analysis.

(ii) Effect of Radiation Blocking

4. The hypothetical square cavity is open at the top as shown in Figure 4.4.6 to allow ambient air access for ventilation cooling in a conservative manner.

The principal results of the hypothetical square cavity thermal model are tabulated below and compared with the baseline thermal results tabulated in Section 4.4.4.

Model	Peak Clad Temperature (^{o}F)	Margin-to-Limit (^{o}F)
Single Cask Model	703	49
Hypothetical Square Cavity Thermal Model	702.1	50
Peak cladding temperature reported for the limiting heat load MPC-37 Pattern A (See Subsection 4.4.4.1)		

The results show that the presence of surrounding casks has essentially no effect on the fuel cladding temperatures (the difference in the results is within the range of numerical round-off). These results are in line with prior thermal evaluations of the effect of surrounding casks in the NRC approved HI-STORM 100 System in Docket 72-1014.

4.4.3 Test Model

The HI-STORM FW thermal analysis is performed on the FLUENT [4.1.2] Computational Fluid Dynamics (CFD) program. To ensure a high degree of confidence in the HI-STORM FW thermal evaluations, the FLUENT code has been benchmarked using data from tests conducted with casks loaded with irradiated SNF ([4.1.3],[4.1.7]). The benchmark work is archived in QA validated Holtec reports ([4.1.5],[4.1.6]). These evaluations show that the FLUENT solutions are conservative in all cases. In view of these considerations, additional experimental verification of the thermal design is not necessary. FLUENT has also been used in all Holtec International Part 71 and Part 72 dockets since 1996.

4.4.4 Maximum and Minimum Temperatures

4.4.4.1 Maximum Temperatures

The 3-D model from the previous subsection is used to determine temperature distributions under long-term normal storage conditions for both BWR canisters (MPC-89) and PWR canisters (MPC-37, MPC-32ML and MPC-31C). Tables 4.4.2, 4.4.3 and 4.4.5 provide key thermal and pressure results from the FLUENT simulations, respectively. Tables 4.4.12 and 4.4.13 respectively provide the temperature and pressure results from the FLUENT simulation of

[1] The lower computed temperature is an artifact of the use of overstated inlet and outlet loss coefficients in the single cask model. The result supports the conclusion that surrounding casks have essentially no effect on the Peak Cladding Temperatures.

the 15x15I short fuel assembly height based on the methodology discussed in Sub-Section 4.4.1.7. The peak fuel cladding result in these tables is actually overstated by the fact that the 3-D FLUENT cask model incorporates the effective conductivity of the fuel assembly sub-model. Therefore the FLUENT models report the peak temperature *in the fuel storage cells*. Thus, as the fuel assembly models include the fuel pellets, the FLUENT calculated peak temperatures are actually peak pellet centerline temperatures which bound the peak cladding temperatures with a modest margin.

The following observations can be derived by inspecting the temperature field obtained from the thermal models:

- The fuel cladding temperatures are below the regulatory limit (ISG-11 [4.1.4]) under all uniform and regionalized storage scenarios defined in Chapter 1 (Figures 1.2.1a, 1.2.1b, 1.2.1c and 1.2.2) and thermal loading scenarios defined in Tables 1.2.3a, 1.2.3b, 1.2.3c and 1.2.4.

- The limiting fuel temperatures are reached under the Pattern A thermal loading condition defined in Table 1.2.3a in the MPC-37. Accordingly this scenario is adopted for thermal evaluation under on-site transfer (Section 4.5) and under off-normal and accident conditions (Section 4.6).

- The maximum temperature of the basket structural material is within its design limit.

- The maximum temperatures of the MPC pressure boundary materials are below their design limits.

- The maximum temperatures of concrete are within the guidance of the governing ACI Code (see Table 2.2.3).

- The calculated fuel temperature for the 15x15I short fuel assembly (Table 4.4.12) is bounded by the thermal evaluations for the minimum MPC-37 for short fuel (Table 4.4.3). The temperatures of other cask components are similar. It is reasonable to conclude that the temperatures and pressure for the minimum height MPC-37 (short fuel) bounds all scenarios.

The above observations lead us to conclude that the temperature field in the HI-STORM FW System with a loaded MPC containing heat emitting SNF complies with all regulatory temperature limits (Table 2.2.3). In other words, the thermal environment in the HI-STORM FW System is in compliance with Chapter 2 Design Criteria.

Also, all the licensing basis thermal evaluations documented in this chapter are performed for the most limiting thermal scenarios i.e. minimum MPC-37 with heat load pattern A.

altitude on the PCT shall be quantified as part of the 10 CFR 72.212 evaluation for the site using the site ambient conditions.

4.4.4.4 Evaluation of Overpack Heat Shields

As discussed in Sub-section 4.4.1.9 above, a thermal evaluation is performed to evaluate the effect of removal of heat shields from a HI-STORM overpack. The predicted temperatures from this sensitivity study of normal condition of storage are summarized in Table 4.4.14. The peak cladding temperature, basket and MPC component temperatures decrease due to removal of heat shields. As expected, the results demonstrate an increase in overpack component temperatures. However, the overpack component temperatures are below their respective normal temperature limits with significant margins. Therefore, removal of heat shields does not have a detrimental effect on the system' thermal performance.

The temperatures of overpack components increase due to removal of heat shields under normal conditions of storage. This temperature increase is then added to the predicted temperatures of all the off-normal and accident conditions discussed in Section 4.6. The resulting temperatures are still well below their respective temperature limits which demonstrate that safety conclusions made for all the off-normal and accident condition evaluations in Section 4.6 remain valid even after the removal of heat shields from the HI-STORM overpack.

4.4.5 Maximum Internal Pressure

4.4.5.1 MPC Helium Backfill Pressure

The quantity of helium emplaced in the MPC cavity shall be sufficient to yield design operating pressures defined in Table 4.4.15.~~produce an operating pressure of 7.1 and 7.0 atmospheres (absolute) respectively for loading patterns A and B during normal storage conditions defined in Table 4.1.1.~~ Thermal analyses performed on the different MPC designs indicate that this operating pressure requires a certain minimum helium backfill pressure (P_b) specified at a reference temperature (70ºF). The minimum backfill pressure for each MPC type is provided in Table 4.4.7. A theoretical upper limit on the helium backfill pressure also exists and is defined by the design pressure of the MPC vessel (Table 2.2.1). The upper limit of P_b is also reported in Table 4.4.7. To bound the minimum and maximum backfill pressures listed in Table 4.4.7 with a margin, a helium backfill specification is set forth in Table 4.4.8.

To provide additional helium backfill range for less than design basis heat load canisters a Sub-Design-Basis (SDB) heat load scenario is defined below:

(i) MPC-37 under 80% Pattern A Heat Load (Table 1.2.3)
(ii) MPC-37 under 90% Pattern A Heat Load (Table 1.2.3)
(iii) MPC-89 under 80% Design Heat Load (Table 1.2.4)
(iv) MPC-37 under vacuum drying threshold heat load in Table 4.5.1[1].

[1] Threshold scenarios (iv) and (v) are bounded by scenarios (i) and (iii) respectively because the core Region 1

(v) MPC-89 under vacuum drying threshold heat load in Table 4.5.1[1]*.

The storage cell and MPC heat load limits under the SDB scenario (i), (ii) & (iii) are specified in Table 4.4.11. Calculations for bounding scenarios (i), (ii) & (iii) show that the maximum cladding temperature under the SDB scenario meet the ISG-11 temperature limits. The helium backfill pressure limits supporting this scenario are defined in Table 4.4.10. These backfill limits maybe optionally adopted by a cask user if the decay heats of the loaded fuel assemblies meet the SDB decay heat limits stipulated above.

Two methods are available for ensuring that the appropriate quantity of helium has been placed in an MPC:

i. By pressure measurement
ii. By measurement of helium backfill volume (in standard cubic feet)

The direct pressure measurement approach is more convenient if the FHD method of MPC drying is used. In this case, a certain quantity of helium is already in the MPC. Because the helium is mixed inside the MPC during the FHD operation, the temperature and pressure of the helium gas at the MPC's exit provides a reliable means to compute the inventory of helium. A shortfall or excess of helium is adjusted by a calculated raising or lowering of the MPC pressure such that the reference MPC backfill pressure is within the range specified in Table 4.4.8 or Table 4.4.10 (as applicable).

When vacuum drying is used as the method for MPC drying, then it is more convenient to fill the MPC by introducing a known quantity of helium (in standard cubic feet) by measuring the quantity of helium introduced using a calibrated mass flow meter or other measuring apparatus. The required quantity of helium is computed by the product of net free volume and helium specific volume at the reference temperature (70^{o}F) and a target pressure that lies in the mid-range of the Table 4.4.8 pressures.

The net free volume of the MPC is obtained by subtracting B from A, where

A = MPC cavity volume in the absence of contents (fuel and non-fuel hardware) computed from nominal design dimensions

B = Total volume of the contents (fuel including DFCs, if used) based on nominal design dimensions

Using commercially available mass flow totalizers or other appropriate measuring devices, an MPC cavity is filled with the computed quantity of helium.

4.4.5.2 MPC Pressure Calculations

---

assembly heat loads and total cask heat loads are bounded by the Sub-Design Basis heat loads in Table 4.4.11.

The MPC is initially filled with dry helium after fuel loading and drying prior to installing the MPC closure ring. During normal storage, the gas temperature within the MPC rises to its maximum operating basis temperature. The gas pressure inside the MPC will also increase with rising temperature. The pressure rise is determined using the ideal gas law. The MPC gas pressure is also subject to substantial pressure rise under hypothetical rupture of fuel rods and large gas inventory non-fuel hardware (PWR BPRAs). To minimize MPC gas pressures the number of BPRA containing fuel assemblies must be limited to that specified in Chapter 2, Section 2.1~~30~~.

Table 4.4.4 presents a summary of the MPC free volumes determined for the fixed height MPC-89, ~~and~~ lowerbound height MPC-37, MPC-32ML and MPC-31C fuel storage scenarios. The MPC maximum gas pressure is computed for a postulated release of fission product gases from fuel rods into this free space. For these scenarios, the amounts of each of the release gas constituents in the MPC cavity are summed and the resulting total pressures determined from the ideal gas law. A concomitant effect of rod ruptures is the increased pressure and molecular weight of the cavity gases with enhanced rate of heat dissipation by internal helium convection and lower cavity temperatures. As these effects are substantial under large rod ruptures the 100% rod rupture accident is evaluated with due credit for increased heat dissipation under increased pressure and molecular weight of the cavity gases. Based on fission gases release fractions (NUREG 1536 criteria [4.4.1]), rods' net free volume and initial fill gas pressure, maximum gas pressures with 1% (normal), 10% (off-normal) and 100% (accident condition) rod rupture are given in Table 4.4.5. The results of the calculations support the following conclusions:

(i) The maximum computed gas pressures reported in Table 4.4.5 under all design basis thermal loadings defined in Section 4.4 are all below the MPC internal design pressures for normal, off-normal and accident conditions specified in Table 2.2.1.

(ii) The MPC gas pressure obtained under loading Pattern A is essentially same as in Pattern B. Accordingly Pattern A loading condition for pressure boundary evaluation of MPC in the HI-TRAC and under off-normal and accident conditions is retained.

Evaluation of Non-Fuel Hardware

The inclusion of PWR non-fuel hardware (BPRA control elements and thimble plugs) to the PWR basket influences the MPC internal pressure through two distinct effects. The presence of non-fuel hardware increases the effective basket conductivity, thus enhancing heat dissipation and lowering fuel temperatures as well as the temperature of the gas filling the space between fuel rods. The gas volume displaced by the mass of non-fuel hardware lowers the cavity free volume. These two effects, namely, temperature lowering and free volume reduction, have opposing influence on the MPC cavity pressure. The first effect lowers gas pressure while the second effect raises it. In the HI-STORM FW thermal analysis, the computed temperature field (with non-fuel hardware excluded) has been determined to provide a conservatively bounding temperature field for the PWR baskets. The MPC cavity free space is computed based on conservatively computed volume displacement by fuel with non-fuel hardware included. This

approach ensures conservative bounding pressures.

During in-core irradiation of BPRAs, neutron capture by the B-10 isotope in the neutron absorbing material produces helium. Two different forms of the neutron absorbing material are used in BPRAs: Borosilicate glass and B_4C in a refractory solid matrix (At_2O_3). Borosilicate glass (primarily a constituent of Westinghouse BPRAs) is used in the shape of hollow pyrex glass tubes sealed within steel rods and supported on the inside by a thin-walled steel liner. To accommodate helium diffusion from the glass rod into the rod internal space, a relatively high void volume (~40%) is engineered in this type of rod design. The rod internal pressure is thus designed to remain below reactor operation conditions (2,300 psia and approximately 600°F coolant temperature). The B_4C- Al_2O_3 neutron absorber material is principally used in B&W and CE fuel BPRA designs. The relatively low temperatures of the poison material in BPRA rods (relative to fuel pellets) favor the entrapment of helium atoms in the solid matrix.

Several BPRA designs are used in PWR fuel. They differ in the number, diameter, and length of poison rods. The older Westinghouse fuel (W-14x14 and W-15x15) has used 6, 12, 16, and 20 rods per assembly BPRAs and the later (W-17x17) fuel uses up to 24 rods per BPRA. The BPRA rods in the older fuel are much larger than the later fuel and, therefore, the B-10 isotope inventory in the 20-rod BPRAs bounds the newer W-17x17 fuel. Based on bounding BPRA rods internal pressure, a large hypothetical quantity of helium (7.2 g-moles/BPRA) is assumed to be available for release into the MPC cavity from each BPRA containing fuel assembly. For a bounding evaluation the maximum permissible number of BPRA containing fuel assemblies (see discussion at the beginning of this Section) are assumed to be loaded. The MPC cavity pressures (including helium from BPRAs) are summarized in Table 4.4.5 for the bounding MPC-37 (minimum MPC height and heat load Patterns A and B), MPC-32ML, MPC-31C and MPC-89 (design heat load) storage scenarios.

4.4.6 Engineered Clearances to Eliminate Thermal Interferences

Thermal stress in a structural component is the resultant sum of two factors, namely: (i) restraint of free end expansion and (ii) non-uniform temperature distribution. To minimize thermal stresses in load bearing members, the HI-STORM FW system is engineered with adequate gaps to permit free thermal expansion of the fuel basket and MPC in axial and radial directions. In this subsection, differential thermal expansion calculations are performed to demonstrate that engineered gaps in the HI-STORM FW System are adequate to accommodate thermal expansion of the fuel basket and MPC.

The HI-STORM FW System is engineered with gaps for the fuel basket and MPC to expand thermally without restraint of free end expansion. The following gaps are evaluated:

a. Fuel Basket-to-MPC Radial Gap
b. Fuel Basket-to-MPC Axial Gap
c. MPC-to-Overpack Radial Gap
d. MPC-to-Overpack Axial Gap

Table 4.4.1

EFFECTIVE FUEL PROPERTIES UNDER BOUNDING FUEL STORAGE CONFIGURATIONS[Note 1]

	Conductivity (Btu/hr-ft-°F)			
	PWR: Short Fuel		**PWR: Standard Fuel**	
Temperature (°F)	Planar	Axial	Planar	Axial
200	0.247	0.813	0.231	0.759
450	0.443	0.903	0.387	0.845
700	0.730	1.016	0.601	0.951
	PWR: XL Fuel		**BWR Fuel**	
	Planar	Axial	Planar	Axial
200	0.239	0.787	0.283	0.897
450	0.393	0.875	0.426	0.988
700	0.599	0.984	0.607	1.104

PWR: 15x15I Short Fuel		
Temperature (°F)	Planar	Axial
200	0.226	0.763
450	0.386	0.848
700	0.601	0.955

Thermal Inertia Properties		
	Density (lb/ft^3)	Heat Capacity (Btu/lb-°F)[Note 2]
PWR: 15x15I Short Fuel	194.5	0.056
PWR: Short Fuel	165.8	0.056
PWR: Standard Fuel	176.2	0.056
PWR: XL Fuel	187.5	0.056
BWR Fuel	255.6	0.056

Note 1: Bounding fuel storage configurations defined in 4.4.1.1(ii).
Note 2: The lowerbound heat capacity of principal fuel assembly construction materials tabulated in Table 4.2.5 (UO_2 heat capacity) is conservatively adopted.
Note 3: The fuel properties tabulated herein are used in screening calculations to define the limiting scenario for fuel storage (See Table 4.4.2).
(continued next page)

Table 4.4.1 (continued)

EFFECTIVE FUEL PROPERTIES UNDER BOUNDING FUEL STORAGE CONFIGURATIONS

	Conductivity (Btu/hr-ft-°F)			
	PWR: 16x16D		**PWR: VVER-1000**	
Temperature (°F)	Planar	Axial	Planar	Axial
212	0.251	0.854	0.229	0.983
450	0.418	0.935	0.308	1.073
700	0.678	1.042	0.341	1.194

Thermal Inertia Properties		
	Density (lb/ft^3)	Heat Capacity (Btu/lb-°F)[Note 21]
PWR: 16x16D	184.5	0.059
PWR: VVER-1000	183.8	0.06

Note 21: The lowerbound heat capacity of principal fuel assembly construction materials tabulated in Table 4.2.5 (UO_2 heat capacity) is conservatively adopted.

Note 32: The fuel properties tabulated herein are used in screening calculations to define the limiting scenario for fuel storage (See Table 4.4.2).

Table 4.4.2

RESULTS OF SCREENING CALCULATIONS UNDER NORMAL STORAGE CONDITIONS

Storage Scenario	Peak Cladding Temperature, °C (°F)
MPC-37 (Note 2) Minimum Height[1] Reference Height Maximum Height	 **353 (667)** 342 (648) 316 (601)
MPC-32ML (Note 3)	349 (660)
MPC-31C (Note 3)	345 (653)
MPC-89 (Note 2)	333 (631)

Notes:

(1) The highest temperature highlighted above is reached under the case of minimum height MPC-37 designed to store the short height Ft. Calhoun 14x14 fuel. This scenario is adopted in Chapter 4 for the licensing basis evaluation of fuel storage in the HI-STORM FW system.

(2) All the screening calculations for MPC-37 and MPC-89 were performed using a reference coarse mesh [4.1.9] and flow resistance based on the calculations in Holtec report [4.4.2].

~~(2)~~(3) Screening calculations for MPC-32ML and MPC-31C performed using a mesh with similar density as the licensing basis converged mesh adopted for MPC-37 in Section 4.4.1.6.

1 Bounding scenario adopted in this Chapter for all thermal evaluations.

Table 4.4.4 MINIMUM MPC FREE VOLUMES		
Item	**Lowerbound Height MPC-37 (ft^3)**	**MPC-89 (ft^3)**
Net Free Volume*	211.89	210.12
	MPC-32ML (ft^3)	**MPC-31C (ft^3)**
Net Free Volume*	291.23	277.52
**Net free volumes are obtained by subtracting basket, fuel, aluminum shims, spacers, basket supports and DFCs metal volume from the MPC cavity volume.*		

Table 4.4.5 SUMMARY OF MPC INTERNAL PRESSURES UNDER LONG-TERM STORAGE*		
Condition	**MPC-37 (psig) Pattern A/Pattern B**	**MPC-89 (psig)**
Initial maximum backfill** (at 70°F)	45.5/46.0	47.5
Normal: intact rods 1% rods rupture	 96.6/97.9 97.7/99.0	 98.4 99.0
Off-Normal (10% rods rupture)	107.5/108.9	104.0
Accident (100% rods rupture)	191.5/194.4	155.0
* Per NUREG-1536, pressure analyses with ruptured fuel rods (including BPRA rods for PWR fuel) is performed with release of 100% of the ruptured fuel rod fill gas and 30% of the significant radioactive gaseous fission products. ** Conservatively assumed at the Tech. Spec. maximum value (see Table 4.4.8).		

(continued next page)

Table 4.4.5 (continued)

SUMMARY OF MPC INTERNAL PRESSURES UNDER LONG-TERM STORAGE*

Condition	**MPC-32ML (psig)**	**MPC-31C (psig)**
Initial backfill** (at 70°F)	45.5	45.5
Normal: intact rods 1% rods rupture	 91.1 91.8	 91.5 92.2
Off-Normal (10% rods rupture)	98.3	98.7
Accident (100% rods rupture)	163.7	163.9

* Per NUREG-1536, pressure analyses with ruptured fuel rods (including BPRA rods for PWR fuel) is performed with release of 100% of the ruptured fuel rod fill gas and 30% of the significant radioactive gaseous fission products.

** Conservatively assumed at the Tech. Spec. maximum value (see Table 4.4.8).

Table 4.4.6

SUMMARY OF HI-STORM FW DIFFERENTIAL THERMAL EXPANSIONS

Gap Description	Cold Gap U (in)	Differential Expansion δ_i (in)	Is Free Expansion Criterion Satisfied (i.e., U > δ_i)
Fuel Basket-to-MPC Radial Gap	0.125	0.112	Yes
Fuel Basket-to-MPC Minimum Axial Gap	1.5	0.421	Yes
MPC-to-Overpack Radial Gap	5.5	0.128	Yes
MPC-to-Overpack Minimum Axial Gap	3.5	0.372	Yes

Table 4.4.7

THEORETICAL LIMITS* OF MPC HELIUM BACKFILL PRESSURE**

MPC	Minimum Backfill Pressure (psig)	Maximum Backfill Pressure (psig)
MPC-37 Pattern A	41.0	47.3
MPC-37 Pattern B	40.8	47.1
MPC-89	41.9	48.4
MPC-32ML	39.7	50.6
MPC-31C	40.6	50.3

* The helium backfill pressures are set forth in the Technical Specifications with a margin (see Table 4.4.8).

** The pressures tabulated herein are at 70°F reference gas temperature.

Table 4.4.8 MPC HELIUM BACKFILL PRESSURE SPECIFICATIONS		
MPC	**Item**	**Specification**
MPC-37 Pattern A	Minimum Pressure	42.0 psig @ 70°F Reference Temperature
	Maximum Pressure	45.5 psig @ 70°F Reference Temperature
MPC-37 Pattern B	Minimum Pressure	41.0 psig @ 70°F Reference Temperature
	Maximum Pressure	46.0 psig @ 70°F Reference Temperature
MPC-89	Minimum Pressure	42.5 psig @ 70°F Reference Temperature
	Maximum Pressure	47.5 psig @ 70°F Reference Temperature
MPC-32ML	Minimum Pressure	41.5 psig @ 70°F Reference Temperature
	Maximum Pressure	45.5 psig @ 70°F Reference Temperature
MPC-31C	Minimum Pressure	41.5 psig @ 70°F Reference Temperature
	Maximum Pressure	45.5 psig @ 70°F Reference Temperature

Table 4.4.9 MAXIMUM HI-STORM FW TEMPERATURES AT ELEVATED SITES[1]	
Component	**Temperature, °C (°F)**
Fuel Cladding	374 (705)
MPC Basket	360 (680)
Aluminum Basket Shims	275 (527)
MPC Shell	246 (475)
MPC Lid[Note 1]	242 (468)
Overpack Inner Shell	126 (259)
Overpack Body Concrete[Note 1]	86 (187)
Overpack Lid Concrete[Note 1]	112 (234)
Note 1: Maximum section average temperature is reported.	

1 The temperatures reported in this table (all for the bounding scenario defined in Table 4.4.2) are below the design temperatures specified in Table 2.2.3, Chapter 2.

Table 4.4.15 DESIGN OPERATING ABSOLUTE PRESSURES[Note 1]	
MPC-37 Loading Pattern A Loading Pattern B	 7.1 atm 7 atm
MPC-32ML	6.5 atm
MPC-31C	6.3 atm
MPC-89	7 atm
Note 1: Table 4.4.8 helium backfill specifications ensure MPC operating pressures meet or exceed design values tabulated herein.	

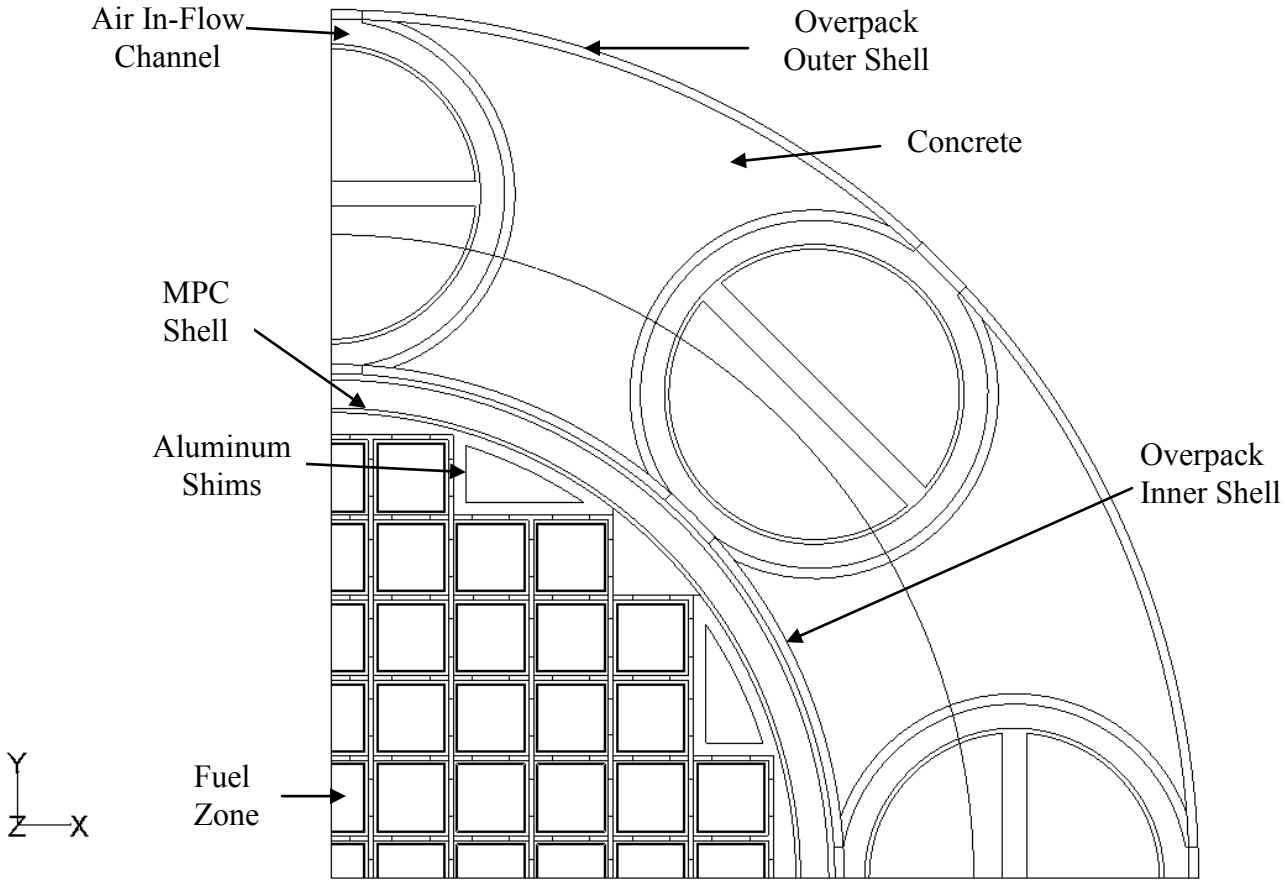

Figure 4.4.2a: Planar View of HI-STORM FW MPC-89 Quarter Symmetric 3-D Model

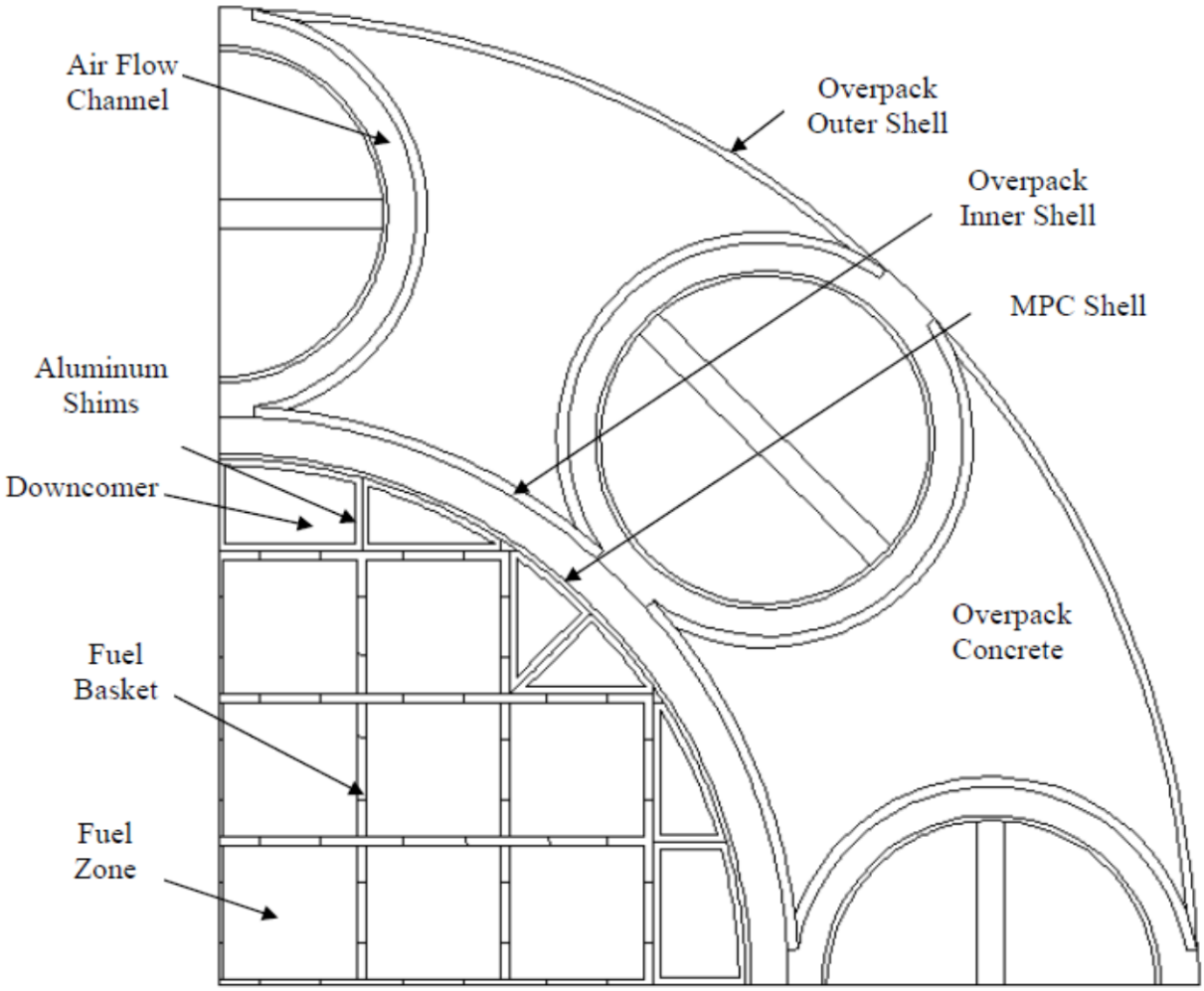

Figure 4.4.2b: Planar View of HI-STORM FW MPC-32ML Quarter Symmetric 3-D Model

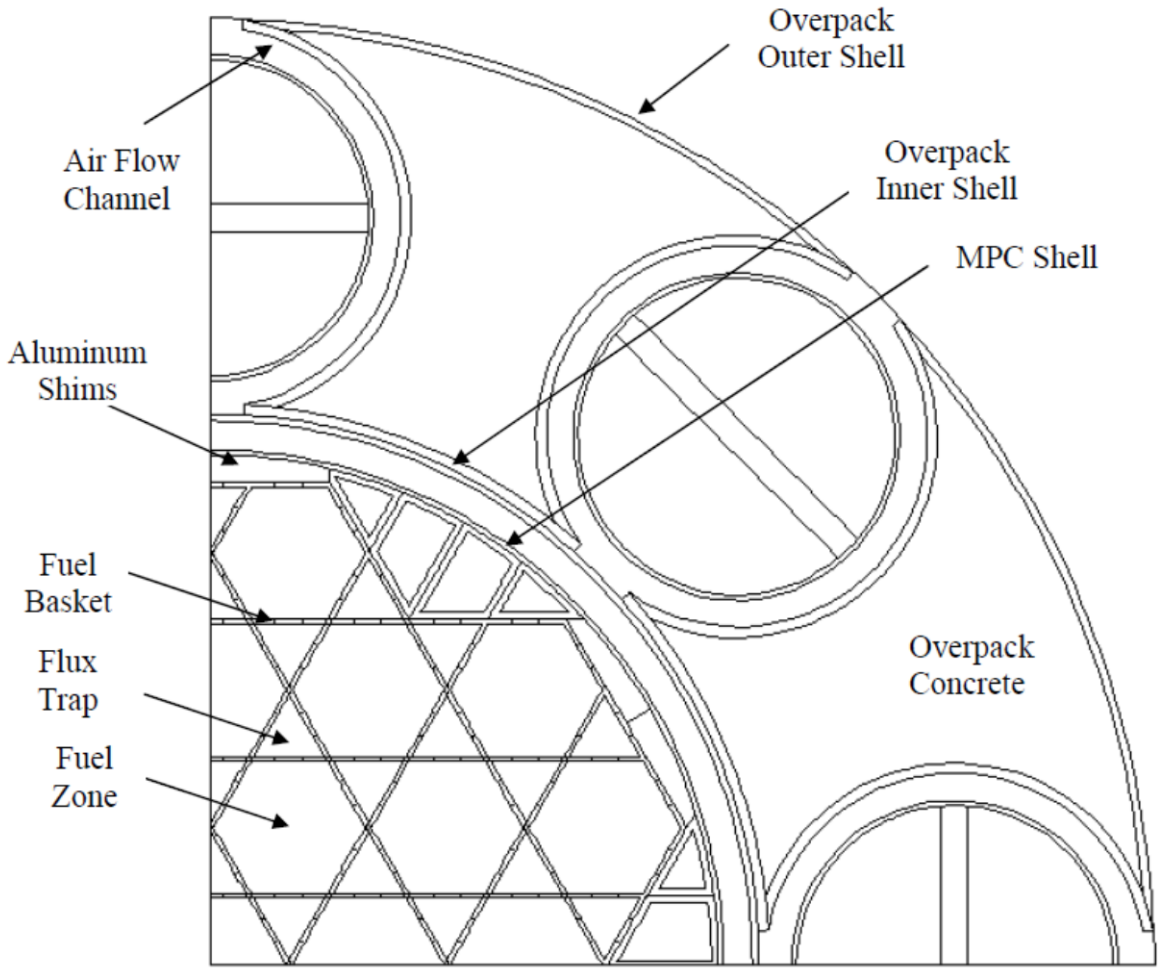

Figure 4.4.2c: Planar View of HI-STORM FW MPC-31C Quarter Symmetric 3-D Model

Mesh No	Total Mesh Size	PCT (^{o}C)	Permissible Limit (^{o}C)	Clad Temperature Margin (^{o}C)
1 (Licensing Basis Mesh)	1,267,474	389	400	11
2	2,678,012	390	400	10
3	5,797,030	389	400	11

The solutions from these grids are in the asymptotic range. The finest mesh (Mesh 3) has about 4.6 times the total mesh size of the licensing basis mesh (Mesh 1). Even with such a large mesh refinement, the PCT is essentially same for all the three meshes. Since the difference of PCT for all these meshes is close to zero, it indicates that an oscillatory convergence or that the "exact" solution has been attained [4.5.1]. To provide further assurance of convergence, grid convergence index (GCI), which is a measure of the solution uncertainty, is computed as 0.566%. The apparent order of the method is calculated as 1.2.

Based on the above results, it can be concluded that the Mesh 1 is reasonably converged and is adopted as the licensing basis converged mesh.

4.5.2.3 Vacuum Drying

The initial loading of SNF in the MPC requires that the water within the MPC be drained and replaced with helium. For MPC-37, MPC-32ML and MPC-89~~s~~ containing moderate burnup fuel assemblies only, this operation may be carried out using the conventional vacuum drying approach upto design basis heat load. In this method, removal of moisture from the MPC cavity is accomplished by evacuating the MPC after completion of MPC draining operation. Vacuum drying of MPC-31C loaded with moderate or high burnup fuel and MPC-37, MPC-32ML & MPC-89~~s~~ containing high burnup fuel assemblies is permitted up to threshold heat loads defined in Table 4.5.1 and 4.5.16. ~~High burnup f~~Fuel drying in MPC-31C~~s~~ generating greater than threshold heat loads require implementation of site-specific vacuum drying time limits. Where such restrictions are deemed not practical the~~is performed by a~~ forced flow helium drying process as discussed in Section 4.5.4 is mandatory.

Prior to the start of the MPC draining operation, both the HI-TRAC VW annulus and the MPC are full of water. The presence of water in the MPC ensures that the fuel cladding temperatures are lower than design basis limits by large margins. As the heat generating active fuel length is uncovered during the draining operation, the fuel and basket mass will undergo a gradual heat up from the initially cold conditions when the heated surfaces were submerged under water. To minimize fuel temperatures during vacuum drying operations the HI-TRAC VW annulus must be water filled. The necessary operational steps required to ensure this requirement are set forth in Chapter 9.

A 3-D FLUENT thermal model of the MPC is constructed in the same manner as described in Section 4.41. The principal input to this model is the effective conductivity of fuel under vacuum drying operations. To bound the vacuum drying operations the effective conductivity of fuel is computed assuming the MPC is filled with water vapor at a very low pressure (1 torr). The methodology for computing the effective conductivity is given in Section 4.4.1 and effective properties of design basis fuel under vacuum conditions tabulated in Table 4.5.8. To ensure a conservative evaluation the thermal model is incorporated with the following assumptions:

i. Bounding steady-state condition is reached with the MPC decay heat load set equal to the limiting heat load (Pattern A in Table 1.2.3a and 1.2.4) for MPCs fueled with Moderate Burnup Fuel and threshold heat load defined in Table 4.5.1 for MPCs fueled with one or more High Burnup fuel assemblies.

ii. The external surface of the MPC shell is postulated to be at the boiling temperature of water 100°C (212°F).

iii. The bottom surface of the MPC is insulated.

iv. MPC internal convection heat transfer is suppressed.

Results of vacuum condition analyses are provided in Subsection 4.5.4.1.

4.5.3 Maximum Time Limit During Wet Transfer Operations

In accordance with NUREG-1536, water inside the MPC cavity during wet transfer operations is not permitted to boil. This requirement is met by imposing time limits for fuel to remain submerged in water after a loaded HI-TRAC VW cask is removed from the pool.

Fuel loading operations are typically conducted with the HI-TRAC VW and its contents (water filled MPC) submerged in pool water. Under these conditions, the HI-TRAC VW is essentially at the pool water temperature. When the HI-TRAC VW transfer cask and the loaded MPC under water-flooded conditions is removed from the pool, the water, fuel, MPC and HI-TRAC VW metal absorb the decay heat emitted by the fuel assemblies. This results in a slow temperature rise of the HI-TRAC VW with time, starting from an initial (pool water) temperature. The rate of temperature rise is limited by the thermal inertia of the HI-TRAC VW system. To enable a bounding heat-up rate determination, the following conservative assumptions are utilized:

i. Heat loss by natural convection and radiation from the exposed HI-TRAC VW surfaces to ambient air is neglected (i.e., an adiabatic heat-up calculation is performed).

1 The MPC thermal model adopted for vacuum drying analysis in this sub-section includes the gap between the intersecting basket panels as 0.4 mm. A sensitivity study of the most limiting thermal scenario (least margins to fuel temperature limit) of vacuum drying condition is performed with this gap as 0.8 mm and discussed in Sub-section 4.5.4.4.

from the MPC cavity. In this case, relatively cooler water will enter via MPC lid ports and heated water will exit from the vent port. The minimum water flow rate required to maintain the MPC cavity water temperature below boiling with an adequate subcooling margin is determined as follows:

$$M_W = \frac{Q}{C_{pW}(T_{max} - T_{in})}$$

where:

M_W = minimum water flow rate (lb/hr)
C_{pw} = water heat capacity (Btu/lb-°F)
T_{max} = suitably limiting temperature below boiling (°F)
T_{in} = water supply temperature to MPC

4.5.4 Analysis of Limiting Thermal States During Short-Term Operations

4.5.4.1 Vacuum Drying

The vacuum drying option is evaluated for the two limiting scenarios defined in Section 4.5.2.2 to address Moderate Burnup Fuel under limiting heat load (Pattern A) and High Burnup Fuel under threshold heat load defined in Table 4.5.1 (MPC-37 and MPC-89) and Table 4.5.16 (MPC-32ML and MPC-31C). The principle objective of the analysis is to ensure compliance with ISG-11 temperature limits. For this purpose 3-D FLUENT thermal models of the MPC-37, MPC-32ML, MPC-31C and MPC-89 canisters are constructed as described in Section 4.5.2.2 and bounding steady state temperatures computed. The results are tabulated in Tables 4.5.6, ~~and~~ 4.5.7, 4.5.17 and 4.5.18. The results show that the cladding temperatures comply with the ISG-11 limits for moderate and high burnup fuel in Table 4.3.1 by robust margins. The analysis presented above supports MPC drying options as summarized in Table 4.5.19.

4.5.4.2 Forced Helium Dehydration

To reduce moisture to trace levels in the MPC using a Forced Helium Dehydration (FHD) system, a conventional, closed loop dehumidification system consisting of a condenser, a demoisturizer, a compressor, and a pre-heater is utilized to extract moisture from the MPC cavity through repeated displacement of its contained helium, accompanied by vigorous flow turbulation. Demoisturization to the 3 torr vapor pressure criteria required by NUREG 1536 is assured by verifying that the helium temperature exiting the demoisturizer is maintained at or below the psychrometric threshold of 21°F for a minimum of 30 minutes. Appendix 2.B of [4.1.8] provides a detailed discussion of the design criteria and operation of the FHD system.

The FHD system provides concurrent fuel cooling during the moisture removal process through forced convective heat transfer. The attendant forced convection-aided heat transfer occurring during operation of the FHD system ensures that the fuel cladding temperature will remain below the applicable peak cladding temperature limit in Table 2.2.3. Because the FHD operation induces a state of forced convection heat transfer in the MPC, (in contrast to the quiescent mode

Table 4.5.8

EFFECTIVE CONDUCTIVITY OF DESIGN BASIS FUEL ~~Note 1~~ UNDER VACUUM DRYING OPERATIONS
(Btu/hr-ft-°F)

Ft. Calhoun 14x14 Note 1		
Temperature (°F)	Planar	Axial
200	0.111	0.737
450	0.273	0.805
700	0.538	0.900
1000	0.977	1.040
Note 1: Ft. Calhoun 14x14 fuel is defined as the design basis fuel under the limiting condition of fuel storage in the minimum height MPC-37 (See Table 4.4.2).		
16x16D Note 2		
Temperature (°F)	Planar	Axial
212	0.095	0.8
450	0.229	0.867
700	0.458	0.962
785	0.558	1.003
VVER-1000 Note 3		
Temperature (°F)	Planar	Axial
212	0.085	0.86
450	0.154	0.927
700	0.206	1.025
Note 2: Design Basis MPC-32ML fuel Note 3: Design Basis MPC-31C fuel		

Table 4.5.16

THRESHOLD HEAT LOADS FOR VACUUM DRYING

MPC Type		Decay Heat Limit per Cell, kW	Number of Cells	Total Decay Heat Limit, kW
MPC-31C	Moderate Burnup Fuel	1.064	31	32.984
	High Burnup Fuel	0.56		17.36
MPC-32ML (Note 1)	High Burnup Fuel	0.897	32	28.704

Note 1: Vacuum drying of Moderate Burnup Fuel permitted upto Design Basis heat load defined in Table 1.2.3b.

Table 4.5.17

MAXIMUM COMPONENT TEMPEARTURES UNDER VACUUM DRYING OPERATIONS OF MPC-32ML

Component	**Temperature @ Threshold Heat (HBF) °C (°F)**	**Temperature @ Design Maximum Heat (MBF) °C (°F)**
Fuel Cladding	384 (723)	481 (898)
MPC Basket	368 (694)	461 (862)
Basket Periphery	304 (579)	369 (696)
Aluminum Basket Shims	263 (505)	314 (597)
MPC Shell	160 (320)	178 (352)
MPC Lid[1]	100 (212)	102 (216)

1 Maximum section average temperature is reported.

Table 4.5.18

MAXIMUM COMPONENT TEMPEARTURES DURING VACUUM DRYING OPERATIONS OF MPC-31C

Component	**Temperature @ HBF Threshold Heat °C (°F)**	**Temperature @ MBF Threshold Heat °C (°F)**
Fuel Cladding	386 (727)	539 (1002)
MPC Basket	351 (664)	475 (887)
Basket Periphery	206 (403)	264 (507)
Aluminum Basket Shims	180 (356)	222 (432)
MPC Shell	131 (268)	144 (291)
MPC Lid[1]	100 (212)	112 (234)

1 Maximum section average temperature is reported.

Table 4.5.19
MPC DRYING OPERATIONS

MPC Type	Fuel	Heat Load Limit (kW)	Method of Drying
MPC-31C	MBF	43.4 (Note 1)	FHD/Vacuum Drying with Time Limit
		32.984	FHD/Vacuum Drying without Time Limit
	HBF	43.4 (Note 1)	FHD/Vacuum Drying with Time Limit
		17.36	FHD/Vacuum Drying without Time Limit
MPC-32ML	MBF	44.16 (Note 1)	FHD/Vacuum Drying without Time Limit
	HBF	44.16 (Note 1)	FHD
		28.704	FHD/Vacuum Drying without Time Limit
MPC-37	MBF	44.09 (Pattern A) 45.0 (Pattern B) (Note 1)	FHD/Vacuum Drying without Time Limit
	HBF	44.09 (Pattern A) 45.0 (Pattern B) (Note 1)	FHD
		34.36	FHD/Vacuum Drying without Time Limit
MPC-89	MBF	46.36 (Note 1)	FHD/Vacuum Drying without Time Limit
	HBF	46.36 (Note 1)	FHD
		34.75	FHD/Vacuum Drying without Time Limit

Note 1: Design Basis heat load.
Note 2:Cyclic drying under time limited vacuum drying operations is permitted in accordance with ISG-11, Rev. 3 requirements by limiting number of cycles to less than 10 and cladding temperature variations to less than 65°C (117°F). Suitable time limits for these cycles shall be evaluated based on site specific conditions and thermal methodology defined in Section 4.5.

[4.2.21] "Thermal Radiation Heat Transfer", Third Edition, Robert Siegel and John R. Howell.

[4.4.1] NUREG-1536, "Standard Review Plan for Dry Cask Storage Systems," USNRC, (January 1997).

[4.4.2] "Pressure Loss Charactersistics for In-Cell Flow of Helium in PWR and BWR Storage Cells", Holtec Report HI-2043285, Revision 6, Holtec International, Marlton, NJ, 08053.

[4.4.3] "Standard for Verification and Validation in Computational Fluid Dynamics and Heat Transfer", ASME V&V 20-2009.

[4.5.1] "Procedure for Estimating and Reporting of Uncertainty due to Discretization in CFD Applications", I.B. Celik, U. Ghia, P.J. Roache and C.J. Freitas (Journal of Fluids Engineering Editorial Policy on the Control of Numerical Accuracy).

[4.6.1] United States Code of Federal Regulations, Title 10, Part 71.

[4.6.2] Gregory, J.J. et. al., "Thermal Measurements in a Series of Large Pool Fires", SAND85-1096, Sandia National Laboratories, (August 1987).

CHAPTER 5 CHANGED PAGES

CHAPTER 5†: SHIELDING EVALUATION

5.0 INTRODUCTION

The shielding analysis of the HI-STORM FW system is presented in this chapter. As described in Chapter 1, the HI-STORM FW system is designed to accommodate both PWR and BWR MPCs within HI-STORM FW overpacks (see Table 1.0.1).

In addition to storing intact PWR and BWR fuel assemblies, the HI-STORM FW system is designed to store BWR and PWR damaged fuel assemblies and fuel debris. Damaged fuel assemblies and fuel debris are defined in Subsection 2.1. Both damaged fuel assemblies and fuel debris are required to be loaded into Damaged Fuel Containers (DFCs).

As described in Chapter 2 (see Table 2.1.1), MPC-37, MPC-32ML and MPC-31C are designed to store various PWR fuel assembly classes. In this chapter, shielding analyses are performed for MPC-37 (for PWR fuel assemblies). For MPC-32ML and MPC-31C, site specific analyses need to use the site specific MPC and fuel type for controlled area boundary dose calculations to show the site's compliance with 10 CFR 72.104. Also, as discussed in Section 5.1, the burnup and cooling times selected for accident conditions represent reasonable upper bound limit, and the heavy metal mass in MPC-32ML and MPC-31C is comparable or less than that in MPC-37. Therefore, it is concluded that the accident condition evaluated in this chapter for MPC-37 is reasonably conservative, and no further site's compliance with 10 CFR 72.106 is required for MPC-32ML and MPC-31C.

PWR fuel assemblies may contain burnable poison rod assemblies (BPRAs), with any number of full-length rods and thimble plug rodlets in the locations without a full-length rod, thimble plug devices (TPDs), control rod assemblies (CRAs) or axial power shaping rod assemblies (APSRs), neutron source assemblies (NSAs), or similarly named devices. These non-fuel hardware devices are an integral yet removable part of PWR fuel assemblies and therefore the HI-STORM FW system has been designed to store PWR fuel assemblies with or without these devices. Since each device occupies the same location within a fuel assembly, a single PWR fuel assembly will not contain multiple devices, with the exception of instrument tube tie rods (ITTRs), which may be stored in the assembly along with other types of non-fuel hardware.

As described in Chapter 1(see Tables 1.2.3 and 1.2.4), the loading of fuel in all HI-STORM FW MPCs will follow specific heat load limitations.

† This chapter has been prepared in the format and section organization set forth in Regulatory Guide 3.61. However, the material content of this chapter also fulfills the requirements of NUREG-1536. Pagination and numbering of sections, figures, and tables are consistent with the convention set down in Chapter 1, Section 1.0, herein. Finally, all terms-of-art used in this chapter are consistent with the terminology of the glossary and component nomenclature of the Bill-of-Materials (Section 1.5).

CHAPTER 6 CHANGED PAGES

6.1 DISCUSSION AND RESULTS

In conformance with the principles established in NUREG-1536 [6.1.1] and 10CFR72.124 [6.1.2], the results in this chapter demonstrate that the effective multiplication factor (k_{eff}) of the HI-STORM FW system, including all biases and uncertainties evaluated with a 95% probability at the 95% confidence level, does not exceed 0.95 under all credible normal, off-normal, and accident conditions. Moreover, the results demonstrate that the HI-STORM FW system is designed and maintained such that at least two unlikely, independent, and concurrent or sequential changes must occur to the conditions essential to criticality safety before a nuclear criticality accident is possible. These criteria provide a large subcritical margin, sufficient to assure the criticality safety of the HI-STORM FW system when fully loaded with fuel of the highest permissible reactivity.

Criticality safety of the HI-STORM FW system depends on the following four principal design parameters:

1. The inherent geometry of the fuel basket designs within the MPC (and the flux trap water gaps in MPC-31C);

2. The fuel basket structure which is made entirely of the Metamic-HT neutron absorber material;

3. An administrative limit on the maximum enrichment for PWR fuel and maximum planar-average enrichment for BWR fuel; and

4. An administrative limit on the minimum soluble boron concentration in the water for loading/unloading fuel in the PWR fuel basket.

The off-normal and accident conditions defined in Chapter 2 and considered in Chapter 12 have no adverse effect on the design parameters important to criticality safety, except for the non-mechanistic tip-over event, which could result in limited plastic deformation of the basket. However, a bounding basket deformation is already included in the criticality models for normal conditions, and thus, from the criticality safety standpoint, the off-normal and accident conditions are identical to those for normal conditions.

The HI-STORM FW system is designed such that the fixed neutron absorber will remain effective for a storage period greater than 60 years, and there are no credible mechanisms that would cause its loss or a diminution of its effectiveness (see Chapter 8, specifically Section 8.9, and Section 10.1.6.3 for further information on the qualification and testing of the neutron absorber material). Therefore, in accordance with 10CFR72.124(b), there is no need to provide a surveillance or monitoring program to verify the continued efficacy of the neutron absorber.

Criticality safety of the HI-STORM FW system does not rely on the use of any of the following aids to the reduction of reactivity present in the storage system:

- burnup of fuel
- fuel-related burnable neutron absorbers
- more than 90 percent of the B-10 content for the Metamic-HT fixed neutron absorber undergirded by comprehensive tests as described in Subsection 10.1.6.3.

The HI-STORM FW system consists of the HI-STORM FW storage cask, the HI-TRAC VW transfer cask and Multi-Purpose-Canisters (MPCs) for PWR (including VVER) and BWR fuel (see Chapter 1, Table 1.0.1). Both the HI-TRAC VW transfer cask and the HI-STORM FW storage cask accommodate the interchangeable MPC designs. The HI-STORM FW storage cask uses concrete as a shield for both gamma and neutron radiation, while the HI-TRAC VW uses lead and steel for gamma radiation and a water-filled jacket for neutron shielding. The design details can be found in the drawing packages in Section 1.5.

While the MPCs are in the HI-STORM FW cask during storage, they are internally dry (no moderator), and thus, the reactivity is very low ($k_{eff} \sim 0.6$). However, the MPCs are flooded for loading and unloading operations in the HI-TRAC VW cask, which represents the limiting case in terms of reactivity. Therefore, the majority of the analyses have been performed with the MPCs in a HI-TRAC VW cask, and only selected cases have been performed for the HI-STORM FW cask.

Confirmation of the criticality safety of the HI-STORM FW system was accomplished with the three-dimensional Monte Carlo code MCNP5 [6.1.4]. K-factors for one-sided statistical tolerance limits with 95% probability at the 95% confidence level were obtained from the National Bureau of Standards (now NIST) Handbook 91 [6.1.5].

To assess the reactivity effects due to temperature changes, CASMO-4, a two-dimensional transport theory code [6.1.6] for fuel assemblies was used. CASMO-4 was not used for quantitative information, but only to qualitatively indicate the direction and approximate magnitude of the reactivity effects.

Benchmark calculations were made to compare the primary code package (MCNP5) with experimental data, using critical experiments selected to encompass, insofar as practical, the design parameters of the HI-STORM FW system. The most important parameters are (1) the enrichment, (2) cell spacing, (3) the ^{10}B loading of the neutron absorber panels, and (4) the soluble boron concentration in the water (for PWR fuel). The critical experiment benchmarking work is summarized in Appendix 6.A.

To assure the true reactivity will always be less than the calculated reactivity, the following conservative design criteria and assumptions were made:

- The MPCs are assumed to contain the most reactive fresh fuel authorized to be loaded into a specific basket design.

- No credit for fuel burnup is assumed, either in depleting the quantity of fissile nuclides or in producing fission product.

- The fuel stack density is assumed to be at 97.5% of the theoretical density for all criticality analyses. This is a conservative value, since it corresponds to a very high pellet density of 99% or more of the theoretical density. Note that this difference between stack and pellet density is due to the necessary dishing and chamfering of the pellets.

- No credit is taken for the ^{234}U and ^{236}U in the fuel.

- When flooded, the moderator is assumed to be water, with or without soluble boron, at a temperature and density corresponding to the highest reactivity within the expected operating range.

- When credit is taken for soluble boron, a ^{10}B content of 18.0 wt% in boron is assumed.

- Neutron absorption in minor structural members is neglected, i.e., spacer grids are replaced by water. This is conservative since studies presented in Section 6.2.1 show that all assemblies are undermoderated, and that the reduction in the amount of (borated or unborated) water within the fuel assembly always results in a reduction of the reactivity. The presence of any other structural material, which would reduce the amount of water, is therefore bounded by those studies, and neglecting this material is conservative. Additionally, the potential neutron absorption of those materials is neglected.

- Consistent with NUREG-1536, the worst hypothetical combination of tolerances (most conservative values within the range of acceptable values), as identified in Section 6.3, is assumed.

- When flooded, the fuel rod pellet-to-clad gap regions (and annular regions of the pellet in VVER fuel) are assumed to be flooded with pure unborated water.

- Planar-averaged enrichments are assumed for BWR fuel. Analyses are presented that demonstrate that the use of planar-averaged enrichments is appropriate.

- Consistent with NUREG-1536, fuel-related burnable neutron absorbers, such as the Gadolinia normally used in BWR fuel and IFBA normally used in PWR fuel, are neglected.

TABLE 6.1.1(a)
BOUNDING MAXIMUM k_{eff} VALUES FOR EACH ASSEMBLY CLASS IN THE MPC-37
(HI-TRAC VW)

Fuel Assembly Class	4.0 wt% ^{235}U Maximum Enrichment†		5.0 wt% ^{235}U Maximum Enrichment†	
	Minimum Soluble Boron Concentration (ppm)	Maximum k_{eff}	Minimum Soluble Boron Concentration (ppm)	Maximum k_{eff}
14x14A	1000	0.8946	1500	0.8983
14x14B	1000	0.9213	1500	0.9282
14x14C	1000	0.9211	1500	0.9277
15x15B	1500	0.9129	2000	0.9311
15x15C	1500	0.9029	2000	0.9188
15x15D	1500	0.9223	2000	0.9421
15x15E	1500	0.9206	2000	0.9410
15x15F	1500	0.9244	2000	0.9455
15x15H	1500	0.9142	2000	0.9325
15x15I	1500	0.9155	2000	0.9362
16x16A	1000	0.9275	1500	0.9366
16x16A[DFC] ††	1000	0.9400	1600	0.9404
16x16B	1000	0.9258	1500	0.9334
16x16C	1000	0.9099	1500	0.9187
17x17A	1500	0.9009	2000	0.9194
17x17B	1500	0.9181	2000	0.9380
17x17C	1500	0.9222	2000	0.9424
17x17D	1500	0.9183	2000	0.9384
17x17E	1500	0.9203	2000	0.9392

† For maximum allowable enrichments between 4.0 wt% ^{235}U and 5.0 wt% ^{235}U, the minimum soluble boron concentration may be calculated by linear interpolation between the minimum soluble boron concentrations specified for each assembly class.

†† Intact Fuel Assembly Class 16x16A loaded in DFCs in all 37 cell locations, if permitted by the certificate of compliance.

TABLE 6.1.1(b)

BOUNDING MAXIMUM k_{eff} VALUES FOR EACH ASSEMBLY CLASS IN MPC-31C (HI-TRAC VW)

Fuel Assembly Class	**Maximum Allowable Planar-Average Enrichment (wt% ^{235}U)**	**Maximum k_{eff}**
V10A	5.0	0.9364
V10B	5.0	0.9348

TABLE 6.1.1(c)

BOUNDING MAXIMUM k_{eff} VALUES FOR EACH ASSEMBLY CLASS IN MPC-32ML (HI-TRAC VW)

Fuel Assembly Class	**4.0 wt% ^{235}U Maximum Enrichment†**		**5.0 wt% ^{235}U Maximum Enrichment†**	
	Minimum Soluble Boron Concentration (ppm)	**Maximum k_{eff}**	**Minimum Soluble Boron Concentration (ppm)**	**Maximum k_{eff}**
16x16D	1500	0.9205	2000	0.9386

† For maximum allowable enrichments between 4.0 wt% ^{235}U and 5.0 wt% ^{235}U, the minimum soluble boron concentration may be calculated by linear interpolation between the minimum soluble boron concentrations specified for each assembly class.

TABLE 6.1.4(a)

BOUNDING MAXIMUM k_{eff} VALUES FOR THE MPC-37
WITH UP TO 12 DFCs

Fuel Assembly Class of Undamaged Fuel	**4.0 wt% ^{235}U Maximum Enrichment for Undamaged Fuel and Damaged Fuel/Fuel Debris †**		**5.0 wt% ^{235}U Maximum Enrichment for Undamaged Fuel and Damaged Fuel/Fuel Debris †**	
	Minimum Soluble Boron Concentration (ppm)	**Maximum k_{eff}**	**Minimum Soluble Boron Concentration (ppm)**	**Maximum k_{eff}**
All 14x14, 16x16††	1300	0.9155	1800	0.9305
All 15x15, all 17x17	1800	0.9032	2300	0.9276

† For maximum allowable enrichments between 4.0 wt% ^{235}U and 5.0 wt% ^{235}U, the minimum soluble boron concentration may be calculated by linear interpolation between the minimum soluble boron concentrations specified for each assembly class.

†† For assembly class 16x16A intact fuel can be loaded with or without DFCs if permitted in the certificate of compliance.

TABLE 6.1.4(b)

BOUNDING MAXIMUM k_{eff} VALUES FOR MPC-31C
WITH UP TO 6 DFCs

Fuel Assembly Class of Undamaged Fuel	**5.0 wt% ^{235}U Maximum Enrichment for Undamaged Fuel and Damaged Fuel**	**5.0 wt% ^{235}U Maximum Enrichment for Undamaged Fuel and Fuel Debris**
	Maximum k_{eff}	**Maximum k_{eff}**
V10A, V10B	0.9423	0.9485

TABLE 6.1.4(c)

BOUNDING MAXIMUM k_{eff} VALUES FOR MPC-32ML
WITH UP TO 8 DFCs

Fuel Assembly Class of Undamaged Fuel	**4.0 wt% ^{235}U Maximum Enrichment for Undamaged Fuel and Damaged Fuel/Fuel Debris †**		**5.0 wt% ^{235}U Maximum Enrichment for Undamaged Fuel and Damaged Fuel/Fuel Debris †**	
	Minimum Soluble Boron Concentration (ppm)	**Maximum k_{eff}**	**Minimum Soluble Boron Concentration (ppm)**	**Maximum k_{eff}**
16x16D	1600	0.9149	2100	0.9347

† For maximum allowable enrichments between 4.0 wt% ^{235}U and 5.0 wt% ^{235}U, the minimum soluble boron concentration may be calculated by linear interpolation between the minimum soluble boron concentrations specified for each assembly class.

by a positive increase in reactivity from the reduction in fuel (which would be counter-intuitive). Therefore, in order not to overstate the conservative effect of the flooded fuel-to-clad gap, the calculations for the variation of the fuel pellet diameter are performed for a flooded gap of constant thickness by also changing the clad ID.

- A discussion in the previous bullet is also applicable to the inner diameter of the annular fuel pellets in VVER fuel.

Since all assemblies have the same principal design, i.e. consist of bundles of cladded fuel rods, most of them with embedded guide/instrument tubes or water rods or channels, the above conclusions apply to all of them, and the bounding dimensions are therefore also common to all fuel assemblies analyzed here. Nevertheless, to clearly demonstrate that the main assumption is true, i.e. that all assemblies are undermoderated, a study was performed for all assembly types where the pellet-to-clad gap (and annular region of the pellet in VVER fuel) is empty instead of being flooded (a conservative assumption for the design basis calculations, see Section 6.4.2.3) The results are listed in Table 6.2.3, in comparison with the results of the reference cases with the flooded gap from Section 6.1 for those assembly types. In all cases, the reactivity is reduced compared to the reference case. This verifies that all assembly types considered here are in fact undermoderated, and therefore validates the main assumption stated above. All assembly types are therefore behaving in a similar fashion, and the bounding dimensions are therefore applicable to all assembly types. This discussion and the corresponding conclusions not only affect fuel behavior, but also other moderation effects, and is therefore further referenced in Section 6.3.1 and 6.4.2

As a result, the authorized contents in Subsection 2.1 are defined in terms of those bounding assembly parameters for each class.

Nevertheless, to further demonstrate that the aforementioned characteristics are in fact bounding for the HI-STORM FW, parametric studies were performed on reference PWR and BWR assemblies, namely PWR assembly class 17x17B and BWR assembly class 10x10A. The results of these studies are shown in Table 6.2.1 and 6.2.2, and verify the bounding parameters listed above. Note that in the studies presented in Tables 6.2.1 and 6.2.2, the fuel pellet diameter and cladding inner diameter are changed together. This is to keep the cladding-to-pellet gap, which is conservatively flooded with pure water in all cases (see Section 6.4.2.3), at a constant thickness, to ensure the studies evaluate the fuel parameters rather than the moderation conditions, as discussed above.

In addition to those dimensions, additional fuel assembly characteristics important to criticality control are the location of guide tubes, water rods, part length rods, and rods with differing dimensions (classes 9x9E/F only). These are identified in the assembly cross sections provided in Appendix 6.B, Section B.4.

In all cases, the gadolinia (Gd_2O_3) normally incorporated in BWR fuel, and Integral Fuel Burnable Absorbers (IFBA) used in PWR fuel was conservatively neglected. However, a partial

gadolinium credit qualifies certain BWR assembly classes with the fuel enrichment above the administrative limit on the maximum enrichment, defined in Chapter 2. For details see Subsection 6.4.10.

Some assembly classes contain partial length rods. There are differences in location of those partial length rods within the assembly that influence how those rods affect reactivity: Assembly classes 9x9A, 10x10A, 10x10B and 10x10F have partial length rods that are completely surrounded by full length rods, whereas assembly class 10x10G has those partial length rods on the periphery of the assembly or facing the water gap, where they directly only face two full length rods (see Appendix 6.B, Section B.4). To determine a bounding configuration for those assembly classes where partial length rods are completely surrounded by full length rods, calculations are listed in Table 6.2.2 for the actual (real) assembly configuration and for the axial segments (assumed to be full length) with and without the partial length rods. The results show that the configurations with only the full length rods present, i.e. where the partial length rods are assumed completely absent from the assembly, is bounding. This is an expected outcome, since LWR assemblies are typically undermoderated, therefore reducing the fuel-to-water-ratio within the rod array tends to increase reactivity. Consequently, all assembly classes that contain partial length rods surrounded by full-length rods are analyzed with the partial length rods absent. For assembly class 10x10G, calculations with different assumptions for the length of the part-length rods are presented in Table 6.2.7, and show that reducing the length of the part length rods reduces reactivity. This means that the reduction in the fuel amount is more dominating than the change in moderation for this configuration. For this class, all rods therefore are assumed full length. Note that in neither of the cases is the configuration with the actual part length rods bounding. The specification of the authorized contents has therefore no minimum requirement for the active fuel length of the partial length rods.

BWR assemblies are specified in Table 2.1.3 with a maximum planar-average enrichment. The analyses presented in this chapter use a uniform enrichment, equal to the maximum planar-average. Analyses presented in the HI-STORM FSAR ([6.0.1], Chapter 6, Appendix 6.B) show that this is a conservative approach, i.e. that a uniform enrichment bounds the planar-average enrichment in terms of the maximum k_{eff}. To verify that this is applicable to the HI-STORM FW, those calculations were re-performed in the MPC-89. The results are presented in Table 6.2.4, and show that, as expected, the planar average enrichments bound or are statistically equivalent to the distributed enrichment in the HI-STORM FW as they do in the HI-STORM 100. To confirm that this is also true for the higher enrichments analyzed here, additional calculations were performed and are presented in Table 6.2.2 in comparison with the results for the uniform enrichment. Since the maximum planar-average enrichment of 4.8 wt% ^{235}U is above the actual enrichments of those assemblies, actual (as-built) enrichment distributions are not available. Therefore, several bounding cases are analyzed. Note that since the maximum planar-average enrichment of 4.8 wt% ^{235}U is close to the maximum rod enrichment of 5.0 wt% ^{235}U, the potential enrichment variations within the cross section are somewhat limited. To maximize the differences in enrichment under these conditions, the analyzed cases assume that about 50% of the rods in the cross section are at an enrichment of 5.0 wt% ^{235}U, while the balance of the rods are at an enrichment of about 4.6 wt%, resulting in an average of 4.8 wt%. Calculations are

TABLE 6.2.3

EFFECT OF THE FLOODING OF THE PELLET-TO-CLAD GAP

Fuel Assembly Class	Maximum k_{eff} at 5.0 wt% ^{235}U Maximum Enrichment		
	Flooded Pellet-to-Clad Gap	Empty Pellet-to-Clad Gap	Difference
14x14A	0.8983	0.8962	-0.0021
14x14B	0.9282	0.9235	-0.0047
14x14C	0.9277	0.9237	-0.0038
15x15B	0.9311	0.9284	-0.0027
15x15C	0.9188	0.9164	-0.0024
15x15D	0.9421	0.9386	-0.0035
15x15E	0.9410	0.9371	-0.0039
15x15F	0.9455	0.9408	-0.0047
15x15H	0.9325	0.9300	-0.0025
15x15I	0.9357	0.9305	-0.0052
16x16A	0.9366	0.9284	-0.0082
16x16A[DFC]	0.9400	0.9340	-0.0060
16x16B	0.9334	0.9297	-0.0037
16x16C	0.9187	0.9144	-0.0043
16x16D	0.9386	0.9350	-0.0036
17x17A	0.9194	0.9160	-0.0034
17x17B	0.9380	0.9335	-0.0045
17x17C	0.9424	0.9375	-0.0049
17x17D	0.9384	0.9323	-0.0061
17x17E	0.9392	0.9346	-0.0046

TABLE 6.2.3 (continued)

EFFECT OF THE FLOODING OF THE PELLET-TO-CLAD GAP

Fuel Assembly Class	Maximum k_{eff}		
	Flooded Pellet-to-Clad Gap	Empty Pellet-to-Clad Gap	Difference
7x7B	0.9317	0.9261	-0.0056
8x8B	0.9369	0.9318	-0.0051
8x8C	0.9399	0.9331	-0.0068
8x8D	0.9380	0.9334	-0.0046
8x8E	0.9281	0.9230	-0.0051
8x8F	0.9328	0.9275	-0.0053
9x9A	0.9421	0.9370	-0.0051
9x9B	0.9410	0.9292	-0.0118
9x9C	0.9338	0.9290	-0.0048
9x9D	0.9342	0.9294	-0.0048
9x9E/F	0.9346	0.9261	-0.0085
9x9G	0.9307	0.9250	-0.0057
10x10A	0.9435	0.9391	-0.0044
10x10B	0.9417	0.9317	-0.0100
10x10C	0.9389	0.9333	-0.0056
10x10F	0.9440	0.9395	-0.0045
10x10G	0.9466	0.9408	-0.0058
V10A	0.9364	0.9200	-0.0164
V10B	0.9348	0.9218	-0.0130

6.3 MODEL SPECIFICATION

6.3.1 Description of Calculational Model

Figures 6.3.1 through 6.3.9~~5~~ show representative cross sections of the criticality models for all considered ~~the two~~ baskets. Figures 6.3.1, 6.3.2, 6.3.6 and 6.3.7~~2~~ show a single cell from each ~~of the two~~ basket~~s~~. Figures 6.3.3, 6.3.4, 6.3.8 and 6.3.9~~4~~ show the entire MPC-37, MPC-89, MPC-31C and MPC-~~89~~32ML basket, respectively. Figure 6.3.5 shows a sketch of the calculational model in the axial direction.

Full three-dimensional calculational models were used for all calculations. The calculational models explicitly define the fuel rods and cladding, the guide tubes, water rods and the channel (for the BWR assembly), the neutron absorber walls of the basket cells, and the surrounding MPC shell and overpack. For the flooded condition (loading and unloading), pure, unborated water was assumed to be present in the fuel rod pellet-to-clad gaps, since this represents the bounding condition as demonstrated in Section 6.4.2.3. Appendix 6.B provides sample input files for typical MPC basket designs

Note that the water thickness above and below the fuel is modeled as unborated water, even when borated water is present in the fuel region.

The discussion provided in Section 6.2.1 regarding the principal characteristics of fuel poison is also important for the various studies presented in this section, and supports the fact that those studies only need to be performed for a single BWR and PWR assembly type, and that the results of those studies are then generally applicable to all assembly types. The studies and the relationship to the discussion in Section 6.2.1 are listed below. Note that this approach is consistent with that used for the HI-STORM 100. The MPC-32ML basket design is very similar to the MPC-37 basket; the only major difference is the increased cell ID and, consequently, the number of storage locations is reduced. Therefore, all studies performed for MPC-37 are directly applicable to MPC-32ML and are not repeated. Also, most of the studies, such as temperature, internal and external moderation effects, etc., discussed in Subsections 6.3.1 and 6.4.2, are applicable to MPC-31C basket as well, since the same behavior (reactivity effect) is expected. However, some MPC-31C basket specific studies are performed and discussed below.

Basket Manufacturing Tolerance: The two aspects of the basket tolerance that are evaluated are the cell wall thickness and the cell ID. The reduced cell wall thickness results in a reduced amount of poison (since the material composition of the wall is fixed), and therefore in an increase in reactivity. The reduced cell ID reduces amount of water between the fuel the poison, and therefore the effectiveness of the poison material. Both effects are simply a function of the geometry, and are independent of the fuel type.

Panel Gaps: Similar to the basket manufacturing tolerance for the cell wall thickness, this tolerance has a small effect on the overall poison amount of the basket, which would affect the reactivity of the system independent of the fuel type.

Eccentric positioning (see Section 6.3.3): When a fuel assembly is located in the center of a basket cell, it is surrounded by equal amounts of water on all sides, and hence the thermalization of the neutrons that occur between the assembly and the poison in the cell wall, and hence the effectiveness of the poison, is also equal on all sides. For an eccentric positioning, the effectiveness of the poison is now reduced on those sides where the assembly is located close to the cell walls, and increased on the opposite sides. This creates a compensatory situation for a single cell, where the net effect is not immediately clear. However, for the entire basket, and for the condition where all assemblies are located closest to the center of the basket, the ~~four~~ assemblies at the center of the basket are now located close to each other, separated by poison plates with a reduced effectiveness since they are not surrounded by water on any side. This now becomes the dominating condition is terms of reactivity increase. This effect is also applicable to all assembly types, since those assemblies are all located close to the center of the basket, i.e. the eccentric position with all assemblies moved towards the center will be bounding regardless of the assembly type.

Wall thicknesses of DFCs: DFCs are used for damaged fuel and fuel debris in selected locations of the basket, but are also permitted to be used for intact fuel of the array/type 16x16A. Generally, DFCs are thin-walled containers, in order to minimize the additional weight to be supported by the basket. For damaged fuel and fuel debris calculations, a wall thickness of 0.025” is used, and studies with larger wall thicknesses show an insignificant effect. However, when DFCs are also used for intact assemblies of the 16x16A array/type, it is shown that there is a noticeable effect when a thicker wall is modeled. Consequently, for DFCs for intact 16x16A fuel, a conservative DFC wall thickness of 0.075” is used to provide manufacturing flexibility. Note that this already a rather thick wall, the same as typically used for storage racks in spent fuel pools, and would therefore present a practical upper limit for any DFC design.

The basket geometry can vary due to manufacturing tolerances and due to potential deflections of basket walls as the result of accident conditions. The basket tolerances are defined on the drawings in Chapter 1. The structural acceptance criteria for the basket during accident conditions is that the permanent deflection of the basket panels is limited to a fraction of 0.005 (0.5%) of the panel width (see Chapter 3). The analyses in Chapter 3 demonstrate that permanent deformations of the basket walls during accident conditions are far below this limit. In fact, the analyses show that the vast majority of the basket panels remain elastic during and after an accident, and therefore show no permanent deflection whatsoever, and that any deformation is limited to small localized areas. Nevertheless, it is conservatively assumed that 2 adjacent cell walls in each cell are deflected to the maximum extent possible over their entire length and width, i.e. that the cell ID is reduced by 0.5% of the cell width, or 0.045” for the MPC-37 cells and 0.030” for the MPC-89 cells. Stated differently, the minimum cell ID based on tolerances was further reduced by the amounts stated above for all cells in each basket to account for the

potential deflections of basket walls during accident conditions. Assuming that all cell sizes are reduced is a simplifying, but very conservative assumption, since cell walls are shared between neighboring cells, so while the deflection of a basket wall would reduce the cell size on one side, it necessarily increases that on the other side of the wall. MCNP5 was used to determine the manufacturing tolerances and deflections that produced the most adverse effect on criticality. After the reactivity effect (positive effect with an increase in reactivity; or negative effect with a decrease in reactivity) of the manufacturing tolerances was determined, the criticality analyses were performed using the worst case conditions in the direction which would increase reactivity. For simplification, the same worst case conditions are used for both normal and accident conditions. For all calculations, fuel assemblies were assumed to be eccentrically located in the cells, since this results in higher reactivities (see Section 6.3.3). Maximum k_{eff} results (including the bias, uncertainties, or calculational statistics), along with the selected dimensions, for a number of dimensional combinations are shown in Table 6.3.2 for ~~both~~ various baskets. The cell ID is evaluated for minimum (tolerance only)~~, minimum with deformation~~, nominal, ~~and an~~ increased value and a bounding with deformation. The wall thickness is evaluated for nominal and minimum values.

Based on the calculations, the conservative dimensional assumptions listed in Table 6.3.3 were determined for the basket designs. Because the reactivity effect (positive or negative) of the manufacturing tolerances is not assembly dependent, these dimensional assumptions were employed for all criticality analyses.

The basket is manufactured from individual slotted panels. The panels are expected to be in direct contact with each other (see Drawings in Chapter 1). However, to show that small gaps between panels would have essentially no effect on criticality, calculations are performed with a postulated 0.06” gap between panels, repeated in the axial direction every 10” in all panels. Since it is expected that the effect of these gaps would be small, these calculations were performed with a larger number of particles per cycle, larger number of inactive cycles, and a larger total number of cycles to improve the statistics of each run, so the real reactivity effect could be better separated from the statistical “noise”. The results are summarized in Tables 6.3.6 and show that the METAMIC gap has a very small effect. Therefore, all calculations are performed without any gaps between panels.

Variations of water temperature in the cask were analyzed using CASMO-4. The analyses were performed for the assembly class 10x10A in the MPC-89, and for the assembly class 17x17B with 2000 ppm soluble boron in the water in the MPC-37. These are the same assemblies and conditions used for the fuel dimension studies in Section 6.2, and shown there to be representative of all assemblies qualified for those baskets. The results are presented in Table 6.3.1, and show that the minimum water temperature (corresponding to a maximum water density) are bounding. This condition is therefore used in all further calculations. This is expected since an increased temperature results in a reduced water density, a condition that is shown in Section 6.4 to result in reduced reactivities.

Calculations documented in Chapter 3 show that the baskets stay within the applicable structural limits during all normal and accident conditions. Furthermore, the neutron poison material is an integral and non-removable part of the basket material, and its presence is therefore not affected by the accident conditions. Except for the potential deflection of the basket walls that is already considered in the criticality models, damage to the cask under accident conditions is limited to possible loss of the water in the water jacket of ~~he~~ HI-TRAC VW. However, this condition is already considered in the calculational models. Other parameters important to criticality safety are fuel type and enrichment, which are not affected by the hypothetical accident conditions. The calculational models of the cask and basket for the accident conditions are therefore identical to the models for normal conditions, and no separate models need to be developed for accident conditions.

6.3.2 Cask Regional Densities

Composition of the various components of the principal designs of the HI-STORM FW system are listed in Table 6.3.4. The cross section set for each nuclide is listed in Table 6.3.8, and is consistent with the cross section sets used in the benchmarking calculations documented in Appendix A. Note that these are the default cross sections chosen by the code.

The HI-STORM FW system is designed such that the fixed neutron absorber will remain effective for a storage period greater than 60 years, and there are no credible means to lose it.

The continued efficacy of the fixed neutron absorber is assured by acceptance testing, documented in Subsection 10.1.6.3, to validate the ^{10}B (poison) concentration in the fixed neutron absorber. To demonstrate that the neutron flux from the irradiated fuel results in a negligible depletion of the poison material over the storage period, an evaluation of the number of neutrons absorbed in the ^{10}B was performed. The calculation conservatively assumed a constant neutron source for 60 years equal to the initial source for the design basis fuel, as determined in Section 5.2, and shows that the fraction of ^{10}B atoms destroyed is less than 10^{-7} in 60 years. Thus, the reduction in ^{10}B concentration in the fixed neutron absorber by neutron absorption is negligible. Therefore, in accordance with 10CFR72.124(b), there is no need to provide a surveillance or monitoring program to verify the continued efficacy of the neutron absorber.

6.3.3 Eccentric Positioning of Assemblies in Fuel Storage Cells

The potential reactivity effect of eccentric positioning of assemblies in the fuel storage locations is accounted for in a conservatively bounding fashion, as described further in this subsection. The calculations in this subsection serve to identify the eccentric positioning of assemblies in the fuel storage locations, which results in a higher maximum k_{eff} value than the centered positioning. For the cases where the eccentric positioning results in a higher maximum k_{eff} value, the eccentric positioning is used for all corresponding cases reported in the summary tables in Section 6.1 and

the results tables in Section 6.4.

To conservatively account for eccentric fuel positioning in the fuel storage cells, three different configurations are analyzed, and the results are compared to determine the bounding configuration:

- Cell Center Configuration: All assemblies centered in their fuel storage cell;
- Basket Center Configuration: All assemblies in the basket are moved as close to the center of the basket as permitted by the basket geometry; and
- Basket Periphery Configuration: All assemblies in the basket are moved furthest away from the basket center, and as close to the periphery of the basket as possible.

It should be noted that the two eccentric configurations are hypothetical, since there is no known physical phenomenon that could move all assemblies within a basket consistently to the center or periphery. However, since the configurations listed above bound all credible configurations, they are conservatively used in the analyses.

In Table 6.3.5, results are presented for all representative conditions. The table shows the maximum k_{eff} value for centered and the two eccentric configurations for each condition, and the difference in k_{eff} between the centered and eccentric positioning. In ~~all~~ most cases, moving the assemblies and DFCs to the periphery of the basket results in a reduction in reactivity, compared to the cell centered position, and moving the assemblies and DFCs towards the center results in an increase in reactivity, compared to the cell centered position. All calculations for these cases are therefore performed with assemblies/DFCs moved towards the center of the basket. However, in case of the MPC-31C basket with damaged fuel/fuel debris in DFCs, the centered positioning is bounding, hence it is used in the design basis calculations.

TABLE 6.3.2

EVALUATION OF BASKET MANUFACTURING TOLERANCES

Box I.D.	**Box Wall Thickness**	**Maximum k_{eff}**
MPC-37 (17x17B, 5.0% Enrichment)		
nominal (8.94")	nominal (0.59")	0.9332
nominal (8.94")	minimum (0.57”)	0.9346
increased (8.96")	minimum (0.57”)	0.9350
minimum (8.92")	minimum (0.57”)	0.9352
minimum, including deformation (8.875")	minimum (0.57”)	0.9374
MPC-89 (10x10A 4.8% Enrichment)		
nominal (6.01")	nominal (0.40")	0.9365
nominal (6.01")	minimum (0.38”)	0.9403
increased (6.03")	minimum (0.38”)	0.9396
minimum (5.99")	minimum (0.38”)	0.9417
minimum, including deformation (5.96")	minimum (0.38”)	0.9428
MPC-31C (V10A, 5.0% Enrichment)		
nominal (9.70")	nominal (0.35")	0.9342
nominal (9.70")	minimum (0.34”)	0.9357
minimum (9.65")	minimum (0.34”)	0.9346
maximum (9.75")	minimum (0.34”)	0.9356
maximum, including deformation (9.79")	minimum (0.34”)	0.9364

TABLE 6.3.3

BASKET DIMENSIONAL ASSUMPTIONS

Basket Type	Box I.D.	Box Wall Thickness
MPC-37	minimum, including deformation(8.875")	minimum (0.57”)
MPC-89	minimum, including deformation (5.96")	minimum (0.38”)
MPC-32ML[1]	minimum, including deformation(9.482")	minimum (0.57”)
MPC-31C	maximum, including deformation(9.79")	minimum (0.34”)

[1] As discussed in Subsection 6.3.1, the basket dimensional assumptions are consistent with MPC-37.

TABLE 6.3.4 (continued)

COMPOSITION OF THE MAJOR COMPONENTS OF THE HI-STORM FW SYSTEM

UO_2-Gd_2O_3, DENSITY 10.686 g/cm^3 5.0 wt% ^{235}U and 3.0 wt% Gd_2O_3	
Nuclide	**Wgt. Fraction**
92235	4.27500E-02
92238	8.12305E-01
8016	1.18916E-01
64152	5.02923E-05
64154	5.55406E-04
64155	3.79519E-03
64156	5.28301E-03
64157	4.06500E-03
64158	6.49316E-03
64160	5.78667E-03

TABLE 6.3.5

REACTIVITY EFFECTS OF ECCENTRIC POSITIONING OF CONTENT
(FUEL ASSEMBLIES AND DFCs) IN BASKET CELLS

CASE	Contents centered (Reference)	Content moved towards center of basket		Content moved towards basket periphery	
	Maximum k_{eff}	Maximum k_{eff}	k_{eff} Difference to Reference	Maximum k_{eff}	k_{eff} Difference to Reference
MPC-37, Undamaged Fuel	0.9327	0.9380	0.0053	0.9143	-0.0184
MPC-37, Undamaged Fuel and Damaged Fuel/Fuel Debris (12 DFCs)	0.9260	0.9276	0.0016	0.9158	-0.0102
MPC-89, Undamaged Fuel	0.9369	0.9435	0.0066	0.9211	-0.0158
MPC-89, Undamaged Fuel and Damaged Fuel/Fuel Debris (16 DFCs)	0.9415	0.9451	0.0036	0.9301	-0.0114
MPC-31C, Undamaged Fuel	0.9344	0.9364	0.0020	0.9271	-0.0073
MPC-31C, Undamaged Fuel and Damaged Fuel (6 DFCs)	0.9423	0.9417	-0.0006	0.9378	-0.0045
MPC-31C, Undamaged Fuel and Fuel Debris (6 DFCs)	0.9485	0.9462	-0.0023	0.9470	-0.0015

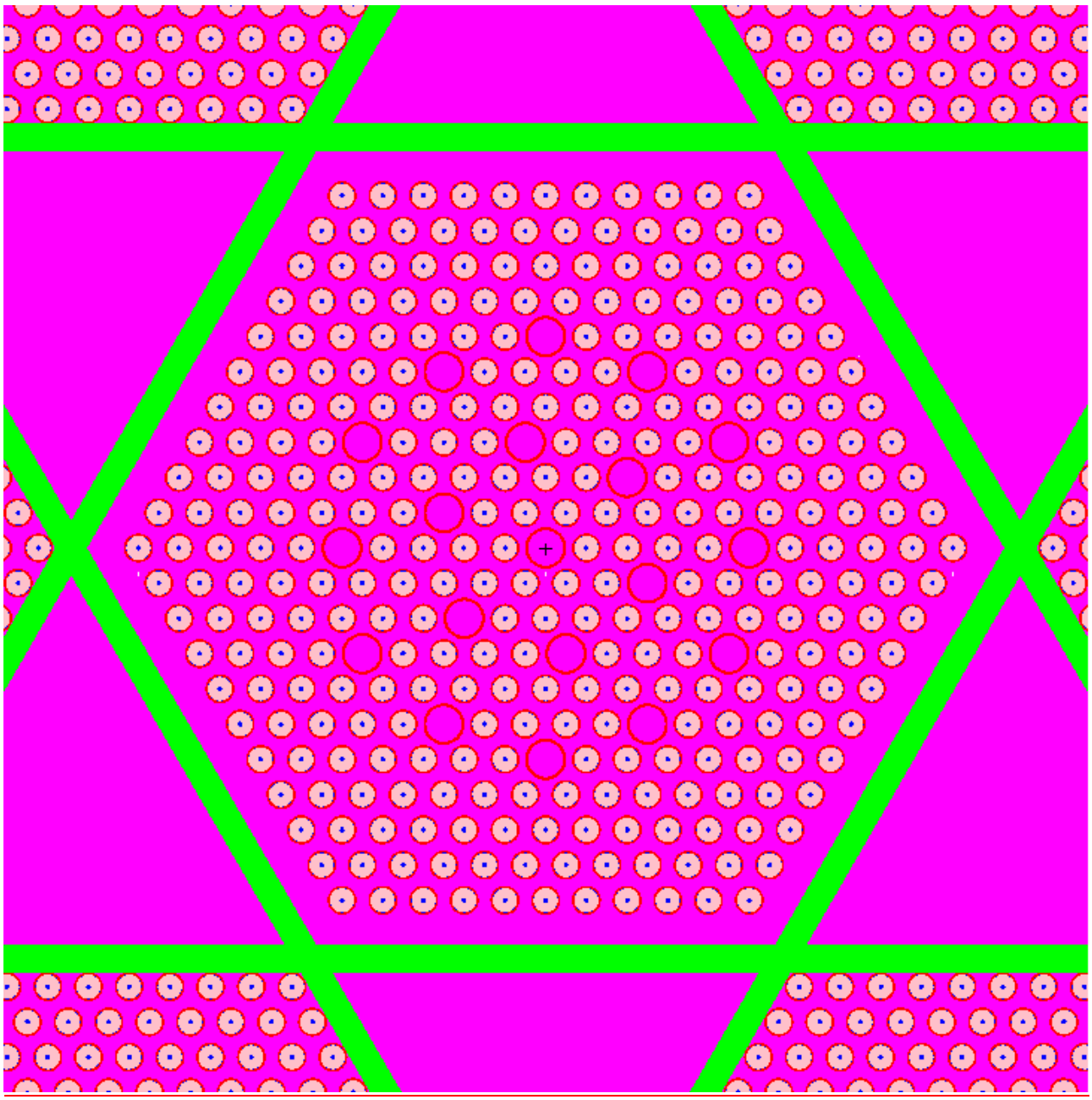

Figure generated directly from MCNP input file using the MCNP plot function. For Cell ID and Cell Wall Thickness see Table 6.3.3. For true dimensions see the drawings in Chapter 1.

Figure 6.3.6: Typical Cell of the Calculational Model (planar cross-section) with representative fuel in MPC-31C

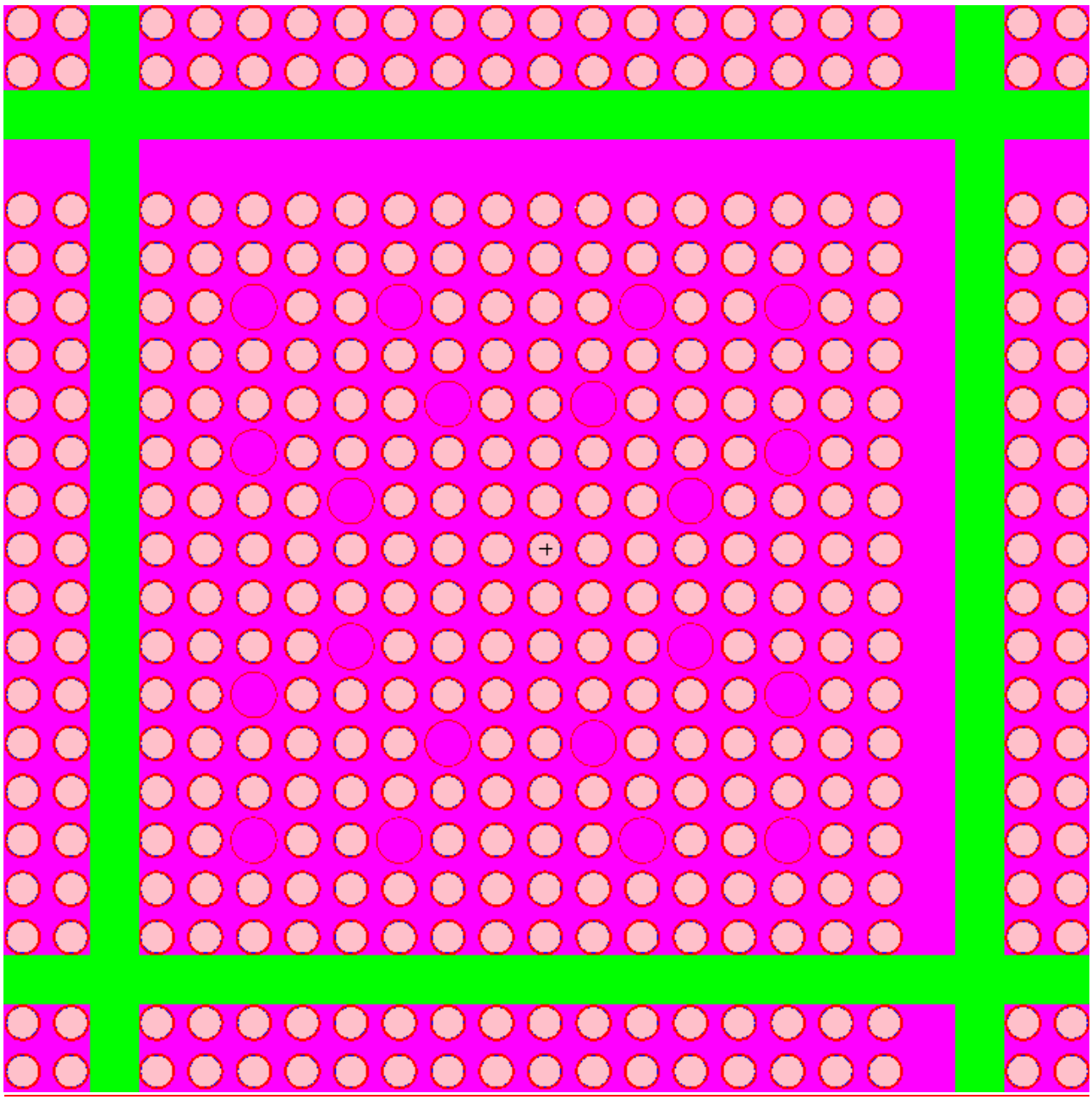

Figure generated directly from MCNP input file using the MCNP plot function. For Cell ID and Cell Wall Thickness see Table 6.3.3. For true dimensions see the drawings in Chapter 1.

Figure 6.3.7: Typical Cell of the Calculational Model (planar cross-section) with representative fuel in MPC-32ML

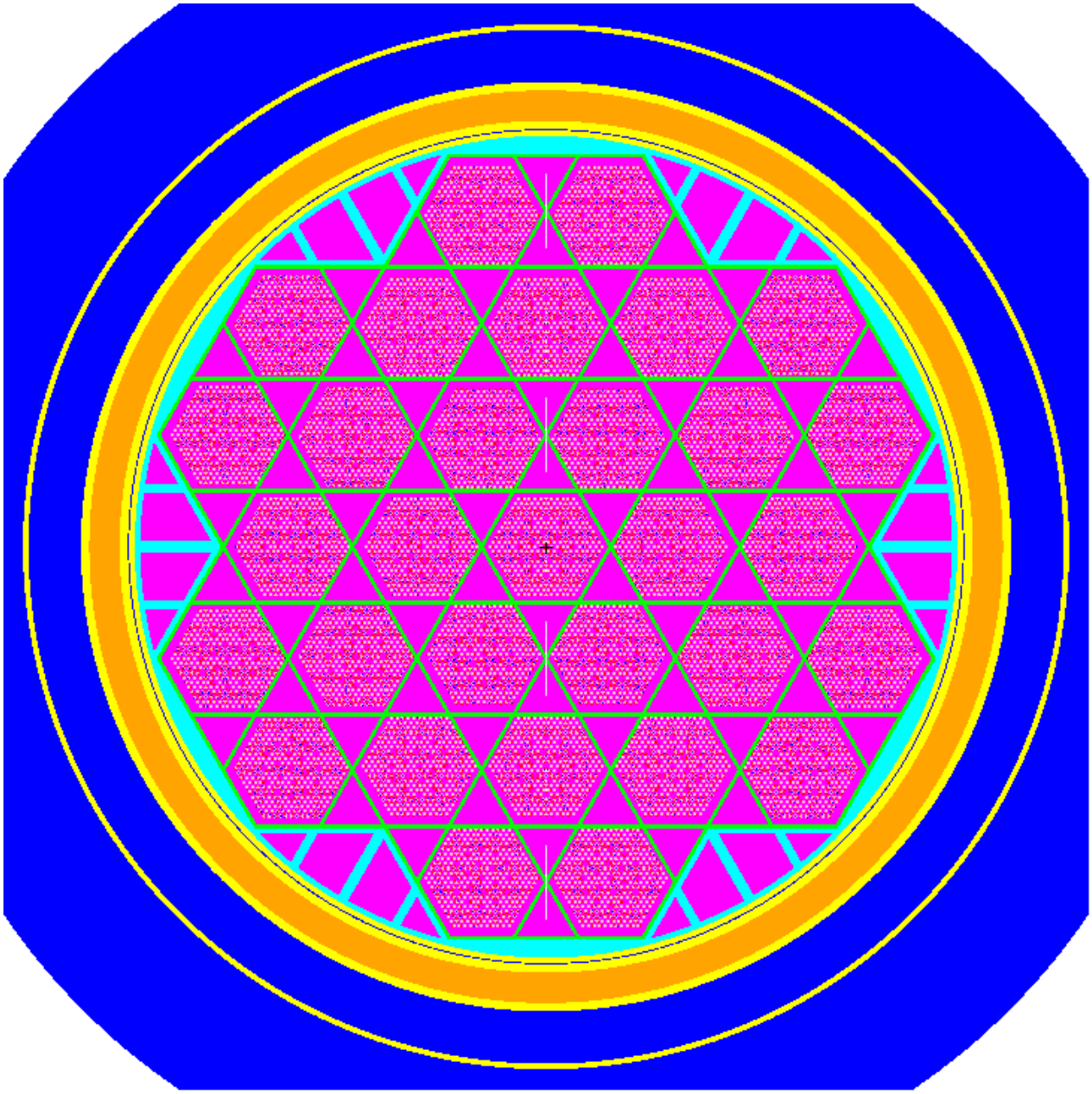

Figure generated directly from MCNP input file using the MCNP plot function. For radial dimensions of the HI-TRAC VW used in the analyses see Table 6.3.7. For true dimensions see the drawings in Chapter 1.

Figure 6.3.8: Calculational Model (planar cross-section) of MPC-31C

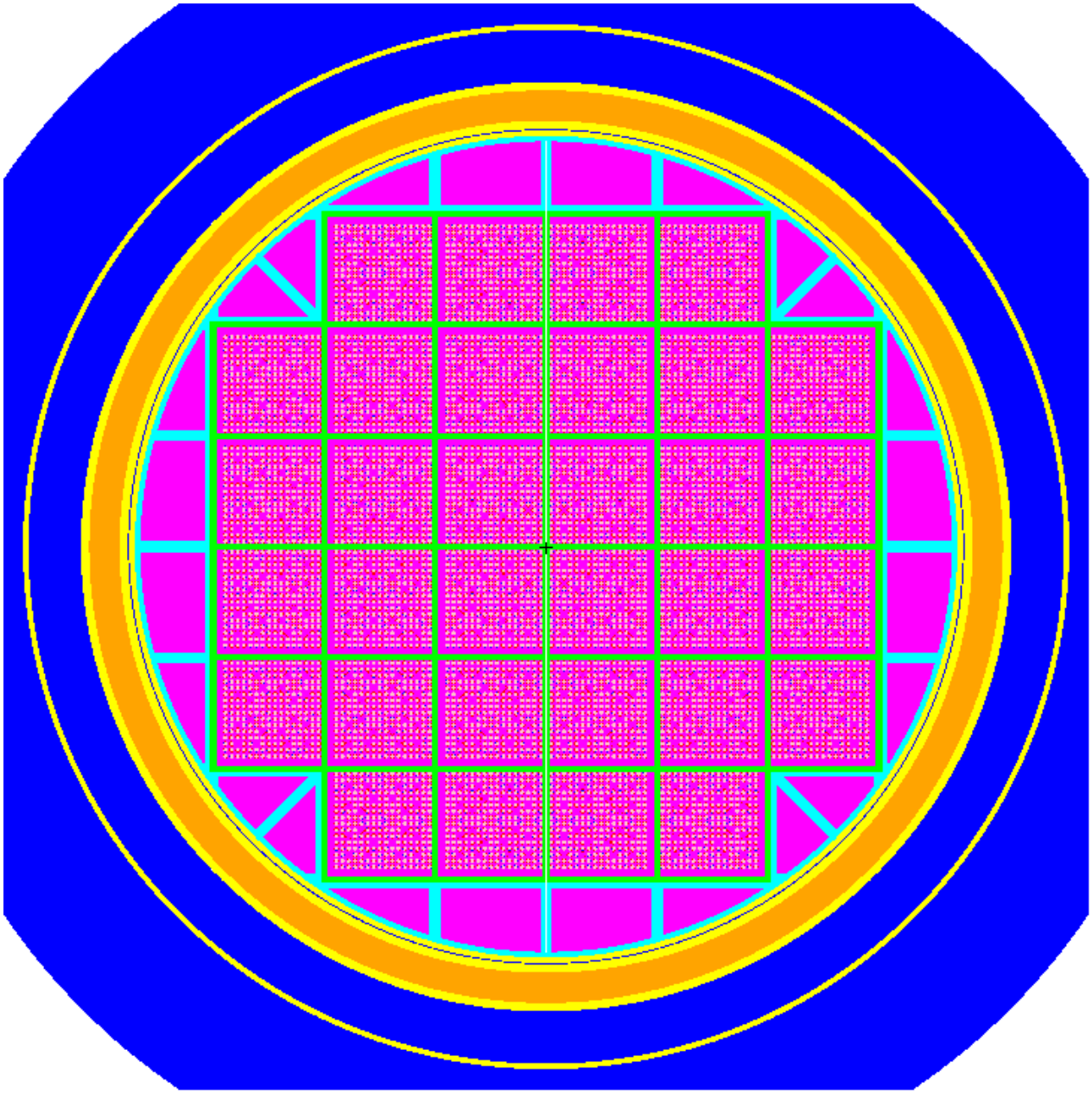

Figure generated directly from MCNP input file using the MCNP plot function. For radial dimensions of the HI-TRAC VW used in the analyses see Table 6.3.7. For true dimensions see the drawings in Chapter 1.

Figure 6.3.9: Calculational Model (planar cross-section) of MPC-32ML

6.4 CRITICALITY CALCULATIONS

6.4.1 Calculational Methodology

The principal method for the criticality analysis is the general three-dimensional continuous energy Monte Carlo N-Particle code MCNP5 [6.1.4] developed at the Los Alamos National Laboratory. MCNP5 was selected because it has been extensively used and verified and has all of the necessary features for this analysis. MCNP5 calculations used continuous energy cross-section data distributed with the code [6.1.4].

The convergence of a Monte Carlo criticality problem is sensitive to the following parameters: (1) number of histories per cycle, (2) the number of cycles skipped before averaging, (3) the total number of cycles and (4) the initial source distribution. The MCNP5 criticality output contains a great deal of useful information that may be used to determine the acceptability of the problem convergence. Based on this information, a minimum of 20,000 histories were simulated per cycle, a minimum of 20 cycles were skipped before averaging, a minimum of 100 cycles were accumulated, and the initial source was specified as uniform over the fueled regions (assemblies). To verify that these parameters are sufficient, studies were performed where the number of particles per cycle and/or the number of skipped cycles were increased. The calculations are presented in Table 6.4.9, and show only small differences between the cases, with the statistical tolerance of those calculations. All calculations are therefore performed with the parameters stated above, except for some studies that are performed with 50000 neutrons per cycle for improved accuracy, and except for the calculations for the HI-STORM, which need less particles for convergence. Appendix 6.D provides sample input files for various ~~the MPC-37 and MPC-89~~ baskets in the HI-STORM FW system.

6.4.2 Fuel Loading or Other Contents Loading Optimization

The basket designs are intended to safely accommodate fuel with enrichments indicated in Section 2.1. The calculations were based on the assumption that the HI-STORM FW system (HI-TRAC VW transfer cask) was fully flooded with clean unborated water or water containing specific minimum soluble boron concentrations. In all cases, the calculations include bias and calculational uncertainties, as well as the reactivity effects of manufacturing tolerances, determined by assuming the worst case geometry.

The discussion provided in Section 6.2.1 regarding the principal characteristics of fuel assemblies and basket poison is also important for the various studies presented in this section, and supports the fact that those studies only need to be performed for a single BWR and PWR assembly types, and that the results of those studies are then generally applicable to all assembly types. The studies and the relationship to the discussion in Section 6.2.1 are listed below. Note that this approach is consistent with that used for the HI-STORM 100.

Calculations for the MPC designs with internal moderators of various densities are shown in Table 6.4.5. Results show that in all cases the reactivity reduces with reducing water density, with both filled and voided guide and instrument tubes for PWR assemblies (see Section 6.4.7). All further calculations are therefore performed with full water density inside the MPCs.

6.4.2.2 Partial Flooding

Calculations in this section address partial flooding in the HI-STORM FW system and demonstrate that the fully flooded condition is the most reactive.

The reactivity changes during the flooding process were evaluated in both the vertical and horizontal positions for ~~all~~ the MPC-37 and MPC-89 designs. For these calculations, the cask is partially filled (at various levels) with full density (1.0 g/cm^3) water and the remainder of the cask is filled with steam consisting of ordinary water at a low partial density (0.002 g/cm^3 or less), as suggested in NUREG-1536. Results of these calculations are shown in Table 6.4.2. In all cases, the reactivity increases monotonically as the water level rises, confirming that the most reactive condition is fully flooded.

6.4.2.3 Clad Gap Flooding

As recommended by NUREG-1536, the reactivity effect of flooding the fuel rod pellet-to-clad gap regions, in the fully flooded condition, has been investigated. Table 6.4.3 presents maximum k_{eff} values that demonstrate the positive reactivity effect associated with flooding the pellet-to-clad gap regions. These results confirm that it is conservative to assume that the pellet-to-clad gap regions are flooded. For all cases, the pellet-to-clad gap regions are assumed to be flooded with clean, unborated water.

6.4.2.4 Preferential Flooding

Two different potential conditions of preferential flooding are considered: preferential flooding of the MPC basket itself (i.e., different water levels in different basket cells), and preferential flooding involving Damaged Fuel Containers.

Preferential flooding of the MPC basket itself for any of the MPC fuel basket designs is not possible because flow holes are present on all four walls of each basket cell at the bottom of the MPC basket. The flow holes are sized to ensure that they cannot be blocked by crud deposits (see Chapter 12). For damaged fuel assemblies and fuel debris, the assemblies or debris are loaded into stainless steel Damaged Fuel Containers fitted with mesh screens which prevent damaged fuel assemblies or fuel debris from blocking the basket flow holes. Preferential flooding of the MPC basket is therefore not possible.

However, when DFCs are present in the MPC, a condition could exist during the draining of the

To identify the configuration or configurations leading to the highest reactivity, a bounding approach is taken which is based on the analysis of regular arrays of bare fuel rods without cladding. Details and results of the analyses are discussed in the following subsections.

Note that since a modeling approach for all MPC designs except MPC-31C is used that bounds both damaged fuel and fuel debris without distinguishing between these two conditions, the term 'damaged fuel' as used throughout this chapter designates both damaged fuel and fuel debris, unless otherwise noted. However, for MPC-31C, the damaged fuel and fuel debris are considered particularly in the separate analyses of regular arrays of cladded and bare fuel rods, respectively.

Note that the modeling approach for damaged fuel and fuel debris is identical to that used in the HI-STORM 100 and HI-STAR 100.

Bounding Undamaged Assemblies

The undamaged assemblies assumed in the basket in those cells not filled with DFCs are those that show the highest reactivity for each group of assemblies, namely

- 9x9E for BWR 9x9E/F, 8x8F and 10x10G assemblies
- 10x10F for BWR 10x10F assemblies
- 10x10A for all other BWR assemblies;
- 16x16A for all PWR assemblies with 14x14 and 16x16 arrays; ~~and~~
- 15x15F for all PWR assemblies with 15x15 and 17x17 arrays;
- 16x16D for all PWR assemblies qualified for MPC-32ML; and
- V10A for all PWR assemblies qualified for MPC-31C.

Since the damaged fuel modeling approach results in higher reactivities, requirements of soluble boron for PWR fuel and maximum enrichment for BWR fuel are different from those for undamaged fuel only. Those limits are listed in Table 6.1.4 (PWR) and Table 6.1.5 (BWR) in Section 6.1. Note that for the calculational cases for damaged and undamaged fuel in the MPC-89, the same enrichment is used for the damage and undamaged assemblies.

Note that for the first group of BWR assemblies listed above (9x9E/F, 8x8F and 10x10G), calculations were performed for both 9x9E and 10x10G as undamaged assemblies, and assembly class 9x9E showed the higher reactivity, and is therefore used in the design basis analyses. This may seem contradictory to the results for undamaged assemblies listed in Table 6.1.2, where the 10x10G shows a higher reactivity. However, the cases in Table 6.1.2 are not at the same enrichment between those assemblies.

All calculations with damaged and undamaged fuel are performed for an active length of 150 inches. There are two assembly classes (17x17D and 17x17E) that have a larger active length for the undamaged fuel. However, the calculations for undamaged fuel presented in Table 6.1.1 show that the reactivity of those undamaged assemblies is at least 0.0050 delta-k lower than that

of the assembly class 15x15F selected as the bounding assembly for the cases with undamaged and damaged fuel. The effect of the active fuel length is less than that, with a value of 0.0026 reported in Table 6.2.1 for a much larger difference in active length of 50 Inches. The difference in active length between the 17x17D/E and 15x15F is therefore more than bounded, and the 15x15F assembly class is therefore appropriate to bound all undamaged assemblies with 15x15 and 17x17 arrays.

Bare Fuel Rod Arrays

A conservative approach is used to model both damaged fuel and fuel debris in the DFCs, using arrays of bare fuel rods:

- Fuel in the DFCs is arranged in regular, rectangular arrays of bare fuel rods, i.e., all cladding and other structural material in the DFC is replaced by water.

- For cases with soluble boron, additional calculations are performed with reduced water density in the DFC. This is to demonstrate that replacing all cladding and other structural material with borated water is conservative.

- The active length of these rods is assumed to be the same as for the intact fuel rods in the basket, even for more densely packed bare fuel rod arrays where it results in a total amount of fuel in the DFC that exceeds that for the intact assembly.

- To ensure the configuration with optimum moderation and highest reactivity is analyzed, the amount of fuel per unit length of the DFC is varied over a large range. This is achieved by changing the number of rods in the array and the rod pitch. The number of rods are varied between 16 (4x4) and 324 (18x18) for BWR fuel, ~~and~~ between 64 (8x8) and 576 (24x24) for PWR fuel, between 289 (17x17) and 676 (26x26) for 16x16D and between 91 (5 hexagonal rows) and 547 (13 hexagonal rows) for V10A.

This is a very conservative approach to model damaged fuel, and to model fuel debris configurations such as severely damaged assemblies and bundles of individual fuel rods, as the absorption in the cladding and structural material is neglected.

Further, this is a conservative approach to model fuel debris configurations such as bare fuel pellets due to the assumption of an active length of 150 inch (BWR and PWR). The actual height of bare fuel pellets in a DFC would be significantly below these values due to the limitation of the fuel mass for each basket position.

All calculations are performed for full cask models, containing the maximum permissible number of DFCs together with undamaged assemblies.

As an example of the damaged fuel model used in the analyses, Figure 6.4.1 shows the basket cell of an MPC-37 with a DFC containing a 14x14 array of bare fuel rods.

Note that the discussed above approach is applicable to damaged fuel in MPC-31C, with the exception of the cladding presence. This is acceptable since there are no gross defects in the damaged fuel assemblies (for the exact definition see the Glossary), and conservative due to applied model of the array of rods. The evaluation of fuel debris in MPC-31C is consistent with a generic approach employed for the other basket designs. It should be noted that the modeling approach for damaged fuel and fuel debris in the MPC-31C basket is similar to that used in Supplement 6.I.

Principal results are listed in Table 6.4.6, ~~and~~ 6.4.7, 6.4.11 and 6.4.12 for the MPC-37, MPC-89, MPC-31C and MPC-~~89~~32ML, respectively. In all cases, the maximum k_{eff} is below the regulatory limit of 0.95.

For the HI-STORM 100, additional studies for damaged fuel assemblies were performed to further show that the above approach using arrays of bare fuel rods are bounding. The studies considered conditions including

- Fuel assemblies that are undamaged except for various numbers of missing rods
- Variations in the diameter of the bare fuel rods in the arrays
- Consolidated fuel assemblies with cladded rods
- Enrichment variations in BWR assemblies

Results of those studies were shown in the HI-STORM 100 FSAR, Table 6.4.8 and 6.4.9 and Figure 6.4.13 and 6.4.14 (undamaged and consolidated assemblies); HI-STORM 100 FSAR Table 6.4.12 and 6.4.13 (bare fuel rod diameter); and HI-STORM 100 FSAR Section 6.4.4.2.3 and Table 6.4.13 (enrichment variations). In all cases the results of those evaluations are equivalent to, or bounded by those for the bare fuel rods arrays. Since the generic approach of modeling damaged fuel and fuel debris is unchanged from the HI-STORM 100, these evaluations are still applicable and need not be re-performed for the HI-STORM FW.

6.4.5 Fuel Assemblies with Missing Rods

For fuel assemblies that are qualified for damaged fuel storage, missing and/or damaged fuel rods are acceptable. However, for fuel assemblies to meet the limitations of undamaged fuel assembly storage, missing fuel rods must be replaced with dummy rods that displace a volume of water that is equal to, or larger than, that displaced by the original rods.

6.4.6 Sealed Rods replacing BWR Water Rods

Some BWR fuel assemblies contain sealed rods filled with a non-fissile material instead of water rods. Compared to the configuration with water rods, the configuration with sealed rods has a

6.4.9 Low Enriched, Channeled BWR fuel

The calculations in this subsection show that low enriched, channeled BWR fuel with indeterminable cladding condition is acceptable for loading in all storage locations of the MPC-89 without placing those fuel assemblies into DFCs, hence classifying those assemblies as undamaged. The main characteristics that must be assured are:

- The channel is present and attached to the fuel assembly in the standard fashion; and
- The channel is essentially undamaged; and
- The maximum planar average enrichment of the assembly is less than or equal to 3.3 wt% ^{235}U

This analysis covers older assemblies, where the cladding integrity is uncertain, and where a verification of the cladding condition is prohibitive. An example of this type of fuel is the so-called CILC fuel, which has potential corrosion-induced damaged to the cladding but does not have grossly breached spent fuel rods.

The presence of the essentially undamaged and attached channel confines the fuel rods to a limited volume and the low enrichment, required for all assemblies in the MPC, limits the reactivity of the fuel even under optimum moderation conditions. Due to the uncertain cladding condition, the analysis of this fuel follows essentially the same approach as that for the Damaged Fuel and Fuel Debris, i.e. bare fuel rod arrays of varying sizes are analyzed within the confines of the channel. This is an extremely conservative modeling approach for this condition, since reconfiguration is not expected and cladding would still be present. The results of this conservative analysis are listed in Table 6.4.8 and show that the system remains below the regulatory limit with these assemblies in all cells of the MPC-89, without DFCs.

These results confirm that even with unknown cladding condition the maximum k_{eff} values are below the regulatory limit when fully flooded and loaded with any of the BWR candidate fuel assemblies, therefore if the cladding is not grossly breached and the fuel assembly structurally sound it can be considered undamaged when loading in an MPC-89.

6.4.10 BWR Fuel with a Partial Gadolinium Credit

A list of the qualified BWR fuel assembly classes, with the associated maximum allowable enrichment (up to 4.8 wt% ^{235}U) and the bounding maximum k_{eff} value, is presented in Table 6.1.2. However, such highly enriched BWR fuel assembly is usually operated with the gadolinium bearing fuel rods, hereinafter referred to as Gd rods, which are typical fuel rods but with the burnable absorber - Gadolinia (Gd_2O_3), embedded in the fuel matrix. Therefore, the analysis is performed and documented in this subsection to qualify all 10x10 assembly classes with the increased enrichment up to 5.0 wt% ^{235}U using a partial credit for Gd rods. The limiting conditions are determined, and the administrative requirements are set forth to ensure that the

maximum k_{eff} value, including all applicable biases and uncertainties, is below 0.95 with a substantial safety margin, sufficient to offset any potential uncertainties in the condition of the BWR fuel assembly with Gd rods.

Withheld in Accordance with 10 CFR 2.390

In summary, all 10x10 fuel assembly classes with the fuel enrichment of up to 5.0 wt% ^{235}U are qualified for loading into the MPC-89 basket using a partial credit for Gd rods with the following administrative requirements:

- The Gd rod loading is not less than 3.0 wt% Gd_2O_3;
- The Gd rods located in the peripheral row of the fuel lattice cannot be credited;
- At least one Gd rod is required for 10x10A, 10x10B and 10x10F fuel assembly classes;
- Not less than two Gd rods are required for 10x10C and 10x10G classes.

TABLE 6.4.3

REACTIVITY EFFECT OF FLOODING THE PELLET-TO-CLAD GAP

~~Pellet-to-Clad Condition~~	~~**Maximum k_{eff}**~~	
	~~**MPC-37 (17x17B, 5.0% ENRICHMENT)**~~	~~**MPC-89 (10x10A, 4.8% ENRICHMENT)**~~
~~dry~~	~~0.9335~~	~~0.9391~~
~~flooded with unborated water~~	~~0.9380~~	~~0.9435~~
Case	**Maximum k_{eff}**	
	Dry	**Flooded with unborated water**
MPC-37 (17x17B, 5.0% Enrichment)	0.9335	0.9380
MPC-89 (10x10A, 4.8% Enrichment)	0.9391	0.9435
MPC-31C (V10A, 5.0% Enrichment)	0.9200	0.9364
MPC-32ML (16x16D, 5.0% Enrichment)	0.9350	0.9386

TABLE 6.4.11

MAXIMUM k_{eff} VALUES IN MPC-31C WITH UNDAMAGED (V10A) AND DAMAGED FUEL

Rod Array inside the DFC, Hexagonal Rows	**Damaged Fuel (Cladded)**	**Fuel Debris (Bare)**
5	0.9307	0.9236
7	0.9381	0.9281
8	0.9423	0.9408
9	0.9403	0.9485
10	0.9365	0.9434
11	0.9338	0.9323
13	0.9314	0.9249

TABLE 6.4.12

MAXIMUM k_{eff} VALUES IN MPC-32ML WITH UNDAMAGED (16x16D) AND DAMAGED FUEL

Bare Rod Array inside the DFC	**Maximum k_{eff}, 4.0 wt%**	**Maximum k_{eff}, 5.0 wt%**
17x17	0.9123	0.9303
19x19	0.9142	0.9332
20x20	0.9149	0.9342
21x21	0.9146	0.9344
22x22	0.9144	0.9347
23x23	0.9140	0.9336
24x24	0.9136	0.9331
26x26	0.9122	0.9315

TABLE 6.4.13

Withheld in Accordance with 10 CFR 2.390

Figure 6.4.2: **Withheld in Accordance with 10 CFR 2.390**

6.7 REFERENCES

[6.0.1] HI-STORM 100 FSAR, NRC Docket 72-1014, Holtec Report HI-2002444, Latest revision

[6.0.2] "Criticality Analyses for the HI-STORM FW System", Holtec Report HI-2094432 Rev.0 (proprietary)

[6.1.1] NUREG-1536, Standard Review Plan for Dry Cask Storage Systems, USNRC, Washington, D.C., January 1997.

[6.1.2] 10CFR72.124, "Criteria For Nuclear Criticality Safety."

[6.1.3] not used

[6.1.4] "MCNP - A General Monte Carlo N-Particle Transport Code, Version 5"; Los Alamos National Laboratory, LA-UR-03-1987 (2003).

[6.1.5] M.G. Natrella, Experimental Statistics, National Bureau of Standards, Handbook 91, August 1963.

[6.1.6] "CASMO-4 Methodology", Studsvik/SOA-95/2, Rev. 0, 1995.

"CASMO-4 A Fuel Assembly Burnup Program, Users Manual," SSP-01/400, Rev. 1, Studsvik Scandpower, Inc., 2001.

"CASMO-4 Benchmark Against Critical Experiments", Studsvik/SOA-94/13, Studsvik of America, 1995.

[6.4.1] J.M. Cano, R. Caro, and J.M Martinez-Val, "Supercriticality Through Optimum Moderation in Nuclear Fuel Storage," Nucl. Technol., 48, 251-260, (1980).

[6.4.2] NUREG/CR-7194, Technical Basis for Peak Reactivity Burnup Credit for BWR Spent Nuclear Fuel in Storage and Transportation Systems, USNRC, Washington, D.C., April 2015.

APPENDIX 6.A: BENCHMARK CALCULATIONS

Withheld in Accordance with 10 CFR 2.390

APPENDIX 6.B: MISCELLANEOUS INFORMATION

6.B.1 Sample Input File MPC-37
6.B.2 Sample Input File MPC-89
6.B.3 Analyzed Distributed Enrichment Patterns for Higher Enrichments
6.B.4 Assembly Cross Sections
6.B.5 Sample Input File MPC-31C
6.B.6 Sample Input File MPC-32ML

6.B.1 Sample Input File MPC-37

Withheld in Accordance with 10 CFR 2.390

6.B.2 Sample Input File MPC-89

Withheld in Accordance with 10 CFR 2.390

6.B.3 Analyzed Distributed Enrichment Patterns

Withheld in Accordance with 10 CFR 2.390

6.B.4 Assembly Cross Sections

Withheld in Accordance with 10 CFR 2.390

6.B.5 Sample Input File MPC-31C

Withheld in Accordance with 10 CFR 2.390

6.B.6 Sample Input File MPC-32ML

Withheld in Accordance with 10 CFR 2.390

CHAPTER 11 CHANGED PAGES

11.3 ESTIMATED ON-SITE CUMULATIVE DOSE ASSESSMENT

This section provides the estimates of the cumulative exposure to personnel performing loading, unloading and transfer operations using the HI-STORM FW system. This section uses the shielding analysis provided in Chapter 5, the operations procedures provided in Chapter 9 and the experience from the loading of many MPCs to develop a realistic estimate of the occupational dose.

The dose rates from the HI-STORM FW overpack, MPC lid, HI-TRAC VW, and HI-STAR 100 overpack are calculated to determine the dose to personnel during the fuel loading and unloading operations. No assessment is made with respect to background radiation since background radiation can vary significantly by site.

The estimated occupational dose is governed by three principal parameters, namely:

i. The dose rate emanating from the MPC.
ii. Average duration of human activity in the radiation elevated space.
iii. Relative proximity of humans to the radiation source.

The dose rate accreted by the MPC depends on its contents. Regionalized storage has been made mandatory in the HI-STORM FW MPC-37 to reduce its net radiation output. The duration of required human activity and the required human proximity, on the other hand, are dependent on the training level of the personnel, and user friendliness of ancillary equipment and the quality of fit-up of parts that need to be assembled in the radiation field.

To provide a uniform basis for the dose estimates presented in this chapter, the reference MPC contents data, available HI-TRAC VW weight, etc., are set down in Table 11.3.1.

Using Table 11.3.1 data, the dose data for fuel loading (wet to dry storage) is provided in Table 11.3.2. The dose for the reverse operation (dry to wet storage) is summarized in Table 11.3.3.

For each step in Table 11.3.2, the task description, average number of personnel in direct radiation field, exposure duration in direct radiation field and average dose rate are identified. The relative locations refer to all HI-STORM FW overpacks. The dose rate location points around the transfer cask and overpack were selected based on actual experience in loading HI-STORM 100 Overpacks. Cask operators typically work with workers entering and exiting the immediate cask area. To account for this, an average number of workers and average dose rates are used. The tasks involved in each step presented in Table 11.3.2 are not provided in any specific order.

Table 11.3.1 ASSUMED PARAMETERS FOR DOSE ESTIMATE UNDER SHORT-TERM OPERATIONS AND UNDER LONG-TEM STORAGE		
	Item	**Value**
1.	**MPC-Contents (MPC-37)[1]**	**45,000 MWD/MTU and 4.5 years**
2.	**Weight of HI-TRAC VW Full of Fuel and Water**	**125 tons**
3.	**HI-STORM Concrete Density**	**150 lb/cubic feet**

[1] The case of MPC-37 is used but similar results are expected for ~~the MPC-89~~ all MPC types.

CHAPTER 13 CHANGED PAGES

13.2.8 MPC

a. Basket material composition, properties, dimensions, and tolerances for criticality control.

b. Canister material mechanical properties for structural integrity of the confinement boundary.

c. Canister and basket material thermal properties and dimensions for heat transfer control.

d. Canister and basket material composition and dimensions for dose rate control.

13.2.9 HI-STORM FW Overpack

a. HI-STORM overpack material mechanical properties and dimensions for structural integrity to provide protection of the MPC and shielding of the spent nuclear fuel assemblies during handling and storage operations.

b. HI-STORM overpack material thermal properties and dimensions for heat transfer control.

c. HI-STORM overpack material composition and dimensions for dose rate control.

13.2.10 HI-TRAC VW Transfer Cask

a. HI-TRAC transfer cask material mechanical properties and dimensions for structural integrity to provide protection of the MPC and shielding of the spent nuclear fuel assemblies during loading, unloading and handling operations.

b. HI-TRAC transfer cask material thermal properties and dimensions for heat transfer control.

c. HI-TRAC transfer cask material composition and dimensions for dose rate control.

13.2.11 Verifying Compliance with Fuel Assembly Decay Heat, Burnup, and Cooling Time Limits

The examples below demonstrate how the user of the system can determine if fuel assemblies, including NFH, are acceptable for loading in either the MPC-37 or the MPC-89 in accordance with the allowable decay heat, burnup, and cooling time for the approved contents. A similar thought process is applicable to fuel assembly acceptability determinations for all MPC types.

B 3.3 SFSC Criticality Control

B 3.3.1 Boron Concentration

BASES	
BACKGROUND	A TRANSFER CASK with an empty MPC is placed in the spent fuel pool and loaded with fuel assemblies meeting the requirements of the Certificate of Compliance. A lid is then placed on the MPC. The TRANSFER CASK and MPC are raised to the top of the spent fuel pool surface. The TRANSFER CASK and MPC are then moved into the preparation area where the MPC lid is welded to the MPC shell and the welds are inspected and tested. The water is drained from the MPC cavity and drying is performed. The MPC cavity is backfilled with helium. Then, the MPC vent and drain cover plates and MPC closure ring are installed and welded. Inspections are performed on the welds. For those MPCs containing PWR fuel assemblies credit is taken in the criticality analyses for boron in the water within the MPC. To preserve the analysis basis, users must verify that the boron concentration of the water in the MPC meets specified limits when there is fuel and water in the MPC. This may occur during LOADING OPERATIONS and UNLOADING OPERATIONS.
APPLICABLE SAFETY ANALYSIS	The spent nuclear fuel stored in the SFSC is required to remain subcritical ($k_{eff} \leq 0.95$) under all conditions of storage. The HI-STORM FW SFSC is analyzed to store a wide variety of spent nuclear fuel assembly types with differing initial enrichments. For all PWR fuel loaded in the MPC-37 or MPC-32ML, credit was taken in the criticality analyses for neutron poison in the form of soluble boron in the water within the MPC. Compliance with this LCO preserves the assumptions made in the criticality analyses regarding credit for soluble boron.

(continued)

BASES	
LCO	Compliance with this LCO ensures that the stored fuel will remain subcritical with a $k_{eff} \leq 0.95$ while water is in the MPC. LCOs 3.3.1 ~~.a~~ provides the minimum concentration of soluble boron required in the MPC water for the MPC-37 and MPC-32ML. The amount of soluble boron is dependent on the initial enrichment of the fuel assemblies to be loaded in the MPC. Fuel assemblies with an initial enrichment less than or equal to 4.0 wt. % U-235 require less soluble boron than those with initial enrichments greater than 4.0 wt. % U-235. For initial enrichments greater than 4.0 wt. % U-235 and up to 5.0 wt. % U-225, interpolation is permitted to determine the required minimum amount of soluble boron. All fuel assemblies loaded into the MPC-37 or MPC-32ML are limited by analysis to maximum enrichments of 5.0 wt. % U-235. The LCO also requires that the minimum soluble boron concentration for the most limiting fuel assembly array/class and classification to be stored in the same MPC be used. This means that the highest minimum soluble boron concentration limit for all fuel assemblies in the MPC applies in cases where fuel assembly array/classes are mixed in the same MPC. This ensures the assumptions pertaining to soluble boron used in the criticality analyses are preserved.
APPLICABILITY	The boron concentration LCO is applicable whenever an MPC-37 or MPC-32ML has at least one PWR fuel assembly in a storage location and water in the MPC. During LOADING OPERATIONS, the LCO is applicable immediately upon the loading of the first fuel assembly in the MPC. It remains applicable until the MPC is drained of water. During UNLOADING OPERATIONS, the LCO is applicable when the MPC is reflooded with water. Note that compliance with SR 3.0.4 assures that the water to be used to flood the MPC is of the correct boron concentration to ensure the LCO is satisfied upon entering the Applicability. A note has also been added to the APPLICABILITY that states that this LCO is not applicable if burnup credit is being utilized.

(continued)